

**COMPARATIVE ENERGY PERFORMANCE  
ASSESSMENT OF HEMP-CLAY  
AS BUILDING BLOCK MATERIAL**

**A Thesis Submitted to  
the Graduate School of Engineering and Sciences of  
İzmir Institute of Technology  
in Partial Fulfillment of the Requirements for the Degree of**

**MASTER OF SCIENCE**

**in Architecture**

**by  
Betül ERGÜN**

**July 2022  
İZMİR**

## ACKNOWLEDGEMENTS

This thesis becomes a reality with the kind support and help of many individuals and institutions. I would like to extend my sincere thanks to all of them.

I would first like to express my sincere gratitude to my supervisor Assoc. Prof. Dr. Zeynep DURMUŞ ARSAN for her decisive support and helpful manner. She supported me in formalizing my enthusiasm for research on natural building materials, steered me in the right direction, and widened my horizons about academic life.

I am equally grateful to my advisor Prof. Dr. Sedat AKKURT for his contribution with informative comments and guidance about the design of experiments and material characterization methods of this thesis.

I would also like to thank the expert who precisely performed thermal conductivity tests of the research samples: Dr. Ebru HANCIOĞLU from Geothermal Energy Research and Application Center in Izmir Institute of Technology (IZTECH). I secondly thank the Center for Material Research of IZTECH for giving me an opportunity to carry out material characterization tests for this thesis.

I'm grateful to the entrepreneur Ulaş Oğrak and the Bloksan Brick Factory in Turgutlu for providing me necessary raw materials to produce experimental samples for the research. I also thank the administration of the Department of Civil Engineering in IZTECH for giving me the allowance to do experiments in their Material Laboratory and use all facilities in the laboratory.

Most importantly, I must express my profound gratitude to my dear parents for their support and continuous encouragement throughout my years of study and whole life. None of this would be possible without the love and patience of my family. I am grateful to them for letting me be myself.

# ABSTRACT

## COMPARATIVE ENERGY PERFORMANCE ASSESSMENT OF HEMP-CLAY AS BUILDING BLOCK MATERIAL

Bio-based and earthen building materials have recently started to be used again in seeking sustainable materials to combat climate change. Hemp-based building materials stand out as energy-efficient materials due to their favorable thermal properties, although they still have unstandardized features that vary by location. This study aims to investigate the thermal properties and energy performance of hemp-clay building blocks which are produced with local hemp and clay in the western Aegean region of Turkey for today and the future, leading up the research on hemp-based building materials in the Mediterranean region.

The methodology of the research consists of laboratory experiments on material and building energy simulations via DesignBuilder software. Building block samples were produced with 27 different hemp-clay mixtures and tested using a quick thermal conductivity meter. Subsequently, the thermal performance of selected hemp-clay block was compared with conventional wall infill materials such as hollow clay brick, autoclaved aerated concrete, and lightweight pumice block via simulations of the annual energy consumption of an existing residential building in Izmir. Simulation scenarios were generated keeping wall thickness and U-value as constant for the climate of 2020, 2050, and 2080.

Hemp-clay building blocks reduced the heating and cooling demands of the case building by 21% and 14%, respectively in 2020. Their energy performance outperformed the other materials' performances even if the scenario walls have the same U-value as hemp-clay walls in today's and the future's climate conditions. Consequently, the hemp-clay building blocks are apparent as a promising material to be improved in Turkey.

# ÖZET

## BİNA BLOK MALZESİ OLARAK KENEVİR-KİLİN KARŞILAŞTIRMALI ENERJİ PERFORMANS DEĞERLENDİRMESİ

İklim değışikliđi ile mücadele için sürdürülebilir malzeme arayışında, bio-malzemeler ve toprak esaslı yapı malzemeleri son zamanlarda yeniden kullanılmaya başlanmıştır. Kenevir bazlı yapı malzemeleri, yere göre değışkenlik gösteren, standardize edilmemiş özelliklere sahip olsa da olumlu ısıl özellikleri nedeniyle enerji verimli yapı malzemeleri olarak öne çıkmaktadır. Bu çalışmanın asıl hedefi, Türkiye'nin batı Ege bölgesindeki yerel kenevir ve kil kullanılarak üretilen kenevir-kil bina bloklarının ısıl özellikleri ile günümüz ve gelecekteki enerji performansını araştırmak ve Akdeniz bölgesindeki kenevir-bazlı yapı malzemesi üzerine yapılacak araştırmaların önünü açmaktır.

Araştırmanın metodolojisi, malzeme üzerine yürütülen laboratuvar çalışmaları ve DesignBuilder programı ile yapılan bina enerji simülasyonlarından oluşmaktadır. Bina blok numuneleri 27 farklı kenevir-kil karışımı ile üretilmiş ve ısıl geçirgenlik ölçüm cihazı ile test edilmiştir. Sonrasında seçilen kenevir-kil bloğun enerji performansı, İzmir'de mevcut bir konut yapısının yıllık enerji tüketimi simülasyonları üzerinden, delikli kil tuğla, gazbeton ve hafif ponza blok gibi konvansiyonel duvar dolgu malzemeleri ve kenevir-beton tuğla ile karşılaştırılmıştır. Simülasyon senaryoları duvar kalınlığının ve U değerinin sabit tutulması ile 2020, 2050 ve 2080 yılları için üretilmiştir.

Üretilen kenevir-kil bina bokları 2020 yılında yapının ısıtma ve soğutma ihtiyaçlarını sırasıyla %21 ve %14 oranlarında azaltmıştır. Diğer duvarların U değerleri kenevir-kil duvarlarla aynı bile olsa hem günümüz hem de gelecek iklim şartlarında kenevir-kil bina bloklarının enerji performansı daha üstündür. Sonuç olarak, kenevir-kil bina blokları Türkiye'de geliştirilmesi gereken umut verici bir malzeme olarak görülmektedir.

# TABLE OF CONTENTS

LIST OF FIGURES .....	viii
LIST OF TABLES .....	x
LIST OF ABBREVIATIONS .....	xi
CHAPTER 1. INTRODUCTION .....	1
1.1. Problem Statement .....	1
1.2. Aim and Objectives .....	5
1.3. Limitations and Assumptions .....	7
1.4. Outline of the Thesis .....	8
CHAPTER 2. LITERATURE REVIEW .....	10
2.3. Hemp and Hemp-Based Building Materials .....	10
2.3.1. Hemp and Its Area of Use .....	10
2.3.1. Hemp Use in Construction .....	12
2.4. Hemp in Turkey .....	15
2.5. Studies on Hemp-Base Building Materials .....	16
2.5.1. Thermal Properties of Hemp-Based Building Materials.....	16
2.5.2. Mechanical Properties of Hemp-Based Building Materials.....	20
2.5.3. Acoustical Properties of Hemp-Based Building Materials.....	22
CHAPTER 3. MATERIAL AND METHODS .....	24
3.1. Simulation Study .....	24
3.1.1. Selection of the Case Building .....	26
3.1.2. General Information About the Case Building .....	26
3.1.3. Building Components and Construction Techniques.....	30
3.1.4. Monitoring Process.....	33
3.1.5. Weather File Generation.....	35
3.1.6. Modeling Process.....	35

3.1.7. Calibration of the Simulation Model.....	40
3.2. Experimental Study .....	41
3.2.1. Selection of Raw Materials .....	42
3.2.1.1. Hemp .....	42
3.2.1.2. Clay .....	43
3.2.1.3. Lime.....	43
3.2.2. Characterization of Materials .....	44
3.2.2.1. Bulk Density Measurement .....	44
3.2.2.2. Grain Size Distribution Tests .....	44
3.2.3. Chemical Composition Tests .....	48
3.2.4. Production of Hemp-Clay Test Blocks .....	50
3.2.4.1. Mixing of Materials .....	50
3.2.4.2. Moulding of the Mixture .....	52
3.2.4.2. Drying of the Test Blocks .....	53
3.2.5. Characterization of Hemp-Clay Blocks .....	53
3.2.5.1. Density Measurement .....	54
3.2.5.2. Thermal Conductivity Test .....	54
3.3. Determination of Simulation Scenarios .....	55
CHAPTER 4. RESULTS AND DISCUSSION.....	58
4.1. Monitoring Results .....	58
4.1.1. Temperature .....	58
4.1.2. Relative Humidity.....	61
4.2. Calibration Results .....	64
4.3. Results of Material Characterization .....	67
4.3.1. Bulk Density.....	67
4.3.2. Grain Size Distribution.....	67
4.3.3. Chemical Composition.....	68
4.4. Results of Hemp-Clay Block Characterization.....	71
4.4.1. Specific Density.....	72
4.4.2. Thermal Conductivity.....	73
4.5. Simulation Results.....	75

CHAPTER 5. CONCLUSION.....	81
5.1. Concluding Regarding Results .....	81
5.3. Further Study .....	84
REFERENCES.....	86
APPENDIX A.....	95

# LIST OF FIGURES

<b><u>Figure</u></b>	<b><u>Page</u></b>
Figure 2.1. Parts of the hemp plant and areas of usage.....	11
Figure 2.2. Hemp-lime building techniques: shuttering (a), spraying (b), and block masonry (c) .....	14
Figure 3.1. Flowchart of the research methodology.....	25
Figure 3.2. Location of Izmir province in a broad context.....	27
Figure 3.3. Aerial view of the case building on the neighborhood scale.....	28
Figure 3.4. Typical floor plan of the case building and the case unit (the case unit was indicated with red dot lines).....	29
Figure 3.5. Aluminum frame window at the corner (a), PVC framed window (b) and the french balcony with a sliding door (c) on the north façade.....	32
Figure 3.6. The exact locations of external and internal data loggers placed in the study room (indicated with red dots).....	34
Figure 3.7. Abstracted site plan of the case building.....	36
Figure 3.8. Digital model in Design Builder (case unit is indicated with black dot lines).....	37
Figure 3.9. Floor plan of the case unit that was modeled in DesignBuilder.....	37
Figure 3.10. Hemp stalks (a) on the field and hemp hurds (b) in the laboratory. ....	43
Figure 3.11. Soil deposit (a) in the factory site and the soil (b) supplied for the study .....	43
Figure 3.12. The sieve shaker and stacks are ready to work .....	45
Figure 3.13. Soil suspension prepared for hydrometer testing (a) and reading of hydrometer (b).....	47
Figure 3.14. Solid components of the hemp-clay materials were prepared to be tested...	48
Figure 3.15. Raw materials prepared for mixing (a), slurry mix of clay and water (b) and hemp-clay mix ready for moulding (c).....	51
Figure 3.16. Hemp-clay block samples in steel moulds (a) and (b).....	52
Figure 3.17. Hemp-clay blocks are left for drying in the laboratory.....	53
Figure 3.18. Measurement of weight (a) and thermal conductivity testing (b).....	54
Figure 4.1. Indoor and outdoor air temperatures for the whole year with the trendline....	60

<b><u>Figure</u></b>	<b><u>Page</u></b>
Figure 4.2. Monitored indoor and outdoor temperatures in January 2021.....	60
Figure 4.3. Monitored indoor and outdoor temperatures in July 2021.....	61
Figure 4.4. Indoor and outdoor relative humidity values for the monitored year.....	63
Figure 4.5. Recorded relative humidity values of indoor and outdoor in January 2021 (Shaded area depicts the RH interval for indoor comfort) .....	63
Figure 4.6. Recorded relative humidity values of indoor and outdoor in July 2021 (Shaded area depicts the RH interval for indoor comfort) .....	64
Figure 4.7. Simulated and monitored air temperature in January.....	66
Figure 4.8. Simulated and monitored air temperature in July.....	66
Figure 4.9. Grain size distribution curve according to both sieve and hydrometer analysis.....	68
Figure 4.10. XRD pattern of clay specimen.....	69
Figure 4.11. XRD pattern of lime specimen.....	69
Figure 4.12. SEM images of hemp (a), clay (b), and lime (c).....	71
Figure 4.13. Effect of hemp:binder ratio and lime additive on thermal conductivity.....	74
Figure 4.14. Heating and cooling energy consumption of different wall infills within the wall same thickness.....	75
Figure 4.15. Annual energy consumption of different wall infill materials with and without an insulation layer.....	77
Figure 4.16. Annual energy consumption of different wall infill materials in 2020, 2050 and 2080.....	78
Figure 4.17. Heating energy consumption of different wall infills in 2020, 2050, and 2080.....	80

# LIST OF TABLES

<b><u>Table</u></b>	<b><u>Page</u></b>
Table 3.1. Technical specifications of the case unit.....	30
Table 3.2. Technical specifications of data loggers .....	33
Table 3.3. Material properties of openings inserted into the simulation model.....	38
Table 3.4. Component properties of materials inserted in DesignBuilder.....	38
Table 3.5. Acceptable limits of error indices.....	40
Table 3.6. Sieve number and mesh openings in millimeters.....	46
Table 3.7. Mixing proportions of hemp, binder, and the additive.....	50
Table 3.8. Wall layers and material properties regarding the first series of scenarios.....	56
Table 3.9. Wall layers and material properties regarding the second series of scenarios.....	57
Table 4.1. Monitored outdoor and indoor temperature values.....	59
Table 4.2. Monitored relative humidity values for outdoor and indoor.....	62
Table 4.3. CV-RMSE and MBE values for each month.....	65
Table 4.4. Mechanical sieve analysis results.....	67
Table 4.5. Hydrometer analysis results.....	68
Table 4.6. XRF results of clay specimen.....	70
Table 4.7. XRF results of the lime specimen.....	70
Table 4.8. Density results of hemp-clay samples after demoulding and drying.....	72
Table 4.9. Thermal conductivity results of hemp-clay samples.....	74
Table 4.10. Annual energy consumption results of all scenarios and change ratio according to the base scenario.....	76
Table 4.11. Annual energy consumption of 8 scenarios in 2020, 2050 and 2080 and their change ratios according to the present.....	79
Table A.1. Activity, opening and HVAC input parameters of the study room, bedroom and master bedroom.....	95
Table A.2. Activity, opening and HVAC input parameters of the kitchen, living room and bathroom.....	98

## LIST OF ABBREVIATIONS

$T_m$	:monitored air temperature for the interior
$T_{ma}$	:the average of monitored temperature values
$T_s$	:simulated air temperature for the interior
.epw	:Energy Plus Weather
AAC	:Aerated autoclaved concrete
ASHRAE	:The American Society of Heating, Refrigerating and Air Conditioning Engineers
ASTM	:The American Society for Testing and Materials
BES	:building energy simulation
BRE	:Building Research Establishment
CV-RMSE	:Root Mean Square Error
HCB	:Hollow clay brick
HVAC	:Heating, Ventilating and Air Conditioning
IEA	:International Energy Agency
IPCC	:Intergovernmental Panel on Climate Change
IPMVP	:International Performance Measurement and Verification Protocol
LPB	:Lightweight pumice blocks
M&V	:Measurement and Verification for Federal Energy Projects
MBE	:Mean Bias Error
PVC	:polyvinyl chloride
RH	:relative humidity
SEM	:Scanning Electron Microscopy
SHGC	:solar heat gain coefficient
T	:temperature
THC	:tetrahydrocannabinol
UNCC	:United Nations Climate Change
UNEP	:United Nations Environment Programme
XRD	:X-Ray Diffraction
XRF	:X-Ray Fluorescence

# CHAPTER 1

## INTRODUCTION

### 1.1. Problem Statement

In recent years, nations have started to take significant actions to combat climate change just after several economic crises and environmental catastrophes. However, hazardous effects of climate change in the not-so-distant future are predicted and well-known since the 1970s (United Nations Climate Change [UNCC] 2019). According to Intergovernmental Panel on Climate Change (IPCC), increasing greenhouse gas emissions in the atmosphere which are directly related to the consumption of fossil fuels such as coal, oil, and gas for energy production is the main reason for global warming and hence, climate change (IPCC 2014). Thereby, the actions which are taken by nations and guaranteed via global agreements intend to prevent greenhouse gas emissions, by minimizing energy consumption, replacing fossil fuels with renewable sources, and providing sustainable growth in general (Fawzy et al. 2020).

Most industries are responsible to limit their carbon emissions as carbon dioxide accounts for the vast majority of greenhouse gases in the atmosphere. Buildings and the construction industry cause 40% of global CO<sub>2</sub> emissions. Any enhancement in the construction industry regarding energy consumption and greenhouse gas emissions will be more effective among others. As a result, sustainability and energy efficiency of buildings have inevitably been the focus of the construction industry lately (United Nations Environment Programme [UNEP] 2021).

Embodied energy and embodied carbon of materials are key concepts in the comprehension of energy studies. The sum of energy that is used in the production, transportation, and implementation of building materials is called embodied energy of building materials (Hu 2020; (International Energy Agency [IEA] 2016). Likewise, the embodied carbon of a building material accounts for the total carbon, which is emitted during its lifecycle, starting from the raw material supply until its application. A

considerable part of consumed energy and emit carbon in the construction industry is directly related to the production of building materials. To provide sustainable production and energy efficiency in the sector, embodied energy and carbon of building materials need to be decreased. The most effective ways to decrease energy used in the production process are using renewable sources, finding energy-efficient production methods, and preferring alternative materials which need low energy to be manufactured. From an architectural perspective, it is helpful to select sustainable materials with low embodied energy and carbon in the design process (Glass, Dainty, and Gibb 2008). Although architectural history in the last century has been shaped by the structural possibilities provided by cement, it is an undeniable fact that it is time to switch to more environmentally friendly material alternatives (Hammond and Jones 2008).

Sustainable materials are made from renewable resources using slightly low energy and can be reused or recycled. If the definition of sustainability is considered, sustainable materials need to be produced allowing future generations access to natural sources at the same level without harming the environment, which has low-embodied energy and low carbon emissions (Santillo 2007). At this point, bio-based materials have gained attention in packaging, automotive, consumer goods, and others but also in the building industry. Bio-based building materials are obtained from bacterial, agricultural by-products, and animal-based products such as wood, straw, hemp, flax, wool, seaweed, and mycelium (Jones and Brischke 2017; Madurwar, Ralegaonkar, and Mandavgane 2013). Some of these materials have been used in buildings for centuries like earth and hence, are not newly invented materials. However, studies on up-gradation and modernization have emerged in recent years as an act towards climate change. For instance, stabilized earth brick production, rammed earth techniques and 3D printed earth building are new trends in earth construction (Ben-Alon 2020; Perrot, Rangeard, and Courteille 2018; Hamard et al. 2016). However, to be truly sustainable for building materials, those raw materials should be harvested and processed in environmentally friendly methods. Besides, end products should provide high thermal performance by reducing the use of energy in buildings. Accordingly, hemp-based building materials come to the forefront for reaching sustainable building targets (Ahmed et al. 2022)

Hemp-based building materials are produced with fibers or the woody core of the hemp plant. Fibers are used to produce batts and mats which are applied for the roof, floor, and wall insulation. Besides, they are used as fiber additives in wall plasters and concrete mixes to increase tensile strength. The woody core of the hemp, on the other

hand, is called hemp hurds or hemp shive. This part of the plant is chopped into small pieces to create a composite material combined with various binders such as lime, clay, gypsum, and cement. Hemp-lime material is commonly called hempcrete (Bevan and Woolley 2008)

Hempcrete is a combination of hemp hurds, lime, and water. Except for lime production, this composite material does not require any heating process which makes it an energy-efficient and low-carbon material. Raw materials are mixed in convenient proportions and can be used in building components such as walls, roofs, and floors. Hemp plant absorbs carbon dioxide from the atmosphere act as a carbon sink throughout their plant life and grows very fast in 3-4 months. These properties make hempcrete building material a carbon-negative, sustainable, and nature-friendly alternative. However, the energy-intensive process of lime production increases the embodied energy and carbon of the material. As expressed in studies by Busbridge (2009) and Mazhoud et al. (2021), lime can be replaced by clay, keeping the performance of the material similar, but decreasing the embodied energy and carbon of the material sharply. Raw earth consisting of a high amount of clay minerals does not need any burning process to be used as a binder of the material, unlike lime.

Earth is also used as a building material since ancient times in many different forms. Earthen building materials and techniques have been transferred for ages, all over the world (Pacheco-Torgal and Jalali 2012). The number of earthen building stocks used by 20-25% of the world population in developing countries has declined over several decades as modern architectural practices have abandoned earthen building techniques on behalf of concrete and cement (Marsh and Kulshreshtha 2022). In contrast, in highly developed countries, earth construction has been gaining popularity again, not only through means of the reapplication of old techniques but also in the development of new application areas for sustainability. The unlimited availability, energy efficiency, and recycling features of raw earth make it appealing for the research of innovative construction techniques. Earth, as a binder, is used in the production of hemp-clay building material, as well. Hemp-clay is not a widely used name for this material. It is mentioned in a couple of research articles by Fernea et al. (2019), Mazhoud et al. (2017), Brümmer et al. (2017), Busbridge (2009), and Glé et al (2021). There is one company that produces hemp-clay blocks in the mass market of Spain and names their product Cannabric. These blocks have been already used in new housing constructions and retrofit projects (Cannabric n.d.).

The production of hempcrete with raw earth instead of lime increases the energy efficiency of the material, making it more sustainable, natural, and worker-friendly (Busbridge 2009). Since the earth is non-standardized and heterogeneous material, it needs to be studied locally with local hemp material before use in buildings. The proportion of hemp in the mix plays a crucial role in the material properties of the block, such as density, thermal conductivity, thermal capacity, and mechanical strength.

There is no solid evidence that hemp has been used for construction in Anatolia. It can be predicted that fibers of hemp may have been added to adobe mixtures. Hemp has been harvested for seeds and fibers for years in Turkey. As by-products, hemp shives are used only for animal bedding. To farmers in Turkey, growing hemp was onerous and not profitable since 2019. In the last years, the industrial hemp cultivation areas have started to increase rapidly (Başer and Bozoğlu 2020). The only hemp-based market product in the construction industry is hemp insulation batt, while the usage of hemp shives to form a composite building material is barely known (Izoguard n.d.; Biokenevir n.d.). It is necessary to experiment with hemp-clay composite used in the production of building block that is made of local hemp and clay material. Measuring physical properties and thermal performance lead us to make significant conclusions about the future possibilities of this novel building material in the local context.

Today, the building materials industry in Turkey offers a limited variety of wall-infill materials produced as building blocks. The most used wall blocks are hollow clay bricks (HCB), aerated concrete blocks (AAC), and lightweight pumice blocks (LPB) in the last few years. These products require a huge amount of energy to be manufactured and release CO<sub>2</sub> excessively into the atmosphere during production processes (Kara and Kayılı 2021). In seeking sustainable building products to combat climate change, experimental and comparative studies about hemp and earth-based local building material can arouse enterprises on the development of such materials. It is necessary to analyze the potential of hemp clay as a building block material and to compare its thermal properties and energy performance with conventional materials based on experimental and simulation data.

## 1.2. Aim and Objectives

The major aim of the thesis is to assess the thermal and energy performance of hemp-clay building block material in residential blocks through comparisons with the most common wall infill block materials in Turkey regarding the annual energy consumption in the Mediterranean climate. Since such material has not been produced in Turkey before, and there is no specification regarding its properties, it has emerged as a secondary aim to find out the thermal properties of the hemp clay blocks which are produced with local hemp and clay from the Aegean region of Turkey. These two aims of the study were fulfilled by completing the following objectives:

- To experience and document the production of hemp-clay composite material made from the raw materials of the Aegean region.
- To determine the appropriate proportions of mixture components (hemp hurds, clay, water, and lime additive) leading to further research.
- To measure the physical and thermal properties of novel material empirically.
- To simulate the thermal and energy performance of hemp-clay material among the other conventional materials on a building scale.
- To determine the energy performance of hemp clay building blocks in future climate conditions through comparisons.
- To provide a preliminary understanding of hemp-clay material as an energy-efficient and sustainable building block for the future in Turkey.

In line with these aims and objectives, experiments and simulation studies containing different research questions were conducted to feed each other. For the experimental part of the study, the main target is to obtain the hemp-clay building block that gives the best thermal properties. Hemp hurds, clay, water, and lime as an additive were the variables of the experiment. The proportions of these ingredients in the blocks were changed to answer relevant research questions:

- What are the physical properties of local hemp and clay?
- In which proportions should hemp and clay combine to be shaped a block?

- How does a small amount of lime additive change the material's thermal properties?
- How do hemp: binder, hemp: clay, and clay: water ratio affect the material's density and thermal conductivity?
- In the end, in which interval do the densities and thermal conductivities of hemp-clay blocks range?
- How similar are the material properties of the novel hemp-clay building block to the hempcrete building block which is produced by selected companies in the US, UK, and Europe?

For the simulation study, physical and thermal properties belonging to the superior hemp-clay building block sample were used as comparative parameters in the simulation model. As this novel material is proposed as a wall infill material for typical residential buildings, hollow clay brick, aerated autoclaved concrete, and pumice blocks were selected as the most used wall materials to compare through simulations. The comparisons are based on the annual energy consumption of a flat in a typical residential block in 2020, 2050, and 2080's climates. In the formation of this part, the following research questions were considered:

- Do hemp-clay wall blocks increase the thermal transmittance value (U-value) of a wall and decrease the energy consumption of a building?
- Do hemp-clay building materials provide enough energy performance in the western Aegean region of Turkey?
- Do hemp-clay building materials show better thermal performance in comparison with hollow clay brick, aerated autoclaved concrete, and lightweight pumice blocks?
- How does the thermal capacity of the materials affect energy consumption when the walls have the same U-value?
- In which way does climate change affect the energy consumption of a flat in a typical residential block in the western Aegean region of Turkey?
- In future climates, 2050's and 2080's, what is the most energy-efficient wall material among hemp-clay blocks, hempcrete blocks, HCB, AAC, and LPB? Does hemp-clay have the ability to replace other building blocks in the future?

### 1.3. Limitations and Assumptions

During the research, some limitations arose in several sections of the study. Assumptions about documentation and simulations were made to focus on answering research questions. Limitations and assumptions are stated as follows:

- Accessibility of the case building selected for the study was limited due to Pandemic restrictions between March 2020 and June 2021. To be able to monitor the building for the whole year, the most accessible residential block was selected.
- The case flat was occupied during the monitoring process and the occupancy pattern of the rooms could not be collected properly. An overall occupancy pattern was created to insert into the simulation model.
- Documents regarding the plans, sections, and component details of the case building could not be reached. The flat in the residential building was observed and surveyed to create plans and a 3D simulation model. Materials that were used in the building were assumed as the conventional building materials of the Izmir region. The material properties were adopted from the standard of TS-825 Thermal Insulation Requirements for Buildings (Turkish Standards Institution 2008)
- Hempcrete building block material was inserted as the fifth material in simulations as it is the reference block material in experiments regarding the density and thermal conductivity properties. Material properties of hempcrete block material were adopted from the specification sheet released by the IsoHemp company (Isohemp 2022).
- In the determination of simulation scenarios, hemp-clay building blocks, hempcrete, HCB, AAC, and LPB were assumed as wall infill materials for both exterior and interior walls of the case building, keeping the concrete structure as existing and not changing the thickness of the existing walls.
- In scenarios, cement plasters for conventional wall blocks (HCB, AAC, and LPB) and hemp-lime plaster for hempcrete and hemp-clay building blocks were selected as hemp-based materials require vapor permeable renders due to their nature.

## 1.4. Outline of Thesis

This thesis comprises six chapters. In the first chapter, the research problem in general and specific to the topic was explained. The significance of decarbonization in the construction industry on building a sustainable future was introduced in the context of embodied energy and the carbon emission rate of building materials. It is expressed why hemp-clay as a building block material needs to be investigated which has the potential to be a material of the future as its low-carbon and energy-efficient features when compared with conventional building block materials. After the problem statement, the general aim of the thesis was clarified in Section 1.2. Followingly, research objectives were proposed, and research questions were listed regarding both the experimental part and simulation parts of the study. Limitations regarding the scope of the study and assumptions related to the study methods were also declared in this chapter.

In the following chapter, the literature review presents the background of the study. It includes recent studies and innovations on hemp-based building materials following the brief history of the hemp plant and hemp-based building materials. Studies on characterization and performance assessment of hempcrete and hemp-clay conducted in Europe are presented interrelatedly.

In the third chapter, the materials and methods which were used in the study are clarified in detail. It prefaces information about case building, monitoring process, and creation of simulation models in DesignBuilder software. Parameters considered for the determination of simulation scenarios are stated and followingly, simulation scenarios are listed to compare hemp-clay building blocks with hempcrete, HCB, AAC, and LPB in today's and future climates. Under the experimental study sub-section, characterization and testing methods of raw materials are explained to show grain size distribution and chemical composition, which is followed by mixing methods of hemp-clay building block samples. The thermal conductivity test method of hemp-clay building block samples is also presented in this chapter.

Results of monitoring, calibration, grain size distribution, and chemical composition tests of raw materials are presented in the fourth chapter. Moreover, the density and thermal conductivity results of produced hemp-clay building block samples are documented discussing the effect of mixing parameters. Finally, results of simulation scenarios that have different wall infill materials in climate conditions of 2020, 2050, and

2080 are demonstrated in comparison. The change ratio in percentage on heating, cooling, and annual energy consumptions are presented when the exterior and interior wall materials in scenarios are changed with hemp-clay building block, hempcrete building block, AAC, and LPB, as the base model has exterior and interior walls which are made of HCB.

The fifth chapter encapsulates the concluding remarks of this study by relating them to the research questions presented in Chapter 1. It is finalized with possible further studies about hemp-based building materials' characterization and energy performance.

## CHAPTER 2

### LITERATURE REVIEW

#### 2.1. Hemp and hemp-based building materials

In this thesis, 'hemp' refers to industrial hemp which is a cultivar of the *Cannabis Sativa* family. Industrial hemp has a tetrahydrocannabinol (THC) value of lower than 0.3%, unlike marijuana which is used for the psychoactive effects of THC (Johnson 2014). General information about the hemp plant, hemp usage in history, and at present, hemp usage in the construction and building examples built with hemp are presented in the following sub-sections.

##### 2.1.1. Hemp and its areas of use

Hemp is one of the oldest cultivated plants, dating back to China's Neolithic Age (around 8500 years ago) (Li 1974). It is an annual plant that has a thin stem with a diameter of 0.6-1.9 cm, varying between 120 and 450 cm in height. Its anatomy consists of leaves, seeds, roots, and stalks (Figure 2.1). The stalk contains fibers and hurds of hemp (Oran Kalkınma Ajansı 2019). Each part of the plant has a variety of usage areas such as textile, paper, medicine, bio-fuel, cosmetics, automotive, and building material (Karche and Singh 2019).

It is predicted that the preliminary purpose of harvesting hemp is to make fabric and ropes from fibers concerning cloth pieces found in an archaeological pot in China (Li 1974). Latter, hemp flowers and seeds were used in folk medicine. As the hemp plant can adapt to climatic conditions easily and does not require much effort to grow, it has spread from Central Asia to India, Egypt, and Europe, respectively. Hemp seeds reached Europe around 2000 BC (Zuardi et al. 2006). Throughout history, hemp fiber was grown mostly for its strong fibers to make ropes and clothes for sailing due to its high durability. Hemp seeds were used for some basic needs such as making lamp oil and food.

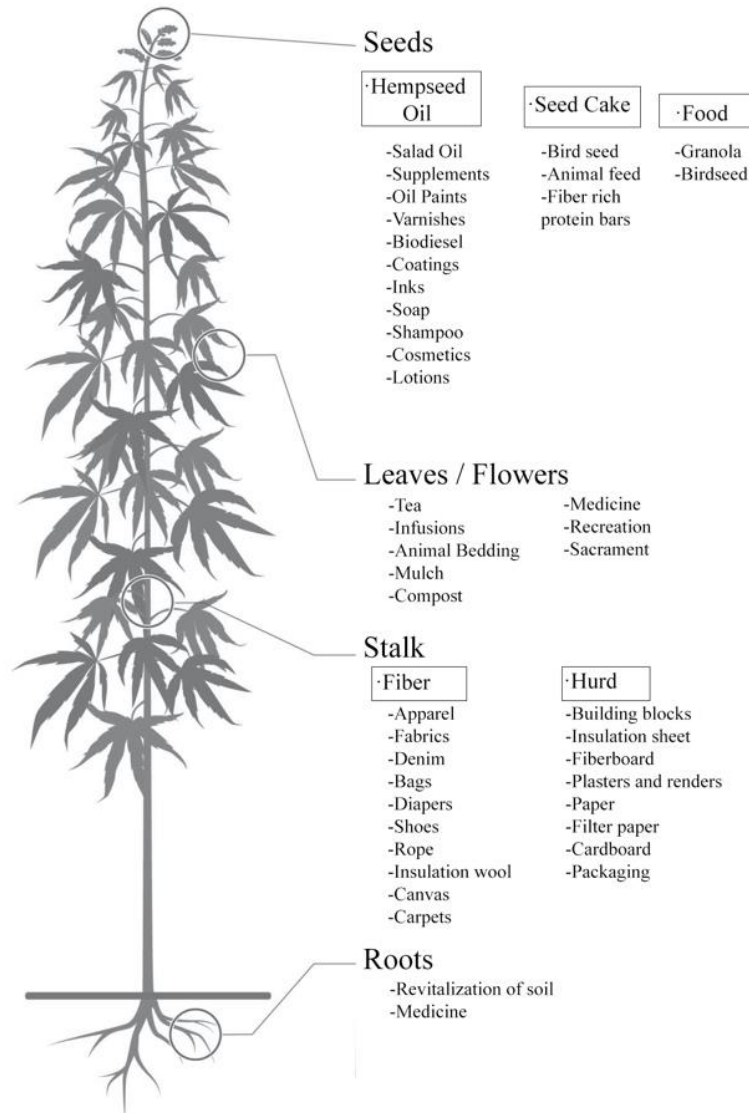


Figure 2.1. Parts of the hemp plant and areas of usage  
(Source: Onay (2020), Hemp New Zealand, n.d.)

Although hemp was the most cultivated agro product worldwide in the 1900s, its production declined sharply owing to the rapid development of the cotton industry. Synthetic fibers from petroleum started replacing hemp fibers in textile and other industries after World War I (Onay 2020; Aydođan et al. 2020). Moreover, the fact that all types of hemp cultivation were banned by the U.S. Government with the Marihuana Tax Act of 1937 gave rise to the prohibition and disesteem of industrial hemp in other countries in Europe (Kaya and Oner 2020) . Since the 2000s, the largest part of hemp production was made in Asia. After that time, hemp gained its popularity again in Europe

in the seek for sustainable material solutions against climate change. It is recorded that in 2018, Europe produced 75.4% of hemp in the world (Özdamar 2021).

Today, it is accepted that hemp is used in the production of more than 50.000 products (Cherney and Small 2016). Hemp seeds are used to produce edible oil, biodiesel, and personal hygiene products while fibers are used to produce textile products, insulation batts, interior plastics, and door panels of cars. Hemp hurds, as by-products of the fiber harvesting process, is used in the papermaking and also building material industry to produce fiberboards, building blocks, and cast-in-place walls (Johnson 2014; Özdamar 2021; Onay 2020). The commercial usage areas of each part of the hemp can also be seen in Figure 2.1. The usage of hemp fibers and hemp hurds in buildings will be explained in the following section.

### **2.1.2. Hemp Use in Construction:**

Evidence for the earliest use of hemp in construction was found in the clay plaster composition at Ellora Cave in India. It is indicated that hemp additive in the clay plaster increased durability despite severe climatic conditions, preserving the plaster layer for 1500 years (Singh, Mamania, and Shinde 2018). According to many online sources, Sarthe Bridge in France is documented as the oldest construction in which hemp fibers were used in the making of mortar, dating back to the 6<sup>th</sup> century (Gołębiewski 2018). Hemp fibers were found as an additive material in mortars and plasters of historic buildings as they improved tensile strength and vapor permeability. In Japan, a traditional house from 1698 was made from hemp stalks which formed the interior walls and the roof (Özdamar 2021). All this evidence from historic building state that hemp has been used as a building material for centuries. However, the first use of hemp as a modern building material was for the renovation of “La Maison d’ Turque” in Nugent-sur-Seine, France in 1986. Charles Rasetti, known as the innovator of hempcrete, used the hemp-lime mix to repair walls of the wooden frame building. Accordingly, hemp fibers and hemp hurds have been used increasingly in building construction, especially in France and the UK (Allin 2005).

Today, hemp fibers derived from the waste of hemp seed harvesting are used to produce hemp wool insulation batts. This agricultural by-product has a thermal

conductivity value of 0.040 W/mK and a density of 35 kg/m<sup>3</sup>. Besides its high thermal performance and sustainability features, it stands out as a healthy building material, as it does not contain volatile organic compounds (VOCs) which harm human health (Hempitecture n.d.). Hemp wool insulation batts can be applied inside and outside of walls, between the roof rafters, laying on the floor, and under the roof tiles, which provides a thermal capacity of 1600 J/kgK. (Izoguard n.d.; ECI n.d.) . In addition, hemp fibers are used to enhance the tensile strength and thermal performance of plasters (Isohemp 2022; Hempire n.d.). Hemp-lime interior plasters show high water vapor permeability and thermal performance. Their moisture buffer value is twice higher than the value of gypsum plaster. Their thermal conductivity value is 0.2 W/mK, which is lower than the gypsum (0.48-0.8 W/mK) (Brahim Mazhoud et al. 2016).

Hemp hurds which is the woody core of hemp stalk constitutes the aggregate of composite building materials. These chopped aggregates are mixed with different binders, especially lime, clay, and gypsum, to produce monolithic walls, insulation boards, building blocks, and framed wall panels. With a suitable type and amount of binder, hemp-based building composites are qualified as breathable, non-toxic, sustainable building materials with low embodied energy and high thermal performance. Lime is the most widely used binder with hemp hurds, and this composite is called hemp-lime or hempcrete, referencing the concrete (Magwood 2016; Bevan and Woolley 2008).

In general, the hemp-lime building material cannot be used as a load-bearing element due to its poor mechanical properties, yet rather preferred for thermal envelope applications and thus, requires a structural frame that carries loads of the building. However, there are three techniques in basics to apply hemp-lime composite material in buildings (Figure 2.2). The most common method of hemp-lime is to cast a hemp-lime mixture in between a formwork, shaping the walls of the building. A wet mix of hemp hurds, lime, and water is cast in the formwork and tapped either by hand or by compression tools in vertical layers of 200-300 mm, and then, shuttering is taken off after 24 hours (Bevan and Woolley 2008; Stanwix and Sparrow 2014). The second method is to spray wet hemp-lime material on the wall frames or between the rafters. For spraying, special equipment is needed and the mixture composition can be different from the tapped hemp-lime mixture for allowance of fluidity and stickiness (Degrave-Lemeurs, Glé, and Hellouin de Menibus 2018). Besides these two cast-in-situ methods, hemp-lime material can be precast to produce building blocks and wall frames (Hemp Block USA n.d.; Hemp Block Australia n.d.).



Figure 2.2. Hemp-lime building techniques: shuttering (a), spraying (b), and block masonry (c) (Source: Lane 2022).

Building with hemp-lime blocks or hempcrete can be defined as a revolutionary system innovated in the last years. Raw materials of hemp and lime were mixed and shaped in moulds to manufacture blocks in the factory to be carried to the worksite after drying for four weeks in general. Hempcrete blocks can be produced in different densities ranging between 300 and 600 kg/m<sup>3</sup>, sizes, and shapes in the factory according to the needs (Isohemp 2022). Precast building blocks are used to infill structural wall frames in

general as non-load-bearing wall materials. They are wet and tied up with a thin lime mortar to build walls (Stanwix and Sparrow 2014). In addition to hemp-lime building blocks, there are new developments in the hemp block sector. Cannabric brick company which is based in Spain produces load-bearing and non-load-bearing hemp-clay building blocks (Cannabric n.d.). Just Biofiber Canada and Hemp Block USA companies produce interlocking hempcrete blocks which can be used as load-bearing wall elements as well (Hemp Block USA n.d.; JustBioFiber n.d.). Moreover, hempcrete wall panels are produced in the factory area to fasten the building component production process on the construction site providing thermal advantages (American Lime Technology n.d.) .

In conclusion, regarding the components of the composite material and techniques, building with hemp is a low-carbon and sustainable construction method which requires low energy for raw material extraction, production, and application (Özdamar 2021).

## **2.2. Hemp in Turkey**

Hemp is called ‘kenevir’, ‘kendir’ and ‘kınnap’ in Turkish. As the oldest domestically grown plant, it was used in Anatolia for more than 7000 years. As mentioned by Özdamar (2021), archaeological studies demonstrated evidence of hemp use in the Çatalhöyük settlement by finding a piece of hemp-woven fabric found in a pot. It is predicted that since that time, hemp was one of the most grown and used plants in Anatolia, as its fibers were used to produce many kinds of textile products such as ropes, cloths, sacks, and rugs (Aytaç, Ayan, and Arslanoğlu 2017). The fiber-rich hemp plant was an essential raw material for the naval forces of the Ottoman empire. Most of the hemp harvesting was made in the Black Sea and Aegean region (Aydoğan et al. 2020). Besides the use of hemp for its fibers, it is known that hemp seeds and flowers are used for food and medical purposes as well (Özdamar 2021).

Turkey was in 10<sup>th</sup> place worldwide in hemp production at the beginning of the foundation with 10.000 hectares of land. Hemp cultivation areas started to decrease rapidly starting from the 1930s due to global restrictions, world wars, and the introduction of cotton in Anatolia (Akpınar and Nizamoğlu 2019). To revitalize hemp production, the first hemp factory was founded in Kastamonu in 1946. However, due to its economic

loss, it was closed in 1951. Another factory founded in 1949 in Taşköprü produced sacks and paper using hemp which was harvested in the region for 4 years and then, replaced the hemp with cheaper imported materials. Seka paper company used the harvested hemp in the country to make paper products until 2004. Due to the import of cheaper raw materials, hemp use and hence its cultivation has decreased gradually (Oran Kalkınma Ajansı 2019). It is stated that the cultivated area of hemp is 6 hectares in Turkey in 2014 (Özdamar 2021).

The regulation published in 2016 gave allowance to 19 provinces in Turkey to grow hemp plants, in the name of Hemp Cultivation and Control of Regulations. Several incentives and hemp research institutes in Samsun and Yozgat provinces have provided an increase in hemp production. The last numbers indicate that Turkey's hemp cultivation areas for fibers and seeds extended to 435 hectares in 2020. However, harvesting land hemp which was done for fibers accounts for only 10 hectares in total (Ordu Ticaret Borsası 2021). This is mostly due to the absence of the industry which requests hemp fiber or hemp hurds in Turkey and systematized fiber decortication machines (Başer and Bozoğlu 2020).

### **2.3. Studies on Hemp-Based Building Materials**

As mentioned in Section 2.1.2, it is known that the first modern use of hemp in buildings was around 40 years ago for the renovation of a timber house in France. Since that date, the hemp-binder composite material was improved mostly by craftsmen on site and then became the topic of scientific investigations. According to Hirst (2013), scientific studies started by Garcia-Jaldon (1992), Courgey (1993), and Van der Werf (1994) in the early 1990s regarding the characterization and building applications of novel material. As studies between 1990 and 2002 are published in French (Cordier 1999; L. Arnaud and Cerezo 2002), these were not included in the literature survey of the thesis. Starting from 2003, studies on mechanical, thermal, and acoustic properties of the hemp-lime composite, characterization of hemp-binder composite, and investigations on hemp-clay building material have been done in many countries from France and UK to New Zealand and Israel. These are examined and presented under the following sub-sections in detail.

### **2.3.1. Thermal Properties of Hemp-Based Building Materials**

Evrard and Herde (2005) presented the hygrothermal properties of lime and hemp concrete according to the measurements which were made at Fraunhofer-Institut for Building Physics in Holzkirchen, Germany. Measurements were done on wall mixture samples that were produced 3 years ago. The moisture sorption behavior of lime hemp concrete with a density value of  $480 \text{ kg/m}^3$ , was analyzed by changing the relative humidity of the experimental chamber. It is concluded that hemp material shows similar sorption behavior to wood products. The thermal storage capacity and thermal conductivity of this novel material were measured as  $1550 \text{ J/kgK}$  and  $0,11 \text{ W/mK}$ , respectively. Transient conditions were simulated with WUFI 4.0 Software to point out its specific behavior. Building envelopes with lime hemp material created in the simulation model were exposed to thermal shock, cycles of thermal changes, and hygric shock. In this early work, Evrard (2005) concluded that the transient thermal performance of hemp-based wall material was superior to permanent performance calculations and need to be studied further.

The transient performance of the material is also highlighted in the Final Report on the Construction of the Hemp Houses at Haverhill, Suffolk in the UK (Yates 2002). Building Research Establishment (BRE) monitored two hemp houses and two brick houses starting from their construction until their occupation to find relative qualities, environmental impacts, and construction costs as well. As one of the findings of this comprehensive work, the thermal conductivity value of lime hemp walls was measured as  $0.08 \text{ W/mK}$ . The most important finding of the report was the fact that hemp houses showed better thermal comfort in real climate conditions than the predicted performances as the thermal capacity and hygroscopic properties of the hemp material provide 1 to 2 degrees higher air temperature with the same heat flux. Later, the region of  $0.08$  and  $0.09 \text{ W/mK}$  was accepted as a reference value for the thermal conductivity of lime hemp material by many authorities (Bevan and Woolley 2008) . Moreover, after the examination of hygroscopic properties, many studies claimed that simulations at the whole building level taking into account hygrothermal phenomena have a significant effect on thermal performance predictions of such materials (Tran Le et al. 2010; Collet et al. 2013; Ahlberg, Georges, and Norlén 2014).

Evrard (2006) investigated the effect of building practice parameters such as mixing method, water input, and implementation on hygrothermal properties of hemp lime wall material. In this work, the mean dry thermal conductivity of the material at 10 °C was found 0,115 W/mK. It is concluded that the water content and thermal conductivity of the material do not have a linear relationship and need to be studied.

In another work on lime and hemp concrete blocks (Elfordy et al. 2008) , the influence of the projection process on density, thermal conductivity, and mechanical properties was investigated. It is confirmed that the thermal conductivity of the material increases when the density of the material increases. In this research, measured thermal conductivity values range between 0.179 and 0.485 W/mK while density values change between 417 and 551 kg/m<sup>3</sup> ,. It is also concluded that when the material is projected at a distance of 1 meter into the mould, density, compressive strength, and thermal conductivity values are obtained as the highest. The influence of the application method of lime and hemp concrete was studied by Collet and Pretot (2014). For this study, hemp concrete samples were produced by spraying method for walls, floor, and roof, and moulding method for walls in different hemp:binder ratios. The density of sprayed hemp concrete for walls was found between 374 and 416 kg/m<sup>3</sup>, while thermal conductivity ranges from 0.116 and 0.125 W/mK in linear with the density. The thermal conductivity value of moulded hemp concrete walls was measured at 11% higher than the sprayed.

Another parameter that affects the thermal conductivity value of lime hemp composite is the amount of hemp hurds in the mixture of composite. Benfratello et al. (2013) investigated the effect of the size and amount of hemp shives, or hurds, on thermal conductivity values and structural properties. It is found that as expected, the increase in the amount of hemp shives results in the decrease of thermal conductivity of the material while the granulometry of hemp shives does have a very low influence on the thermal properties. Thermal conductivity values of the hemp lime sample whose densities ranged between 377 and 603 kg/m<sup>3</sup>, changed between 0.0899 and 0.1406 W/mK in this work (Benfratello et al. 2013).

Studies on hemp concrete with different binders than lime, especially unfired clay, were done as well. Wilkinson (2009) experimented with a lime-clay mixture as the binder of hemp composite while Busbridge (2010) produced a couple of hemp-clay samples with lime additives (Wilkinson 2009; Busbridge 2009). For these studies, the aim is to reduce embodied energy and carbon of the hemp composite as the lime production process requires a huge amount of energy and emits greenhouse gases into the atmosphere. As a

comparison, embodied carbon amount of unfired clay and lime is 0.005 and 0.8 kg/CO<sub>2</sub>kg, respectively (Hammond and Jones 2008). In the study of Busbridge (2010), several hemp-clay samples with different hemp: binder ratios were produced in laboratory conditions. The production and drying conditions of these samples were documented. Material properties such as density, thermal conductivity, water content, and strength were measured as well. As a result, the thermal conductivity of hemp-clay material with a density of 318 kg/m<sup>3</sup> was found as 0.1 W/mK which is slightly higher than the hemp-lime material. The author concluded that the clay binder outperforms the lime binder by comparing the material properties and environmental benefits of both materials (Busbridge and Rhydwen 2010).

Hemp-based building materials with clay binder were studied later in the works of Balčiūnas et al. (2013), Vincelas et al. (2017), and (Brümmer, Sáez-Pérez, and Suárez 2018). Vincelas et al. (2017) found the thermal conductivity of hemp-clay samples between 0.08 W/mK and 0.12 W/mK. which is in a similar range with hemp-lime properties in the literature. In parallel with the studies on the mechanical properties of hemp-clay material, experiments with stabilized clay as a binder were conducted to enhance both the thermal and structural properties of such material (Brahim Mazhoud et al. 2021). In this study, hemp material with clay and stabilized clay (with the additive of 5% lime and 5% cement) were compared regarding density, thermal conductivity, and moisture buffer values. It is concluded that clay stabilization increased the thermal conductivity and density values of the hemp material slightly. However, this study is significant to find an agreement between high mechanical strength and low thermal conductivity for hemp-clay building material (Mazhoud et al. 2021).

Lastly, the thermal performance of hemp-clay material based on an experimental study was investigated in the scientific literature. In the study of Haik et al. (2019), test cells made with hemp-clay material, hemp-lime material, and conventional building materials were produced to monitor during winter and summer seasons. According to recorded outdoor air temperatures and indoor air temperatures of test cells, binder type, clay, or lime, did not influence the thermal performance of hemp-based building material. In comparison to other conventional materials such as AAC, HCB, and EPS, cells made with hemp-clay material showed better performance in summer conditions while in winter conditions, AAC cells were slightly better than hemp-clay material. It is deduced that regarding the environmental impacts of conventional materials, hemp-clay material

has clear advantages to reduce energy consumption and carbon emissions providing very similar thermal performance for buildings (Haik, Peled, and Meir 2020).

### **2.3.2. Mechanical Properties of Hemp-Based Building Materials**

The mechanical properties of hemp-lime building materials have been studied in scientific literature since 2000 (Cerezo 2005; L. Arnaud and Cerezo 2002). As mentioned in the previous section, since hemp hurds has a highly porous structure (70-80%) and low density, a combination of hemp hurds and lime binder constitutes a very light material with low thermal conductivity and good insulation properties. However, the compressive strength of such material needs to be analyzed as well to be used as a building material in different building components such as walls, roofs, and floors. Several parameters that would influence the compressive strength of hemp-lime composite material were investigated to help the proper mix design of the material. These parameters are hemp/binder ratio, binder type, compaction hardness, and hemp hurds characteristics.

According to the studies, the mechanical performance of hemp-lime building materials can vary because of their nature. For the study of Evrard (2003), four different lime-hemp concrete mixtures were produced and the compressive strength values of 0.2 – 0.5 MPa were recorded. Evrard (2006) found higher compressive strength values for such material that range from 0.4 to 1.2 MPa, highlighting that the values depend on the composition of mixtures. Other studies show a similar range (0.2 MPa to 1.2 MPa) for the compressive strength value of hemp-lime building material which has a 1:2 hemp/binder ratio in weight (Jami, Karade, and Singh 2019; de Bruijn 2008; Murphy, Pavia, and Walker 2010; E. Hirst et al. 2010). It is expressed that this range of values is not sufficient to be used as load-bearing material, since it is around 1/20 that of concrete (Sutton, Black, and Walker 2011) Therefore, hemp-lime building material requires a load-bearing wooden or concrete framework. As Cerezo (2005) states, apart from this requirement of a framework and lime rendering, any additional thermal insulation, sound insulation, or moisture protection layer becomes redundant to compose a well-functioning wall with hemp-lime building material.

A relationship between binder content, density, compressive strength, and compactness was drawn in many studies (Elfordy et al. 2008; Nguyen et al. 2009; Tronet

et al. 2016). In these studies, it is concluded that the higher binder ratio in the hemp-lime mixture results in higher density and compressive strength. Higher density also can be linked to the compactness of the material. Nguyen et al. (2009) investigated the influence of compactness by producing 7 different samples with manual tamping and compacting device. It is stated that compacting material and aging of the material enhance the compression resistance. High-compacted hemp-lime material showed 2 times better mechanical properties in the study. Moreover, it is mentioned that such material has great deformation capacity when it is heavily compacted, and hence, this provides suitability for use as a building material in high seismic zones (Nguyen et al., 2009). As another parameter, the influence of hemp hurds characteristics was studied by Arnaud and Gourlay (2012). They proved that using finer hemp hurds in the mixture increases the compressive strength of hemp-lime building material in the long-term creating more bonding and fewer pores between hemp hurds.

One of the first studies on the mechanical properties of hemp-clay was conducted by Mazhoud et al. (2017) The authors observed that replacing lime with clay increased the compressive strength of the material slightly. It is found that the compressive strength of hemp-clay samples ranges from 0.39 to 0.48 MPa. They also investigated the influence of clay stabilization with lime-based binder and portland cement. As a result, the stabilization process of clay with less than 10% of additives improved the mechanical performance of the hemp-clay building material (Mazhoud 2017). This is also proved in the study of Brümmer et al. (2018). The research demonstrated that a higher amount of lime additive results in lower compressive strength values and it is necessary to formulate the mixture according to the type of hemp hurds with the proper amount of clay and lime to have an optimum performance of such material (Brümmer et al. 2018). Finally, the potential of hemp-clay composition without any stabilization was investigated by Fernea et al. (2019) According to the results of this study, the compressive strength of hemp-clay composite that has a ratio of 1:3 hemp/binder was found around 1 MPa at the end of 90 day drying period (Fernea et al. 2019).

The mechanical properties of hemp-clay building material and the influencing parameters have not been studied extensively yet in the literature. As hemp's heterogenous nature and variety of hemp types, the composite mixture may require specific formulations and result in different properties.

### 2.3.3. Acoustical Properties of Hemp-Based Materials

Besides the thermal and mechanical properties, the acoustical properties of hemp-based building materials were investigated in a relatively limited number of studies. The sound absorption coefficient is the most effective parameter to assess the acoustical performance of building materials. It is measured in the range 0-1. 0 means that the material reflects all the sound energy while 1 means that the sound is absorbed or transmitted. This value changes from 0.04 to 0.008 for smooth-rendered wall surfaces (Mommertz 2008).

Materials having a porous structure show a higher sound absorption coefficient since the pores provide the dissipation of the sound energy by converting it to heat. Hemp-lime building materials have macropores (between the particles of hemp hurds), mesopores (between hemp hurds and the binder), and micropores (between the binder particles) showing a high porosity in the range of 60-90% (Delannoy et al. 2017). In the low frequency, the sound absorption coefficient of hemp-lime composite ranges between 0.2 and 0.5 depending on the type of binder, compactness, density, and water content (Glé, Gourdon, and Arnaud 2011). However, the hemp-lime wall is usually rendered with a lime-based render that allows moisture transfer through the hemp-lime wall and provides durability. This rendered surface of the hemp-lime wall closes the pores on the surface affecting the sound absorption capacity negatively (Grimes et al. 2013). The influence of the render on the sound absorption property of hemp-lime construction was investigated by Kinnane et al. (2016). It is reported that 10 mm hemp-lime render reduces the sound absorption coefficient of the wall from 0.42 to 0.28. As a result, it is claimed that hemp-lime walls with good acoustical properties reduce the need for additional acoustical treatment (Kinnane et al. 2016).

Later, Lemeurs et al. (2018) carried out an experimental and modeling study that investigate the acoustical performance of hemp-clay and hemp-lime. The research demonstrated that the hemp amount is more effective on the sound absorption coefficient than the binder fluidity and clay type and secondly, hemp-clay and hemp-lime has similar acoustical properties. According to the results of the modeling study, the hemp-clay sample with a density of around  $400 \text{ kg/m}^3$  has a sound absorption coefficient of 0.7 at 500 Hz frequency (Degrave-Lemeurs, Glé, and Hellouin de Menibus 2018). In one of the recent studies, Gle et al. (2021) studied the sound reduction of hemp-clay material at a

wall scale using the intensimetry method. The researchers created two adjacent rooms (an emission room and a reception room) and set up measurement devices between them. Hemp-clay samples of different thicknesses and with different coatings were placed into the adjacent wall to calculate the weighted sound reduction index. It is demonstrated that the sound reduction index increases with the thickness of the hemp-lime wall and the addition of coatings on both surfaces. The weighted sound reduction index for the 10 cm hemp-clay wall with 2 cm clay coatings on both surfaces was found 48 dB. This value is higher than the sound reduction index of a brick wall which is around 40 dB (Philippe Glé et al. 2021).

## CHAPTER 3

### MATERIALS AND METHODS

Comparative energy performance assessment of natural building materials requires a systematic approach. For this study, the performance assessment of novel hemp-clay building blocks was carried out through building energy simulations. Before the modeling and energy simulations of the case building on DesignBuilder Software, data about the existing building and the parameters of the novel material and existing materials which need to be entered into the simulation model were collected.

The methodology of this thesis is explained in three major parts. The first two parts were conducted simultaneously, and the final part is a conjugation of two parts to make conclusions. The structure of the methodology was visualized in a flowchart (Figure 3.1). As seen in Figure 3.1, the first part consists of all steps regarding the simulation study and the other is about the experimental study of the hemp-clay building block. The simulation study includes the data collection about the case building, monitoring of the local climate data, modeling of the building in DesignBuilder Software, the calibration of the simulation model according to the monitored climate data, and the generation of future climate data via Meteororm Version 7 tool (Meteotest 2021). This part of the methodology was explained in Section 3.1. in detail.

Furthermore, the experimental study of the thesis consists of the selection of raw materials which are required to produce hemp-clay test samples, characterization of the materials through sieve analysis and X-ray screening, production of hemp-clay test samples, and the thermal conductivity tests of the dried samples. All these steps were presented in Section 3.2. respectively.

As the final step of the study, all the data collected was used to constitute simulation scenarios and to perform energy simulations. The creation of the simulation scenarios is clarified in Section 3.3.

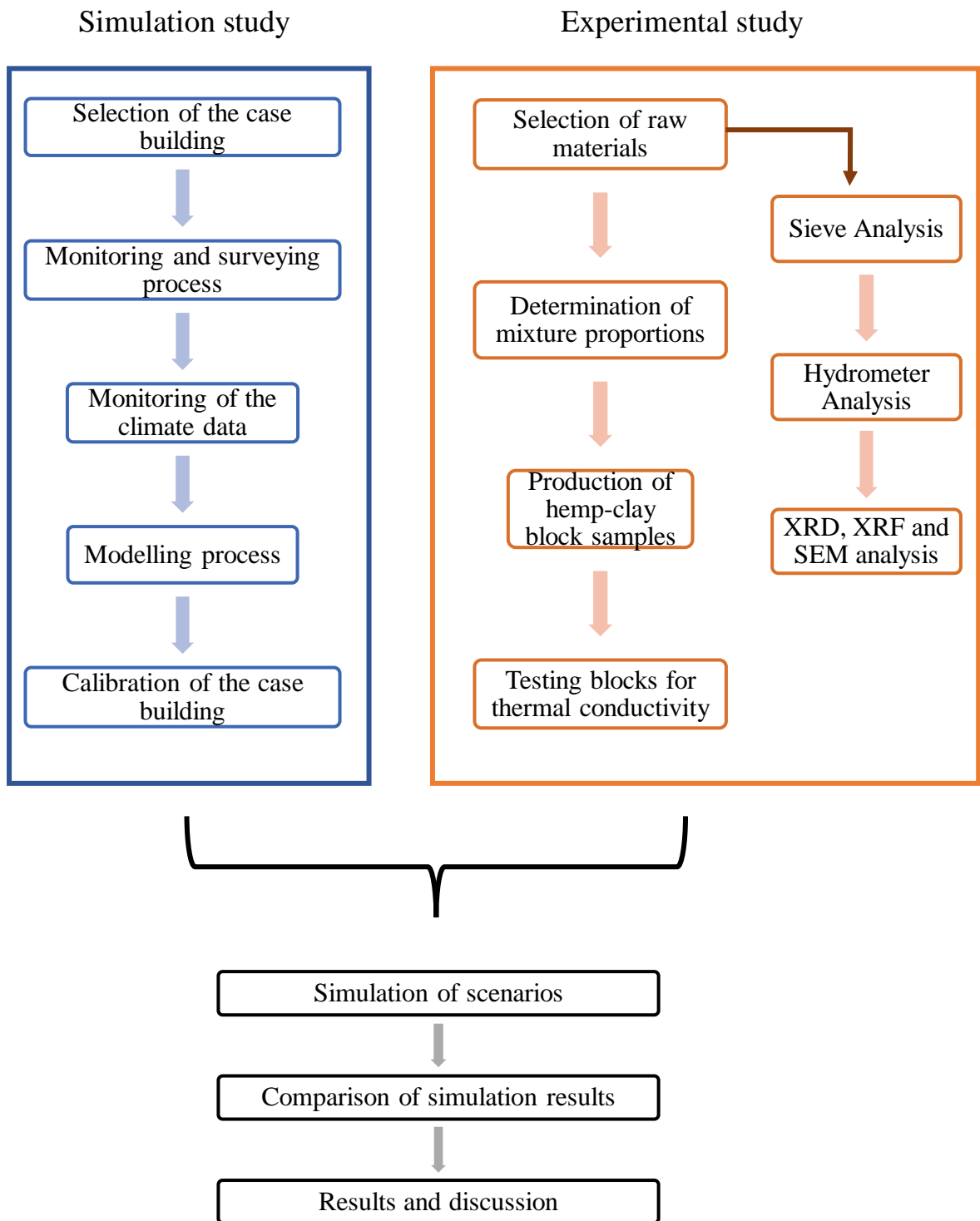


Figure 3.1. Flowchart of the research methodology

The material properties of the novel hemp-clay material and the future climate data file generated were entered as parameters into the calibrated building energy simulation model. 24 different scenarios were simulated, and the results of energy consumption of each scenario were analyzed to assess the thermal performance of the hemp-clay as a building block material comparing with other building materials in the climate conditions of 2020, 2050 and 2080.

### **3.1. Simulation Study**

Under this section of the thesis, materials and methods that were used to carry out the simulation study were explained in detail. These are the selection of the case building, general information about the case building, description of the building components, process of monitoring climate data, modeling of the case building, and the calibration of the simulation model, respectively.

#### **3.1.1. Selection of the Case Building**

For the selection of the case building, three criteria were considered in line with the purpose of the research. The main criterion was the selection of a mainstream, low-rise residential building. A typical housing block as the most constructed building type in Turkey was chosen, considering that using novel hemp-clay material in residential buildings would influence the energy consumption of the construction industry in a more apparent way. The second criterion was the geographical location. Knowing the vulnerability of the Mediterranean region in the face of climate change crises, such as extreme temperature rise and drought, Izmir province located in the Western Aegean region of Turkey was selected. Lastly, due to the restrictions between March 2020 and June 2021 owing to the COVID-19 pandemic, accessibility of the case building for the survey and monitoring was regarded while selecting the case building.

### 3.1.2. General Information and Description of the Case Building

The case building is located in the province of İzmir which is on the coast of the Aegean Sea in the western region of Turkey (Figure 3.2). The case location is under the influence of the Mediterranean climate. The neighborhood of the case building is 10 km far from Urla center and 30 km far from İzmir city center. It is separated from the coastline by an arterial road, consisting of a few general stores, detached houses, and low-rise housing blocks. The case building is quite close to the crossroads and the shore. Its absolute location is 38.36°N and 26.83°E in terms of latitude and longitude. The building is constructed on a ground whose altitude is three meters.



Figure 3.2. Location of İzmir province in a broad context  
(Source: Google Earth, 2022)

The case building is one of three similar housing blocks constructed in 2002 on the same lot. It locates along the northeast-southwest axis facing the southeast. The main façade faces the main street and a series of trees on the street. The location of the building

in-between the neighborhood can be seen in Figure 3.3. While there are shops on the ground floor of the 4-storey building, the upper floors are used only for dwelling purposes. Shops on the ground level have individual entrances from the street. Apartment units share the main entrance from the backyard of the building. The backyard between the housing blocks is also used as a car parking area. An abstracted version of the site plan was drawn based on satellite images taken from Google Earth Pro and on-site observations, which were presented in Figure 3.7 in section 3.1.6.

In total, there are 12 apartment units and 6 commercial units in each one of the housing blocks. Each floor consists of identical 4 apartments that are placed around the vertical circulation area which includes a stairwell and an elevator. The flat roof of the housing block can be reached through this circulation core as well. The identical floor plan of the building can be seen in Figure 3.4 which was drawn in AutoCad 2019 version (AutoCad 2019) after the survey of the block and on-site measurements.



Figure 3.3. Aerial view of the case building on the neighborhood scale  
(Source: Google Earth (2022))

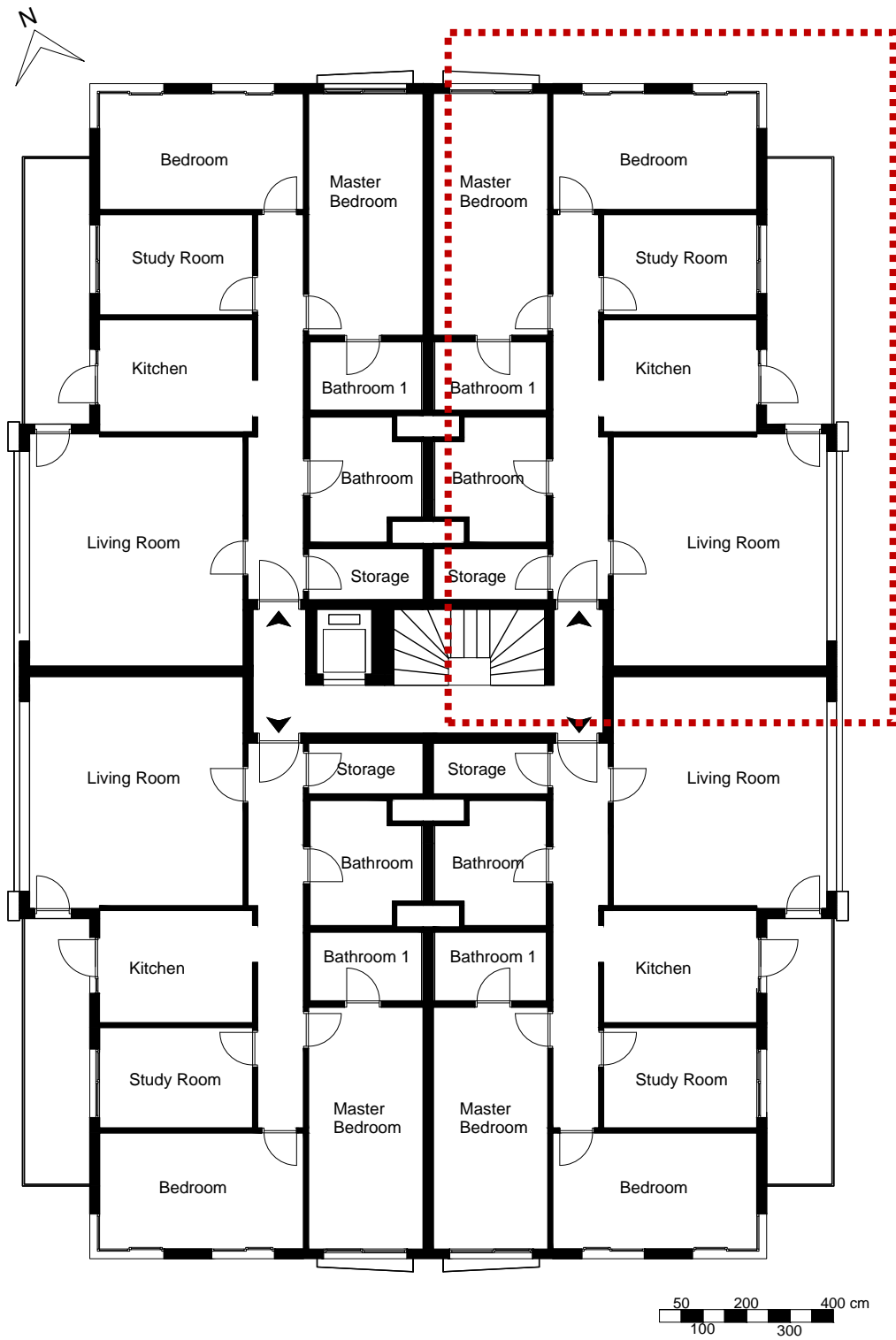


Figure 3.4. Typical floor plan of the case building and the case unit  
 (The case unit was indicated with red dot lines)

### 3.1.3. Building Components and Construction Techniques of the Unit

The case unit which is selected for this study is located on the 2<sup>nd</sup> floor, facing the main street, and to the northeast. The unit consists of three bedrooms (one of these bedrooms is named ‘the study room’ in the following sections), one living room, two bathrooms, one kitchen, and one small storage. Following the entrance, all rooms except the second bathroom are connected by a long corridor. There is a long, narrow balcony that continues along the main façade. The study room, kitchen, and living room have separate doors to the balcony. Technical specifications which belong to the case unit can be seen in Table 3.1.

Table 3.1. Technical specifications of the case unit

<b>FEATURE</b>	<b>VALUE</b>
Floor area (m <sup>2</sup> )	102
Ceiling height (m)	2.62
Surface area of the façades (m <sup>2</sup> )	65.6
Surface area of the adjacent walls (m <sup>2</sup> )	64.7
Glazing area (m <sup>2</sup> )	26.5
Glazing ratio (%)	40.4

#### *Exterior and Interior Walls*

The case building is surveyed by collecting information based on observations, technical measurements, and interviews with users. According to the survey, it is inferred that the construction system of the building is a reinforced concrete frame that is fitted on a raft foundation most probably. Hollow clay bricks of different sizes were used as wall-filling material in the building. Walls were rendered on both sides with cement-based plaster. With these 3 features, it carries the main characteristics of widely used residential blocks in the Western Aegean region.

Furthermore, it is concluded that 19 cm thick hollow clay bricks were used in the exterior walls which have 22.5 cm thickness with its exterior and interior renders. The outer surfaces of the walls were rendered with cement-based rough plaster and house paint without any insulation layer. Only the exterior wall of the living room has a second cladding on it, as this part of the building has curtain walls that are made of aluminum frames and reflective windowpanes.

The finish material of the inner surfaces was gypsum plaster which was applied on a thin and rough cement-based plaster. The inner surfaces of the exterior walls have a thin paint layer. However, paint layers were not regarded in the energy transfer calculations. Besides, internal partition walls between the zones were made of 8.5 cm thick hollow clay bricks. On both the inside and outside of these partitions, rough cement-based and fine gypsum-based plaster were applied respectively, with a total thickness of 1.5 cm. Exceptionally, the interior wall surfaces of bathrooms were finished with ceramic tiles. In this case, the total thickness of the interior walls was measured as 12.5 cm for one side tiling and 14.5 cm for two sides tiling.

### ***Openings***

There are different types of window frames and glazing in the building (Figure 3.5). The curtain walls in the living room and the windows at the corner of the bedroom walls were made of aluminum frames. Windowpanes between aluminum frames have a reflective coating which tends to reduce heat gain and glare and makes the inside invisible during the day.

Other frames in the unit are made of polyvinyl chloride (PVC) which is very common among building materials. The kitchen and the living room have fully glazed doors that open to the balcony with PVC frames, while the study room has sliding glass doors. In addition, the master bedroom has a fully glazed sliding door that opens to a French balcony on the north façade. All rooms have the same type of internal doors which are made of hollow core panels. Lastly, the main entrance door can be classified as a steel door with a wooden finish outlook.



Figure 3.5. Aluminum frame window at the corner (a), PVC framed window (b) and the french balcony with a sliding door (c) on the north façade.

### ***Occupancy Pattern, Heating, Cooling, Lighting, Electrical Equipment***

During the monitoring process, the unit was occupied by a family of 3 members. The retired couple used the living room and kitchen during the day. The study room monitored for the simulation study was occupied by 1 person during the daytime mostly. Bedrooms were occupied at night by all family members. The heating of the unit was provided by a combi boiler consuming natural gas. The heating system was on starting from 13th of October till 20th of April. On the other side, there was no active system for cooling. Cooling was provided by natural ventilation. The lighting of the rooms was in parallel with the occupancy and provided by 100-watt LED bulbs. Electrical equipment used were 2 televisions, 1 computer, 1 washing machine, 1 dishwasher, 1 oven, and 1 kettle in total.

### 3.1.4. Monitoring Process

The case building was equipped with HOBO data loggers (HOBO U12-012) to record indoor and outdoor weather data. These loggers are capable of measuring air temperatures between  $-20^{\circ}\text{C}$  and  $70^{\circ}\text{C}$  and relative humidity between 5% and 95% (Table 3.2.). Indoor dry bulb temperature and relative humidity values were logged in  $^{\circ}\text{C}$  and % respectively for the whole year between the 1st of November 2020 and the 31st of October 2021.

Table 3.2. Technical specifications of data loggers (Onset 2022)

<b>Data Logger</b>	<b>HOBO U12, T/RH/light/external data logger</b>
Measurement range	T: $-20^{\circ}\text{C}$ to $70^{\circ}\text{C}$ , RH: 5% to 95%
Accuracy	$\pm 0.35^{\circ}\text{C}$ from $0^{\circ}\text{C}$ to $50^{\circ}\text{C}$ RH: $\pm 2.5\%$ from 10% to 90%

For indoor measurements, one data logger was placed in the study room at a height of 1.70 meters from the floor, keeping away from abrupt temperature changes relatively. It measured and logged the temperature and relative humidity of the room with an interval of 10 minutes to be used in the calibration process of the simulation model later. Outdoor weather data is also measured in the same way. Another data logger was placed on the external wall of the study room, protecting it from rainwater and direct sunlight. For one year, outdoor temperature and relative humidity at this location were recorded every 10 minutes and used for the generation of weather climate data. Both data loggers were stopped periodically to get logged data, change batteries, and set up again for the record. The location of the data logger placed in the study room is represented in Figure 3.6.

During this monitoring process, the apartment and the monitored room were used actively by the users. The doors of the room were kept open mostly and the curtains were likewise. The door opening in the kitchen to the balcony is used when it is necessary during winter days. For summer days, that door was also left open during the daytime.

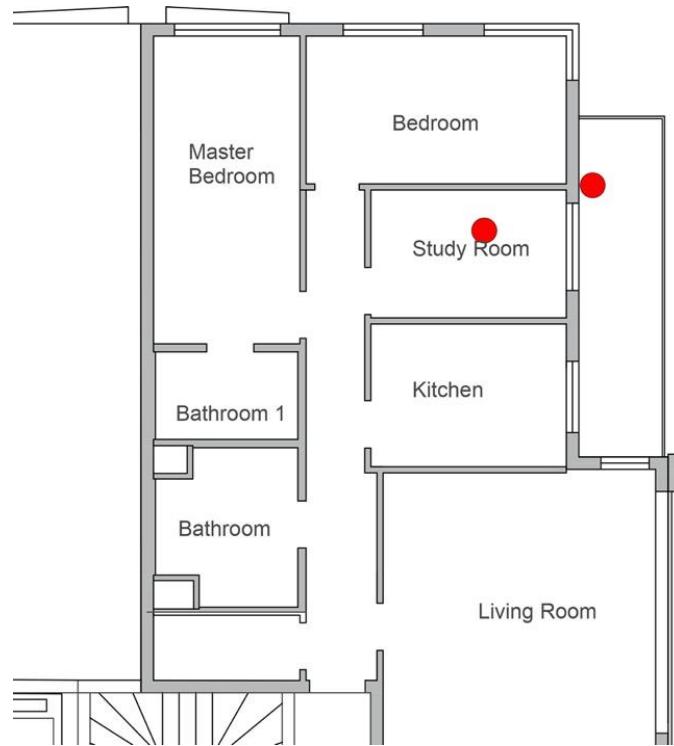


Figure 3.6. The exact locations of external and internal data loggers placed in the study room (indicated with red dots)

### 3.1.5 Weather File Generation

DesignBuilder simulation software requires accurate location information and climate data for the exact results. The altitude and the coordinates of the case building were found via Google Earth and inserted in DesignBuilder. At first, monitored dry bulb temperature and relative humidity in 10-min intervals were converted to hourly weather data in .csv (comma separated values) format, calculating the mean for each hour, as the software produces results in an hourly format. Then, this weather data was converted to .epw (Energy Plus Weather) format through Meteonorm tool to use as the weather parameter in DesignBuilder simulations. Meteonorm software generates accurate yearly weather information for any place on earth, using interpolation models, and enables the conversion of a large variety of weather file formats from one to another (Meteotest, 2021). Thus, this conversion process provided also the missing outdoor weather data for April. This final .epw file was used as a weather data parameter in DesignBuilder.

### 3.1.6 Modelling Process

This study is an investigation of the energy performance of novel and conventional building materials comparing annual heating and cooling energy consumptions of a case building. DesignBuilder energy simulation software was selected to find the consumed energy of the selected case building. This software uses the Energy Plus engine to calculate cooling and heating energy demands based on hourly weather data, offering a user-friendly interface for modeling and inserting parameters. The case building was modeled in detail in DesignBuilder. The modeling process was explained step by step:

- An abstracted site plan of the case building was drawn in AutoCad according to the survey, observations, on-site measurements, and satellite images taken from Google Earth Pro. Figure 3.7 shows simply the roads, city blocks, surrounding blocks, the case building, and the trees along the street.
- According to the drawn site plan, site features, surrounding buildings, and trees were created as 3D objects using component blocks, adiabatic blocks, and building block options in DesignBuilder. The model also involves abstraction to a certain degree due to the failure risk of the engine and extending hours of simulation when it makes calculations with complicated geometries. A 3D model of the site in DesignBuilder which is based on abstracted plans can be seen in Figure 3.9.
- Secondly, the case unit which was indicated with black dot lines in Figure 3.8 was separated into zones creating partition walls (Figure 3.9). Openings, windows, and doors were created on each wall and partition according to the floor plan. Transparent doors on the balcony were created as fully opening window casements to provide a similar heat gain as the existing situation.
- Properties of external walls, internal walls, windows, doors, and the floor were entered according to the data in Table 3.3 and Table 3.4.
- Site data of the building location and the weather file which was generated according to the procedure in the previous section were inserted in the simulation model.

- HVAC preferences were defined. Mechanical ventilation and cooling system were turned off completely due to the absence in the real condition. The heating system was defined as a central heating boiler using natural gas source. It was activated starting in October and ending in May (for more information see Appendix A).
- As defined by users, setpoint temperatures for the heating system is defined as 22°C and heating setback temperature is defined as 19°C (for more information see Appendix A).
- Natural ventilation was fully activated during the summer months.

After all the necessary data were inserted, the digital model was simulated from 1<sup>st</sup> of November 2020 till 31<sup>st</sup> of October 2021, and the simulation results were compared to results taken from data loggers to calibrate the simulation model.

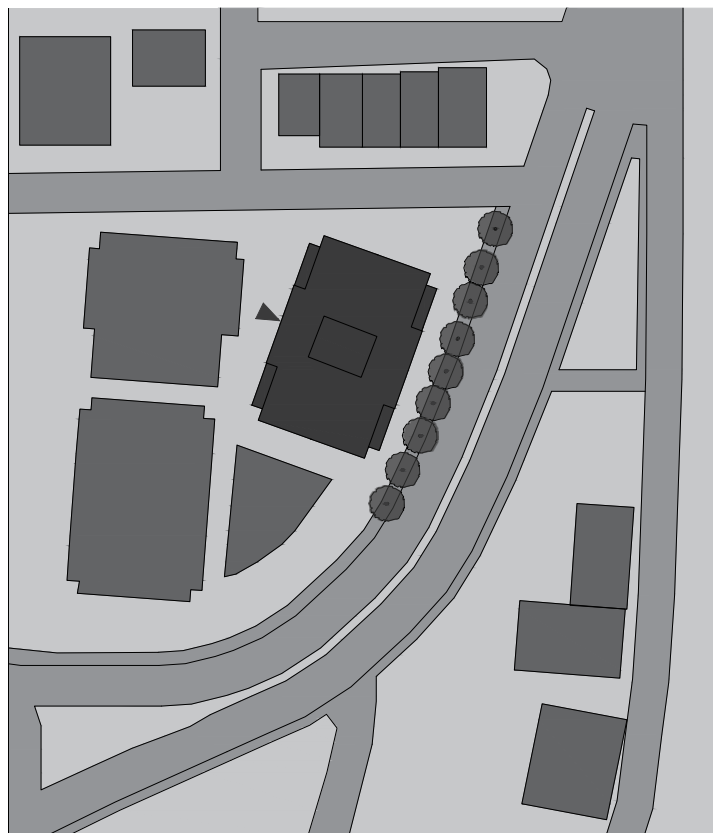


Figure 3.7. Abstracted site plan of the case building.



Figure 3.8. Digital model in DesignBuilder (the case unit is indicated with black dot lines)

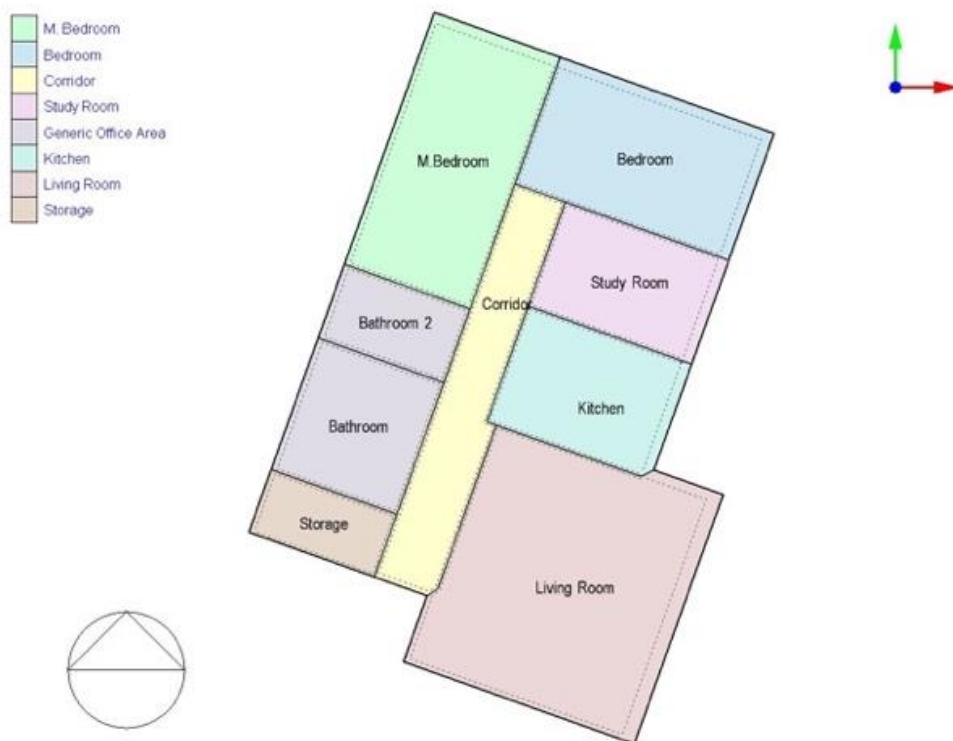


Figure 3.9. Floor plan of the case unit that was modeled in DesignBuilder.

Table 3.3. Material properties of openings inserted into the simulation model.

	U Value (W/m <sup>2</sup> )	Type	Thickness (glass+air+glass)	SHGC	Light Transmission
<b>PVC Framed Windows</b>	<b>2.72</b>	Double Glazing	4-+12+4	0.51	0.8
<b>Aluminium Framed Window</b>	<b>1.7</b>	Double Tempered Glazing	4-+12+4	0.42	0.55
<b>Internal Doors</b>	<b>2.5</b>	Hollow Core Door	4.2	-	-

Table 3.4 Component properties of materials inserted in DesignBuilder.

	U Value (W/m <sup>2</sup> )	Layers	Thickness (cm)	Conductivity (W/m.K)	Specific Heat (J/kg.K)	Density (kg/m <sup>3</sup> )
<b>External Walls</b>	<b>1.3</b>	Rough Cement Plaster	2	1.6	840	2000
		Hollow Clay Brick	19	0.33	840	600
		Rough Cement Plaster	1	1.6	840	2000
		Gypsum Plaster	0.5	0.7	1000	1400
		<b>Total</b>	<b>22.5</b>			
<b>External Wall with Glass Cladding</b>	<b>1.09</b>	Tempered Glass Panel	2	1.4	750	2200
		Cavity Unventilated	7.5	0.3	1000	1000
		Rough Cement Plaster	1.5	1.6	840	2000
		Hollow Clay Brick	19	0.33	840	600
		Rough Cement Plaster	1	1.6	840	2000
		Gypsum Plaster	0.5	0.7	1000	1400
		<b>Total</b>	<b>31.5</b>			

(con. on next page)

Table 3.4. (Cont.)

<b>Internal Walls with Gypsum Plaster</b>	<b>1.84</b>	Gypsum Plaster	0.5	0.7	1000	1400
		Rough Cement Plaster	2	1.6	840	2000
		Hollow Clay Brick	8.5	0.33	840	700
		Rough Cement Plaster	2	1.6	840	2000
		Gypsum Plaster	0.5	0.7	1000	1400
		<b>Total</b>	<b>11.5</b>			
<b>Internal walls with ceramic tiles</b>	<b>1.8</b>	Gypsum Plaster	0.5	0.7	1000	1400
		Rough Cement Plaster	2	1.6	840	2000
		Hollow Clay Brick	8.5	0.33	840	700
		Ceramic Adhesive	0.5	0.7	1000	1400
		Ceramic Tiles	1	1.4	840	2500
		<b>Total</b>	<b>12.5</b>			
<b>Internal Floor</b>	<b>2.8</b>	Reinforced Concrete (with 2% steel)	22	2.5	1000	2400
		<b>Total</b>	<b>22</b>			

### 3.1.7 Calibration Process

In building energy simulation (BES), calibration of the simulation model can be considered a provident approach before starting simulation studies. Although it is not a must for BES research, its significance has been increasingly recognized. Calibration enhances the credibility of the simulations to make profound predictions by matching simulation results to actual observations (Chong, 2021). In addition, there are some metrics to assess calibration performances that are specified by guidelines. CV-RMSE and MBE are the most used statistical indices for the calibration of BES models. Simply, CV-RMSE indicates the proximity of simulation outputs to observed outputs while MBE is an index of overall bias in simulation results.

For the calibration process of this study, ASHRAE Guideline 14-2002: Measurement of Energy and Demand Savings (ASHRAE14-2002 2002), IPMVP: International Performance Measurement and Verification Protocol (IPMVP 2002), and U.S. M & V guidelines (MVFEF): Measurement and Verification for Federal Energy

Projects (M&V guidelines 2008) were considered. These guidelines define different CV-RMSE and MBE limits for monthly and hourly weather data. As this study admits the calibration with hourly data approach, CV-RMSE value should not exceed 30%, 20% and 30% and MBE value should not be over +10%, 20%, and 10% respectively according to ASHRAE-14, IPMVP, and MVFEP (Table 3.5). Equations 3.1 and 3.2 show the formula for CV-RMSE and MBE, respectively.

Acceptable error ranges for hourly comparisons:

$$CV-RMSE (\%) = \frac{100}{T_{ma}} \times \sqrt{\frac{1}{N} \cdot \sum (T_s - T_m)^2} \quad \text{Eq. (3.1)}$$

$$MBE (\%) = \frac{100}{T_{ma}} \times \frac{\sum (T_s - T_m)}{N} \quad \text{Eq. (3.2)}$$

Where:

- N : the number of temperature data
- $T_{ma}$  : the average of monitored temperature values
- $T_s$  : simulated air temperature for the interior
- $T_m$  : monitored air temperature for the interior

Table 3.5. Acceptable limits of error indices

	ASHRAE-14 2014	IPMVP	MVFEP
CV-RMSE (%)	30	20	30
MBE (%)	±10	±20	±10

In addition to this approach, as the second criterion of the calibration, the average energy consumption of the case unit for heating was considered to calibrate the simulation model. The total natural gas consumption of the unit in December 2020 and January 2021 was examined through the natural gas bill. It is aimed that the heating load that is obtained

from the simulations shows similarity with the energy that was consumed in one month. This way, it is provided that the calibrated simulation model would get close to the real situation and come up with more credible results.

At first, a simulation model of the room and building with its components, materials, HVAC system, environmental parameters, and users' activity was created as close to the actual condition of the room. This process is explained in detail in the previous section. Followingly, this initial model was simulated in DesignBuilder and hourly indoor air temperature results of the monitored room were compared with the monitored air temperature values for each month of the year. Hourly error limits between the values coming from the simulation and the monitoring were calculated. Heating energy consumption in January 2021 was compared with the consumption value in the bill.

To obtain the optimum results that meet both requirements (error limits are under the given limits and the monthly energy consumption is close to the real condition), several attempts of simulations were done. These calibration steps were explained briefly as follows:

- The 3D objects of the other units in the building were changed from adiabatic blocks to building blocks.
- The solar heat gain coefficient (SHGC) value of windows was changed from 0.75 to 0.5 to limit overheating due to direct sunlight during morning hours.
- The natural ventilation schedule of the rooms was edited as allowing nighttime ventilation during the summer months.
- The heating setback temperature changed to 23 °C.

As a result of these efforts, the calibrated simulation model was obtained. All parameters and preferences which were defined in the model can be found in Table 1 in Appendix A. With these parameters, CV-RMSE and MBE values for each month of the year were found under the acceptable limits of error indices. Moreover, the heating load of the simulation model for January and December was obtained as the actual energy consumption of the building. Those approved that the model is calibrated and ready for further simulations in the study.

## **3.2 Experimental Study**

In this section, materials and methods regarding the experimental study of this thesis were explained in detail. Firstly, the selection procedure of raw materials and characterization test methods that were made on hemp, clay, and lime were clarified. In the following sections, the production steps of hemp-clay test blocks were elucidated. Lastly, the density and thermal conductivity values of the produced hemp-clay blocks were measured to insert them into the model for simulations.

### **3.2.1 Selection of Raw Materials**

The consumed energy during the transportation of raw materials and end products has a significant effect on the amount of embodied energy and embodied carbon of buildings. In this study, the energy performance of new construction material is investigated. This material is the hemp-clay block which is known to be an energy-efficient material with the possibility of being produced from locally available materials.

#### **3.2.1.1 Hemp**

Hemp hurds was sourced from the industrial hemp grown and harvested in the Menemen region which is located in the north of Izmir city center. After separating from their flowers, seeds, and fibers, hemp stalks which are around 4-meters long were broken into small pieces by harvesting machines in the field. Hemp hurds which is processed by the farmer was supplied in huge bags for this experimental study. The sizes of hemp hurds were in the range of 0-15 mm (Figure 3.10).



Figure 3.10. Hemp stalks (a) on the field and hemp hurds (b) in the laboratory.

### 3.2.1.2. Clay

The soil that is extracted from the Turgutlu region in Manisa province was used as a clay source. Turgutlu is an industrial region bordering Izmir which meets almost 20 percent of the clay brick (terracotta or earthenware) production in Turkey (Şahin, 2001). There is a great number of clay brick-tile factories in the Turgutlu region as the soil in that region is rich in alluvion and easy to process for brick production (Arslan, 2018).



Figure 3.11. Soil deposit (a) in the factory site and the soil (b) supplied for the study (Photography: Betül Ergün, (2021), Location: Turgutlu, Manisa))

The raw soil which is known for its high clay content and used in the production of brick and tile was obtained from a factory in Turgutlu (Figure 3.11). The soil samples were tested for physical properties in Material Laboratory in Civil Engineering Department and chemical compositions in the Center for Materials Research in Iztech.

### **3.2.1.3 Lime**

Hydrated lime was used as an additive in the blocks to find out the effect of a small percentage of lime on the drying process, density, and thermal conductivity. Hydrated lime C80 of a local brand from Izmir was used as a lime additive. It was held in its paper bag under laboratory conditions with a temperature of  $23\pm 5^{\circ}\text{C}$  and relative humidity of  $50\pm 5\%$  during experiments.

## **3.2.2 Characterization of Materials**

The hemp hurds and clay were the main components of hemp-clay blocks while lime was used as an additive. All these were characterized by their physical and chemical properties. The same samples were also observed under electron scanning microscopy to image the physical structure.

### **3.2.2.1. Bulk Density Measurement**

The as-received soil samples were dried in an oven at  $100^{\circ}\text{C}$  for 24 hours. The weights and volumes of both as-received and dried soil samples were measured to calculate densities. Hemp hurds were also measured using the same procedure this time in a 1-liter cup without tapping.

### 3.2.2.2. Grain Size Distribution Tests

Soil grain size distribution states the percentages of aggregate with different diameters in the sample. Soil mined from nature consists of stone, sand, silt, and clay, from coarse to fine, respectively. It is essential to know the grain size distribution of soil that is used in the production of hemp-clay samples, to evaluate the physical behaviors of the sample accordingly. This process includes two tests in order. The first one is Mechanical Sieve Analysis for the separation of larger diameter grains (4.75 mm to 0.075 mm). The other is Hydrometer Analysis which tests grains that are finer than 0.075 mm. These two methods are standardized as ASTM D 422 – Standard Test Method for Particle Size Analysis of Soil (ASTM 2014).

#### *Mechanical Sieve Analysis:*

In the sieve analysis test, a soil sample was passed through the sieves with different size openings which were stacked on top of each other. The pan and sieves from finer to larger were placed on the shaker, the larger sitting on top. Figure 3.12 shows the sieving setup. The number of sieves and opening sizes used in the study was according to the ASTM E11 standard which can be seen in Table 3.6.



Figure 3.12. The sieve shaker and stacks are ready to work  
(Photography: Betül Ergün, (2021))

Table 3.6. Sieve number and mesh openings in mm

Sieve Size or Number	Openings (µm )
#20	850
#40	425
#60	250
#200	75

For this study, sieves number #20, #40, #60, and #200 were used, and sieve analysis tests were performed. The shaker worked for 10 minutes to let the particles pass through the sieves. The percentage of soil left on each sieve was calculated according to the Percent Retained (R) formula (Eq. 3.3).

$$R = \frac{\text{Weight Retained}}{\text{Soil Weight}} \times 100 \quad (\text{Eq. 3.3})$$

In sieve analysis, Cumulative Retained Percentage (C) and Percent Finer (F) are needed to plot the particle size distribution graph. C is the sum of percentages that are retained in sieves with larger openings (Eq. 3.4) and F shows the percentage of soil which is finer than the given size (Eq. 3.5).

$$C_{\#n} = R_{\#n-1} + R_{\#n-2} \dots R_{\#1} \quad (\text{Eq. 3.4})$$

$$F_N = 100 - C_N \quad (\text{Eq. 3.5})$$

### ***Hydrometer Analysis***

Hydrometer analysis is a widely used method to determine the particle size distribution of soil passing a 75 nm sieve. It is standardized by “ASTM- D1140 Standard Test Method for Amount of Material in Soils Finer Than No.200 (75nm) Sieve”. This method is based upon Stoke’s law which estimates that grain settles in liquids as an individual. It states that larger particles settle faster, and the diameter of the particle is

proportional to the square root of its settling velocity. The hydrometer floats lower and lower in the slurry in time and how low it floats is recorded as a function of time. For the study, the suspension was prepared with clay, water, and a dispersing agent according to the standard. The hydrometer was placed in the slurry for each reading and kept in pure water otherwise. The value on the hydrometer is read at the following intervals of elapsed time ( $\Delta T$ ); 2, 5, 15, 30, 60, 250, 1 and 440 minutes and recorded (Figure 3.13).

Using the R-value which is read on the hydrometer, recorded time in minutes, and correction factors of a and b gave in the standard as a function of temperature, the distance between the center of mass of the hydrometer and the point where the hydrometer is read (L), the particle diameter (D) and percent passing were calculated. The following equations were applied for this process.

$$L = 16.3 - 0.163R \quad (\text{Eq. 3.6})$$

$$D = Kx \sqrt{(Lx\Delta T)} \quad (\text{Eq. 3.7})$$

$$P' = \frac{(R-b)a}{M_d} \times 100\% \quad (\text{Eq. 3.8})$$

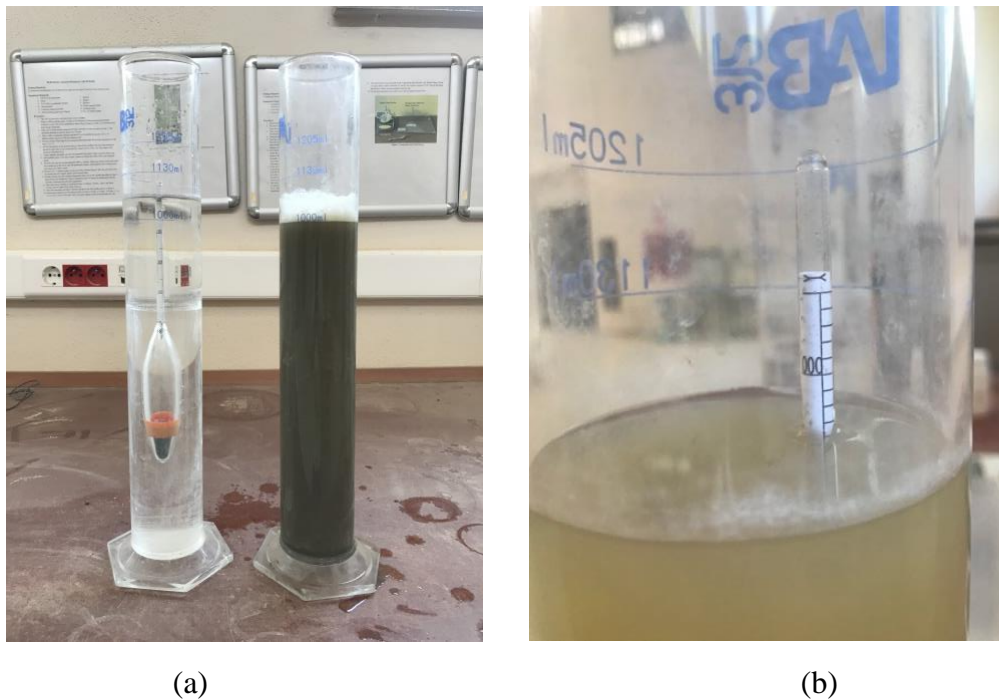


Figure 3.13. Soil suspension prepared for hydrometer testing (a) and reading of hydrometer (b)

### 3.2.3. Chemical Composition Tests

To characterize the binders, clay, and lime, regarding their elemental composition and compounds, complementary analyses that use X-ray sources were performed in the research center. In addition to that, both the hemp hurd, clay, and lime sample was imaged with Scanning Electron Microscopy (SEM) to document the microstructure of the material. For these tests, samples need to be finely ground and homogenized. To prepare the samples for tests, the soil was crushed in a ball mill first and then sieved with a 0.075 mm sieve while the lime was crushed in a small hand grinder to decrease particle size. Three small samples to be tested were taken to the research center (Figure 3.14).



Figure 3.14. Solid components of the hemp-clay materials were prepared to be tested.

#### *XRD*

X-Ray diffraction (XRD) analysis was used to assess the mineral phases of clay and lime. XRD patterns were obtained using Cu K $\alpha$  ( $k = 1.5405 \text{ \AA}$ ) radiation with a Philips X'PERT MPD diffractometer. The diffractometer was scanned from  $4.9^\circ$  to  $80^\circ$  ( $2\theta$ ) in step size of 0.016 and the time per step was 26.7 s. This analysis was made by an expert in the Center of Material Research. The results of the analysis were obtained from the expert and evaluated to indicate the mineralogical compositions of clay and lime.

### ***XRF***

X-Ray Fluorescence (XRF) analysis was used to determine the chemical composition of clay and lime as binders. The major and trace elements of the materials were analyzed using a Spectro IQ II X-ray fluorescence (XRF) spectrometer with wavelength dispersion.

### ***SEM***

Scanning Electron Microscopy (SEM) produces electron beams and scans the sample to create a magnified surface image of the material. This method is used effectively for microanalysis and failure analysis of inorganic materials. Small amounts of clay, lime, and hemp hurds were scanned in SEM by an expert to evaluate the microstructure of materials.

### **3.2.4. Production of Hemp-Clay Blocks**

As the first step of the production process, clay material that was obtained from the factory was sieved using a sieve with a 2 mm mesh size. Grains larger than 2 mm were separated as they can restrain the adherence between the hemp hurds.

Before the determination of the mix ratio of the three main ingredients (hemp hurds, clay and water), various ratios and methods of mixing were tried to find a reasonable range of ratios. A small paste mixing machine in the laboratory was tried but it scattered the material out, causing some changes in the ratio. On the other hand, the cement mixer was too large to mix this amount of mixture. Both methods were eliminated.

In the establishment of mixing proportions, water:binder and hemp:clay ratios were considered in weight. The initial series of blocks have a ratio of 1:5 and 1:4 hemp:binder. For this series firstly 1:2 water:binder ratio was tried, but this did not provide the necessary stickiness between hemp hurds. According to observations on initial tests, proposed mixing proportions were determined.

### 3.2.4.1 Mixing

Mixing proportions of ingredients and specific names that were created for each block series are presented in Table 3.7. H, C, CL, and W mean the hemp hurds, clay, clay with lime, and water, respectively. Additionally, the number at the right of the letter stands for their ratio in the mix. Two series of blocks were produced based on the presence of additives in a binder.

Table 3.7. Mixing proportions of hemp, binder, and the additive.

<b>Sample Name/Ratios</b>	<b>Hemp:Binder (in % by weight)</b>	<b>Clay:Water (in % by weight)</b>	<b>Lime amount in binder (in % by weight)</b>
<b>H1C2W2</b>	1:2	1:1	-
<b>H1C2.5W2.5</b>	1:2.5	1:1	-
<b>H1C3W3</b>	1:3	1:1	-
<b>H1C2W3</b>	1:2	1:1.5	-
<b>H1CL2W2</b>	1:2	1:1	5
<b>H1CL2.5W2.5</b>	1:2.5	1:1	5
<b>H1CL3W3</b>	1:3	1:1	5
<b>H1CL2W3</b>	1:2	1:1.5	5
<b>H1CL2W3_10</b>	1:2	1:1.5	10

For the first series of blocks, the binder was clay with no additive. To see if the ratio of binder influences the physical and thermal features of the samples, the proposed recipes had the ratio of 1: 2, 1:2,5, and 1: 3 and hemp-binder. That means that in the compositions the amount of hemp was constant, and the density of the specimens was influenced only by the mass of the clay binder. On the other hand, the clay:water ratio was kept constant with a ratio of 1:1 for these series.

For the second series of blocks, hemp:binder ratios were the same as those in the first. The binder was altered to contain lime additive with a ratio of 5% for each block.

In this way, it is aimed to observe the effect of lime additives on the physical and thermal properties of hemp-clay blocks.

The production process of the hemp-clay compositions is presented in Figure 3.15. The mixing procedure for each block was operated following the steps: the total amount of the binder was mixed with the half amount of water with a paddle mixer to get a slurry. The other half of the water was added to hemp hurds. Then finally, the slurry was added to wet hemp hurds and mixed by hand until a homogeneous mixture. The fact that two components are moist or wet increases the adherence when mixed as the water is needed to activate clay as a binder.



(a)



(b)



(c)

Figure 3.15. Raw materials prepared for mixing (a), slurry mix of clay and water (b) and hemp-clay mix ready for moulding (c)

### 3.2.4.2 Moulding

In the moulding process of hemp-clay material, cubic and prismatic steel moulds were used. Cubes were standard concrete sample moulds which are produced in 150x150x150 mm sizes. according to TS- EN 1239-1. Other prismatic moulds are in the size of 250x50x75 mm. For each mix, a set of three blocks was made. Two cubic and one prismatic block were produced. The mixed composition was put in moulds layer by layer. Each 5 cm layer of composition was compacted manually until the mould got fulfilled. Hemp-clay blocks after moulding can be seen in Figure 3.16.

### 3.2.4.3. Drying

Samples were demoulded after 3 days and left for drying under laboratory conditions for 28 days before testing. During this time, the air temperature and relative humidity of the laboratory room were monitored with data loggers. Demoulded hemp-clay samples left for drying and the data logger which is placed on the wall can be seen in Figure 3.17.



(a)



(b)

Figure 3.16. Hemp-clay block samples in steel moulds (a) and (b)



Figure 3.17. Hemp-clay blocks are left for drying in the laboratory.

### **3.2.5. Characterization of Hemp-Clay Blocks**

#### **3.2.5.1. Density Measurements**

The weight of each block was measured before and after demoulding with an electronic scale (Figure 3.18a). Measurements were continued every day for 1 week to record changes in the weight of blocks. Any decrease in the weight means that water in the composition evaporates and the samples are drying. The density measurements of the samples in the 28<sup>th</sup> day was accepted as the dry density of the novel hemp-clay building blocks.

#### **3.2.5.2. Thermal Conductivity Tests**

Hemp-clay block samples were tested for thermal conductivity values using KEM QTM 500 type quick thermal conductivity meter in Materials Research Center (Figure 3.18b). For this type of meter, measuring ranges between 0.023 and 11.63 W/mK with 5% precision. Samples were tested 3 times from both the upper face and the side face. A

total of six measurements were averaged to find the ultimate thermal conductivity value of the sample.

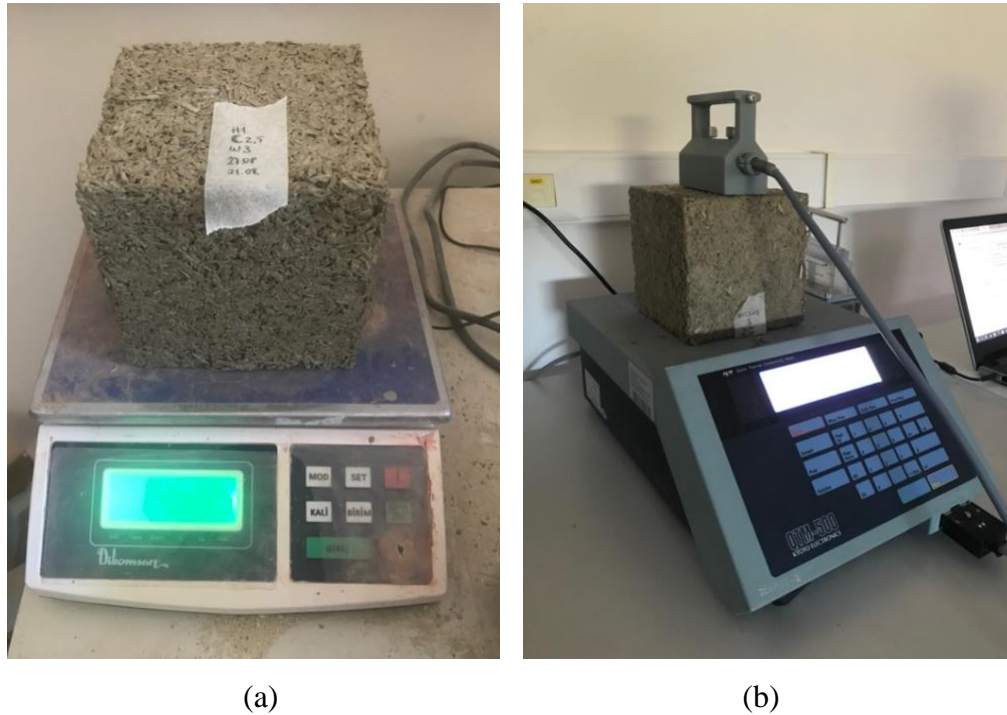


Figure 3.18. Measurement of weight (a) and thermal conductivity testing (b)

### 3.3. Determination of Simulation Scenarios

In the determination of simulation scenarios, variables and constants regarding the wall materials were defined. Two series of scenarios were created for building energy simulations in this study. In the first series, the existing wall thickness of the case building was fixed, and the wall-filling material was changed. As expressed in section 3.1.3, the existing wall material of the case building was hollow clay brick (HCB) with 19 cm and 8.5 cm thicknesses for exterior and interior walls, respectively. This filling layer was rendered with cement-based and gypsum-based plasters. For scenarios 2 and 3, the HCB layer in the exterior and interior walls of the simulation model was changed with aerated autoclaved concrete (AAC) blocks and lightweight pumice blocks (LPB). Material properties of HCB, AAC, LPB, EPS, gypsum, and cement plasters such as thermal conductivity and density were taken from the manual of TS-825 Thermal Insulation

Requirements for Buildings (Turkish Standards Institution 2008). The specific heat capacity of these materials was adopted from the material library of DesignBuilder.

For scenario 4, the hempcrete block was defined as wall material to be able to make a comparison between the experimented hemp-clay block and the hempcrete block which is produced and already used in the buildings. Material properties of the hempcrete block were adopted from the technical data sheet released by the IsoHemp block producer (IsoHemp 2022). Experimented hemp-clay blocks were defined in scenario 5. The hemp-clay block sample with the lowest thermal conductivity value was selected for the energy simulations. In these scenarios 4 and 5, hempcrete and hemp-clay wall infills were completed with insulating hemp lime plasters at both sides of the walls, as hemp materials do not comply with the cement-based plaster due to their high moisture permeability. Material properties of hemp lime plaster were taken from the technical document of Tradical (Tradical 2022). Therefore, plaster types that are compatible with the defined wall-filling material were preferred for each scenario. Table 3.8 shows the external wall layers, their material properties, and U-values regarding the first series of scenarios. These 5 scenarios with different wall materials were simulated for 3 different climate conditions of 2020, 2050, and 2080. As explained in section 3.1.5., weather files belonging to the years 2020, 2050, and 2080 were generated to insert into the simulation model. Thereby, in total, 15 building energy simulation was run for the first series of scenarios.

The second series of scenarios consist of 4 different scenarios. Scenario 5 with the hemp-clay wall option was duplicated in this series. An insulation layer was added to HCB, AAC, and LPB wall options so that they can reach the U-value of the external hemp-clay walls. For scenarios 6, 7 and 8, an insulation layer that was made of expanded polystyrene foam in different thicknesses was added onto the exterior sides of the walls, keeping the thickness of the wall-filling material the same as it is in the first series. Consequently, there are 4 wall options that have different insulation thicknesses, different wall-infill materials, and the same U-value in the second series. The list of wall options with material properties can be seen in Table 3.9. Comparing the energy consumption of these scenarios with the wall options explained, it is investigated if the hemp-clay shows similar performance with the conventional building materials with an insulation layer when they all have the same U-value. Addition to the first series of simulations, 9 more simulations were run for scenarios 6,7 and 8. In total, 24 different simulations were done in DesignBuilder for this study.

Table 3.8. Wall layers and material properties regarding the first series of scenarios.

Year	#	Wall Option	U value (W/m <sup>2</sup> K)	Layers (outside to inside)	Thickness (m)	Thermal Conductivity (W/mK)	Specific Heat Capacity (J/kgK)	Density (kg/m <sup>3</sup> )	
2080	1	HCB (Hollow Clay Brick) (base scenario)	1.66	Cement Plaster	0.02	1.6	840	2000	
				<b>HCB</b>	0.19	0.33	840	600	
				Cement Plaster	0.01	1.6	840	2000	
				Gypsum plaster	0.005	0.7	1400	1000	
	2	AAC (Aerated Autoclaved Concrete Block)	0.97	Cement Plaster	0.02	1.6	840	2000	
				<b>AAC</b>	0.19	0.19	840	600	
				Cement Plaster	0.01	1.6	840	2000	
				Gypsum plaster	0.005	0.7	1400	1000	
	2050	3	LPB (Lightweight Pumice Block)	1.17	Cement Plaster	0.02	1.6	840	2000
					<b>LPB</b>	0.19	0.23	1040	600
					Cement Plaster	0.01	1.6	840	2000
					Gypsum plaster	0.005	0.7	1400	1000
2020	4	Hempcrete	0.32	Hemp-lime plaster	0.02	0.09	1068	887	
				<b>Hempcrete blocks</b>	0.19	0.07	1000	340	
				Hemp-lime plaster	0.015	0.09	1009	887	
	5	Hemp-clay (experimented)	0.47	Hemp-lime plaster	0.02	0.09	1068	887	
				<b>Hemp-clay blocks</b>	0.19	0.11	1550	352	
				Hemp-lime plaster	0.015	0.09	1068	887	

Table 3.9. Wall layers and material properties regarding the second series of scenarios.

Year	#	Wall Option	U value (W/m <sup>2</sup> K)	Layers (outside to inside)	Thickness (m)	Thermal Conductivity (W/mK)	Specific Heat Capacity (J/kgK)	Density (kg/m <sup>3</sup> )
2080	5	Hemp-clay (experimented)	<b>0.47</b>	Hemp-lime plaster	0.02	0.09	1068	887
				Hemp-clay blocks	0.19	0.11	1550	352
				Hemp-lime plaster	0.015	0.09	1068	887
	6	Hollow Clay Brick (HCB) with insulation layer	<b>0.47</b>	Cement plaster	0.02	1.6	840	2000
				EPS	<b>0.06</b>	0.04	710	160
				HCB	0.19	0.33	1030	600
				Cement Plaster	0.01	0.7	840	2000
	7	Aerated Autoclaved Concrete (AAC) with insulation layer	<b>0.47</b>	Gypsum plaster	0.005	1.6	1400	1000
				Cement Plaster	0.02	1.6	840	2000
				EPS	<b>0.044</b>	0.04	710	160
				AAC	0.19	0.19	840	600
				Cement Plaster	0.01	1.6	840	2000
	8	Lightweight pumice block (LPB) with insulation layer	<b>0.47</b>	Gypsum plaster	0.005	0.7	1400	1000
				Cement Plaster	0.02	1.6	840	2000
				EPS	<b>0.051</b>	0.04	710	160
				LPB	0.19	0.23	1040	600
Cement Plaster				0.01	1.6	840	2000	

## CHAPTER 4

### RESULTS AND DISCUSSION

#### 4.1. Monitoring Results

In the first section of Chapter 4, results of monitoring process were presented. The monitored air temperature and relative humidity values of the case building were examined and discussed separately in the following sections.

##### 4.1.1. Temperature

Monitored indoor and outdoor weather data of the study room between 1<sup>st</sup> of November 2020 and 31<sup>st</sup> of October 2021 facing to the southeast were analyzed for each month. The maximum, minimum recorded temperature values and their averages can be seen in Table 4.1. The maximum outdoor temperature was 41.7°C in 17.07.21 at 09:00 a.m. while maximum indoor temperature was recorded as 35.1°C in 06.08.2021 at 14:30 p.m. The minimum temperatures were recorded as 1.5°C and 18.6°C for the outdoor in February and the indoor in December, respectively. Indoor air temperature ranged between 18.6°C and 35.1°C for one year while outdoor air temperature was between 1.5°C and 41.7°C. The alteration trend of indoor and outdoor air temperatures during the monitoring process was depicted in Figure 4.1 as well.

To examine the temperature values for winter weather, indoor and outdoor temperatures for January were graphed in Figure 4.2. It is seen that indoor temperature values range between 19.1°C and 27.6°C with an average of 23.3°C. It fluctuates during the day due to the solar heat gain early in the morning and the changes made in the setpoint temperature of the heating system. On the other side, outdoor temperatures vary in a wider range (from 1.7°C to 28.7°C) with a lower average value of 12.9°C.

The peak points of outdoor temperature during the day show similarity for each day in January. These peaks were recorded around 11:00 a.m. The reason for that can be interpreted as the direct sun exposure at the same hours each day. As the heating system is active 7/24 for the whole month, indoor air temperatures did not get affected by the outdoor temperature changes, except solar heat gain in the morning. Therefore, indoor air temperatures are always higher than the temperature values that are defined as thermal comfort range (19.5°C – 27.5°C) by ASHRAE standards (ASHRAE 2002).

Table 4.1. Monitored outdoor and indoor temperature values.

	Outdoor Air Temperature (°C)			Indoor Air Temperature (°C)		
	T <sub>min</sub>	T <sub>max</sub>	T <sub>avg</sub>	T <sub>min</sub>	T <sub>max</sub>	T <sub>avg</sub>
<b>November, 20</b>	8.8	23.2	16.7	21.1	25.9	23.5
<b>December, 20</b>	7.1	23.6	14.3	<b>18.6</b>	27.5	23.5
<b>January, 21</b>	1.7	28.7	12.9	19.1	27.6	23.3
<b>February, 21</b>	<b>1.5</b>	33.5	13.4	20.2	29.3	24.6
<b>March, 21</b>	4.9	33.5	13.2	20.1	28.7	23.5
<b>April, 21</b>	11.4	37.0	21.4	20.6	26.6	23.5
<b>May, 21</b>	14.3	36.9	23.4	23.5	30.3	26.9
<b>June, 21</b>	16.2	37.3	26.1	25.2	32.9	28.5
<b>July, 21</b>	23.2	<b>41.7</b>	29.8	28.1	30.3	30.5
<b>August, 21</b>	23.4	39.8	30.0	26.8	<b>35.1</b>	30.2
<b>September, 21</b>	16.1	35.3	25.4	23.9	31.4	27.5
<b>October, 21</b>	13.7	28.0	20.0	20.9	28.9	23.5

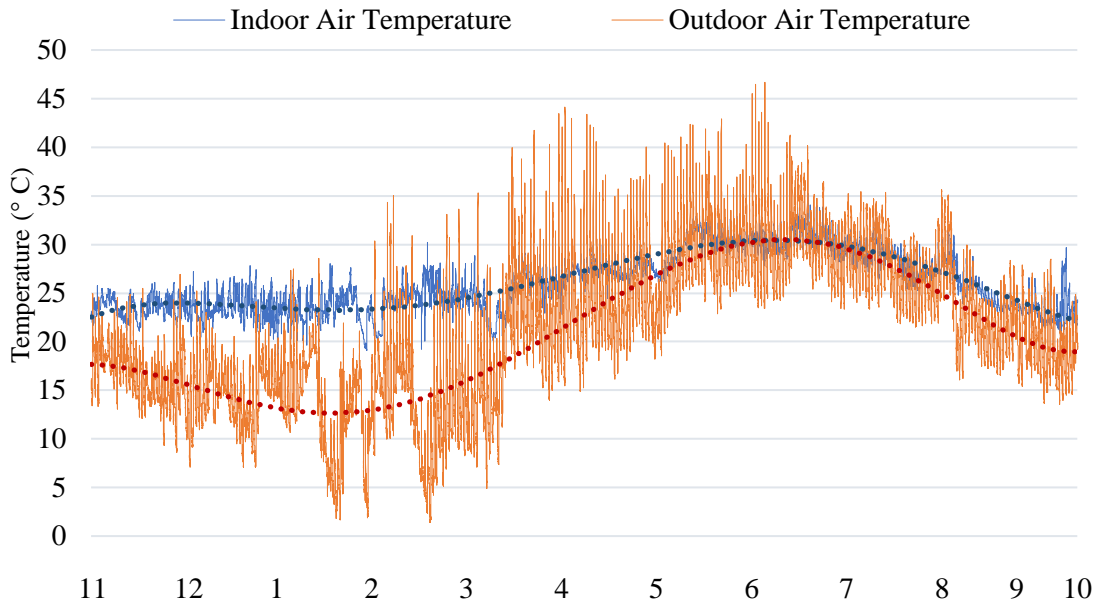


Figure 4.1. Indoor and outdoor air temperatures for whole year with the trendline.

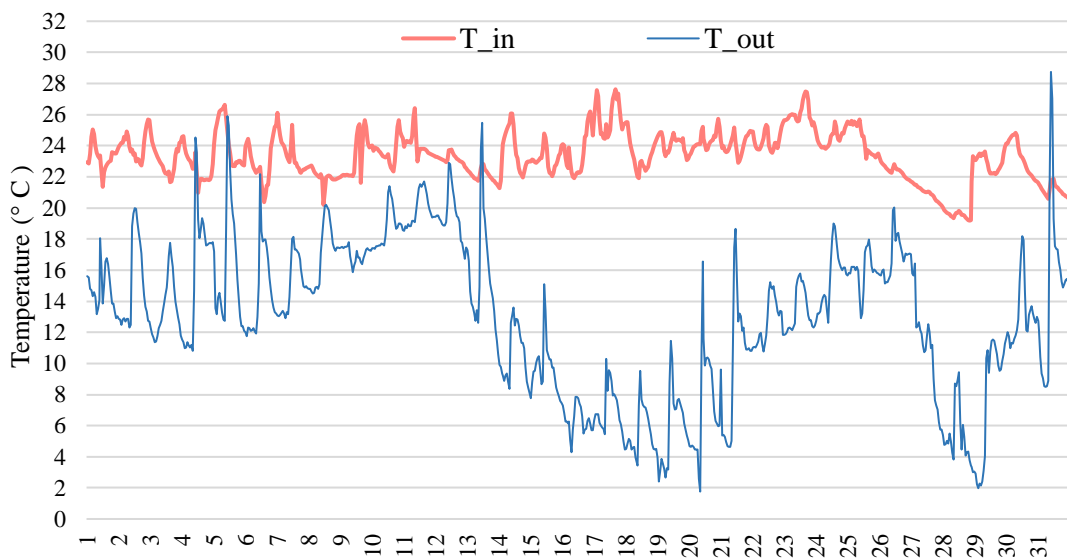


Figure 4.2. Monitored indoor and outdoor temperatures in January 2021.

The effect of sun exposure on data logger and solar heat gain can be observed in the summer days (Figure 4.3). In July, temperature peaks are seen at 09:00 a.m. every day, which is earlier than it is in January. Conversely, temperature drops to its lowest value ( $\cong 23^{\circ}\text{C}$ ) at 05:00 a.m. almost each day. Outdoor air temperatures vary in a range of  $23.2^{\circ}\text{C}$  and  $41.7^{\circ}\text{C}$  while indoor air temperatures change slightly between  $28.1^{\circ}\text{C}$  and

30.3°C. However, the fluctuations of indoor and outdoor temperatures are seen concurrent.

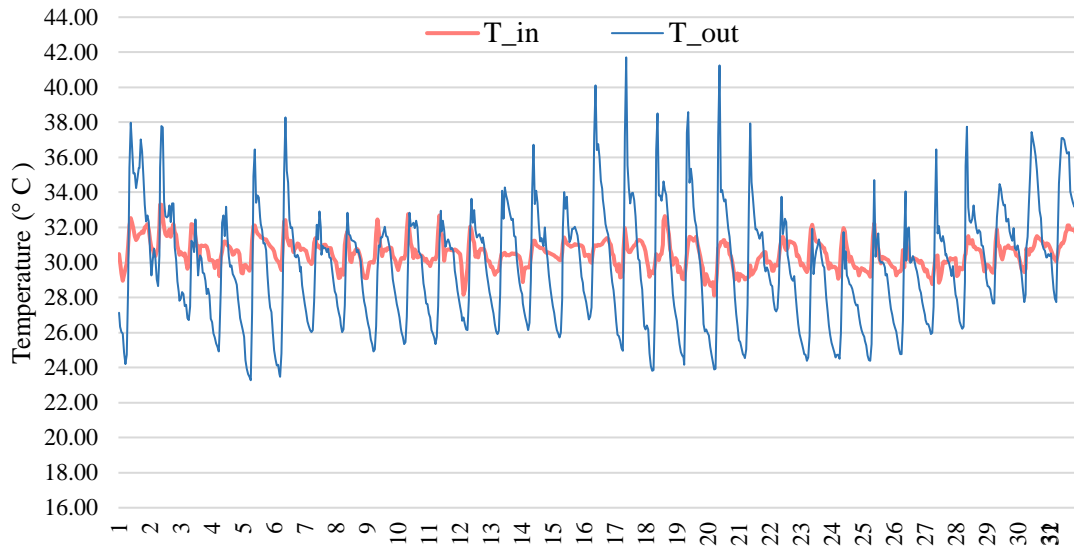


Figure 4.3. Monitored indoor and outdoor temperatures in July 2021.

#### 4.1.2. Relative Humidity

Relative humidity values changes between 17.0% and 91.4% in recorded outdoor weather data (Table 4.2). Indoor and outdoor relative humidity values for the monitored year and the change trend were presented in Figure 4.4. For the whole year, the average of outdoor relative humidity values are higher than 50%. In addition, these averages are always slightly higher in winter months, making the peak with the relative humidity of 75.1% in December. On the contrary, according to recorded indoor weather data, RH values vary less than outdoor RH values, which is between 21.9% and 72.5%. For summer months, average RH values of indoor environment are in relation with those of outdoor due to constant natural ventilation.

In examination of RH values for January 2021, it is observed that indoor and outdoor relative humidity values do not show convergence at most of the time (Figure 4.5).

This is since the heating system kept the indoor air temperature in a defined range on cold days without the effect of outdoor air temperature. Indoor RH values are always lower than the outdoor RH values in percentage and also stay in the defined range of RH value for thermal comfort, which is between 30% and 60% (ASHRAE 2002).

However, in July 2021, indoor RH value exceeded 60% several times due to the rise in outdoor humidity. Although, indoor RH values went up and down in the same direction with the outdoor RH, it did not reach the extreme values of outdoor RH values most of the time (Figure 4.6).

Table 4.2. Monitored relative humidity values for outdoor and indoor

	Outdoor Relative Humidity (%)			Indoor Relative Humidity (%)		
	RH <sub>min</sub>	RH <sub>max</sub>	RH <sub>avg</sub>	RH <sub>min</sub>	RH <sub>max</sub>	RH <sub>avg</sub>
<b>November, 20</b>	29.1	80.0	59.1	34.7	59.7	49.0
<b>December, 20</b>	34.7	89.7	75.1	34.1	68.3	51.6
<b>January, 21</b>	21.8	89.8	67.0	24.1	70.7	47.2
<b>February, 21</b>	18.6	<b>91.4</b>	63.0	<b>21.9</b>	61.7	43.0
<b>March, 21</b>	<b>17.0</b>	85.7	58.4	28.8	54.3	40.3
<b>April, 21</b>	22.0	77.6	47.1	32.9	61.4	50.4
<b>May, 21</b>	17.8	83.4	55.0	31.0	63.6	51.2
<b>June, 21</b>	21.6	86.9	57.3	38.4	65.1	55.1
<b>July, 21</b>	17.9	78.7	54.4	34.4	71.3	55.9
<b>August, 21</b>	19.9	75.3	53.4	29.7	<b>72.5</b>	55.4
<b>September, 21</b>	28.6	75.0	54.2	38.3	67.5	53.1
<b>October, 21</b>	34.9	85.7	61.8	39.7	75.2	55.4

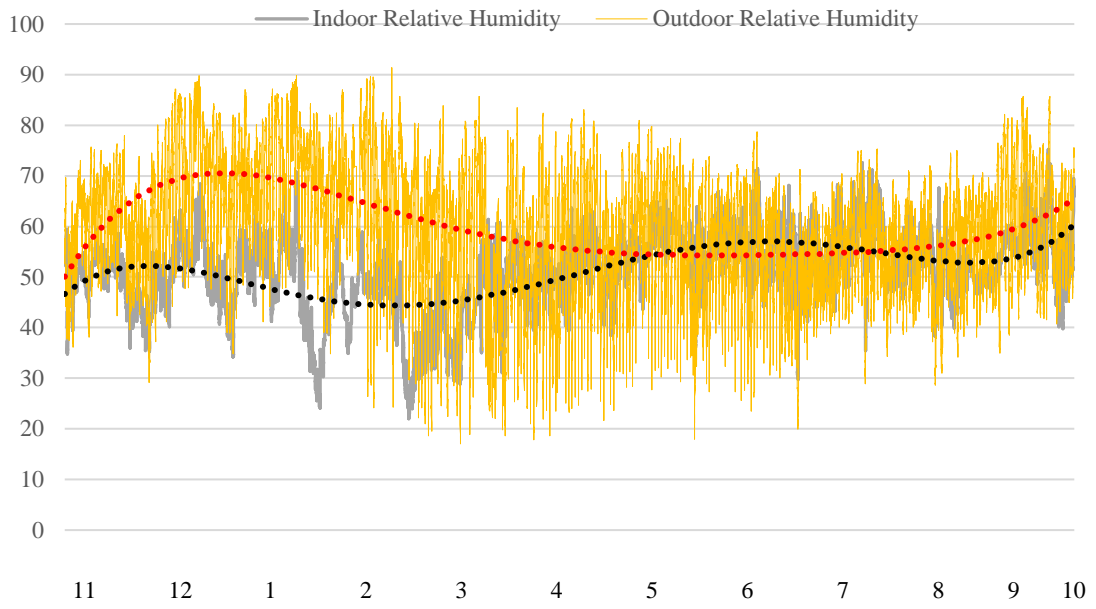


Figure 4.4. Indoor and outdoor relative humidity values for the monitored year.

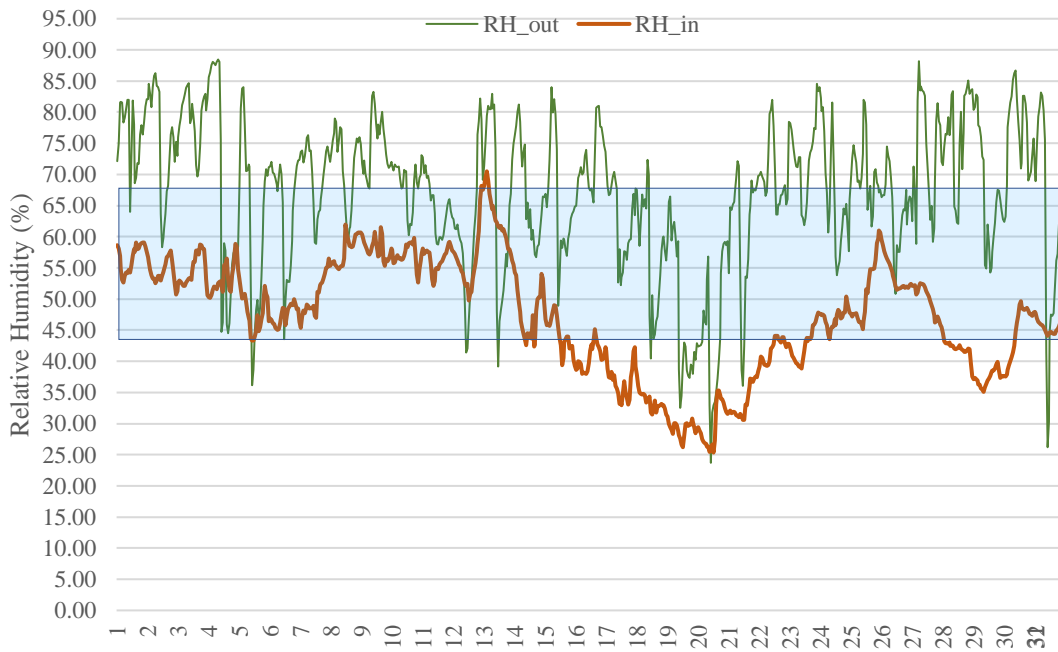


Figure 4.5. Recorded relative humidity values of indoor and outdoor in January 2021 (shaded area depicts the RH interval for indoor comfort)

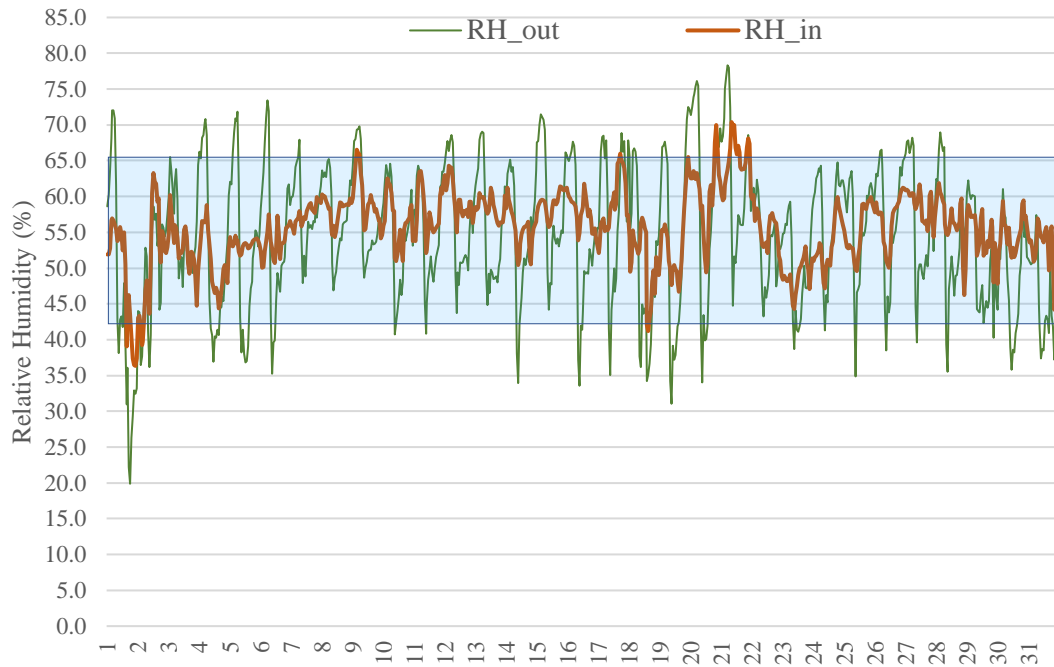


Figure 4.6. Recorded relative humidity values of indoor and outdoor in July 2021  
(shaded area depicts the RH interval for indoor comfort)

## 4.2. Calibration Results

To obtain a confiding simulation model, calibration of the model was evaluated for each month separately. In this process, several attempts were done to keep CV RMSE and MBE values between the limits defined and find a good agreement between the heating load and actual energy consumption. These criterias were explained in detail in chapter 3. As a result of the first simulation trial, CV RMSE value do not exceed the limit of  $\pm 30\%$  while MBEs were higher than 10% for summer months, changing between 1.37% and 14.74%. Accordingly, natural ventilation schedule and solar heat gain coefficient of the windows were changed to cool down the indoor. Finding out the correct relation between the natural ventilation and heating system, simulated indoor air temperatures were approached to the monitored indoor air temperatures. According to results of 4<sup>th</sup> attempt, MBEs for all months were dropped under 10%, changing between 9.3% and -7.84 %, while CV RMSE values changed between 3.95% and 11.07% as desired (Table 4.3). However, heating energy consumption of the simulation model was

far lower than actual condition. Changing the inputs related with internal heat gain of the model, heating energy consumption of the last model is reached to the expected value. It is accepted as the calibrated model.

When the simulated and monitored air temperature values were examined, it is the seen that in January, monitored air temperatures fluctuate randomly in a wide range, due to the changes on occupancy and heating setpoint values (Figure 4.7). However, temperature values that were obtained from the calibrated model do not show a similar trend with the monitored. In July, on the other side, simulated values are always higher than the monitored air temperature values, although they move in a similar trend (Figure 4.8). However, CV RMSE and MBE values stand inbetween the limits for both months, which indicates that the model is calibrated and reliable to be used in simulations.

Table 4.3. CV RMSE and MBE values for each month

	CV RMSE (%)			MBE (%)		
	First Simulation	4 <sup>th</sup> Simulation	Last Simulation	First Simulation	4 <sup>th</sup> Simulation	Last Simulation
<b>January</b>	12.45	8.93	<b>9.8</b>	3.25	-3.56	<b>-4.67</b>
<b>February</b>	14.31	11.07	<b>11.78</b>	6.64	-7.84	<b>-8.94</b>
<b>March</b>	10.64	9.22	<b>9.07</b>	1.37	-3.4	<b>-4.07</b>
<b>April</b>	13.96	9.77	<b>3.49</b>	13.51	9.3	<b>2.3</b>
<b>May</b>	6.66	3.95	<b>5.17</b>	5.82	-1.7	<b>-3.28</b>
<b>June</b>	10.21	3.11	<b>6.83</b>	9.63	0.60	<b>-4.38</b>
<b>July</b>	11.25	6.66	<b>4.3</b>	10.78	6.13	<b>1.3</b>
<b>August</b>	12.12	8.8	<b>5.3</b>	11.71	8.4	<b>3.4</b>
<b>September</b>	13.19	5.2	<b>5.95</b>	12.75	3.7	<b>-2.3</b>
<b>October</b>	15.88	7.35	<b>5.46</b>	14.74	4.74	<b>-0.63</b>
<b>November</b>	7.54	5.81	<b>5.71</b>	4.08	1.13	<b>-3.1</b>
<b>December</b>	9.11	7.85	<b>8.04</b>	2.24	-4.29	<b>-4.96</b>
<b>Average</b>	<b>11.41</b>	<b>7.31</b>	<b>6.74</b>	<b>8.04</b>	<b>1.1</b>	<b>-2.44</b>

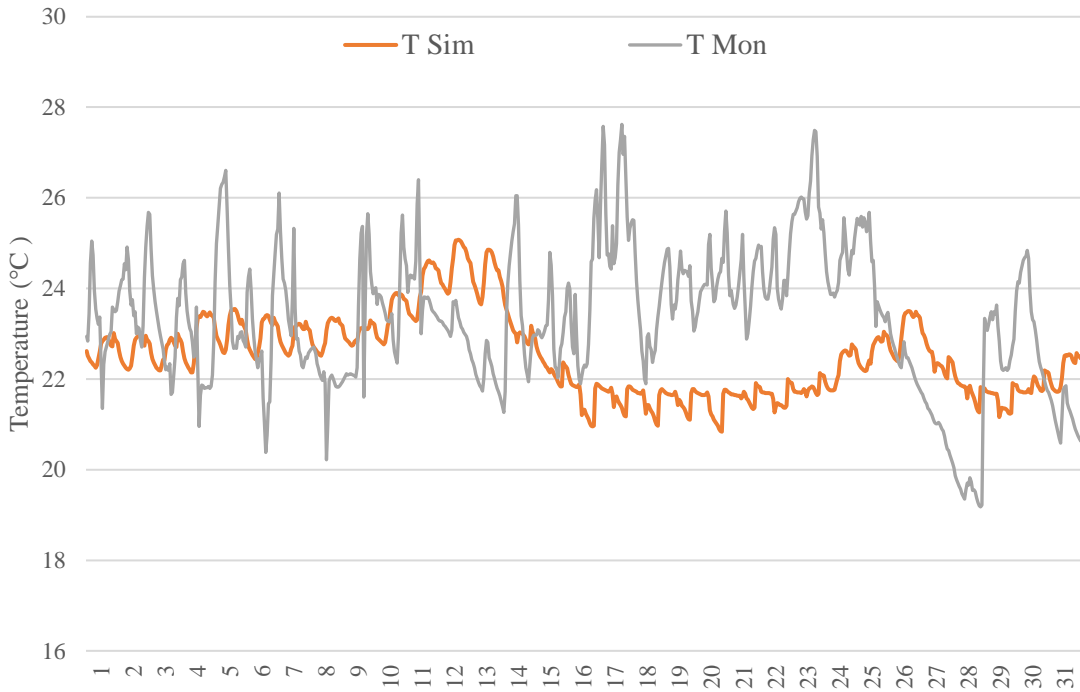


Figure 4.7. Simulated and monitored air temperature in January.

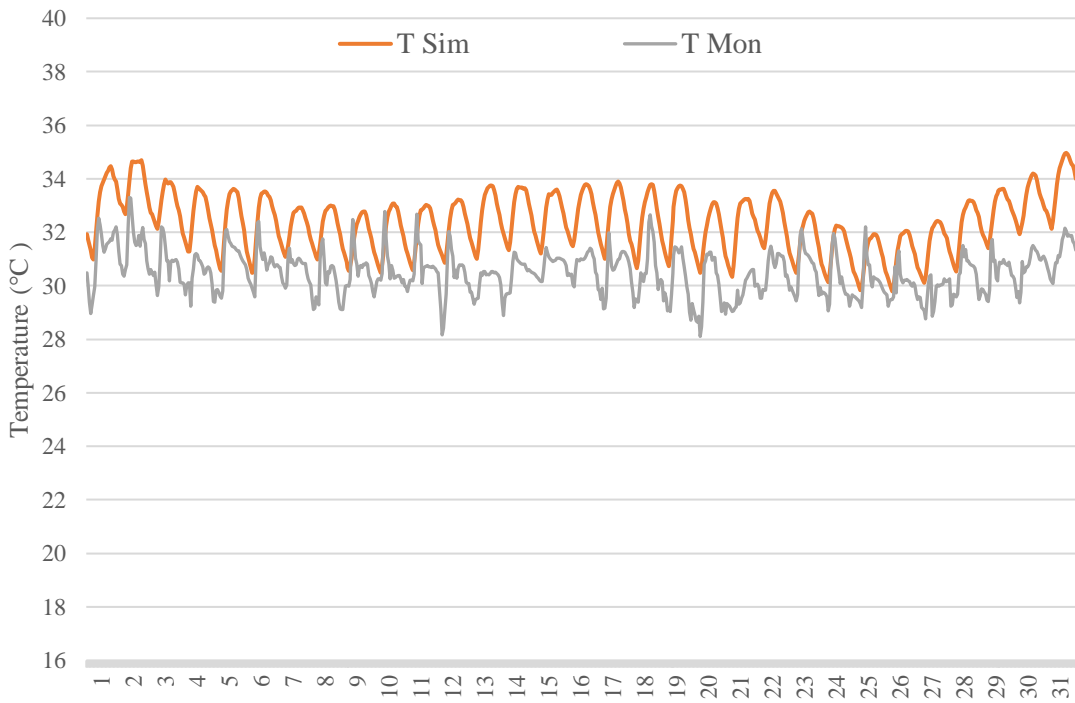


Figure 4.8. Simulated and monitored air temperature in July.

### 4.3. Results of Material Characterization

#### 4.3.1. Bulk Density

All hemp, clay and lime specimens were measured to find out their densities using the procedure explained in Section 2.1.1. The densities were found to be 115, 1200 and 540 kg/cm<sup>3</sup> for hemp, clay and lime, respectively. It is deduced that the hemp hurds as the main filler of the material are extremely lightweight with high porosity ratio, as it is mentioned in earlier studies (Jiang et al. 2018).

#### 4.3.2. Grain Size Distribution

The grain size distribution measurements were performed on the clay specimen which is the main binder of the composite material. Results of mechanical sieve analysis and hydrometer analysis were presented in Table 4.4 and Table 4.5. According to the results, the ratio of fine grains which is composed of silt and clay is 12.2 percent. Gradation curve also can be seen in Figure 4.9.

Table 4.4. Mechanical sieve analysis results.

<b>Diameter Of Grains (mm)</b>	<b>Mass Ratio (%)</b>
<b>2.00 – 0.85</b>	27.25
<b>0.85 – 0.43</b>	24.36
<b>0.43 – 0.25</b>	9.91
<b>0.25 – 0.075</b>	26.28
<b>&lt;0.075</b>	12.2

Table 4.5. Hydrometer analysis results.

t (min)	R (hydrometer reading)	L	Diameter (mm)	Percent Finer %
2	1.018	16.1341	0.0382	27.2
5	1.014	16.1347	0.0242	19.2
15	1.01	16.1354	0.0139	11.2
30	1.009	16.1355	0.0098	9.2
60	1.007	16.1359	0.0069	5.2
250	1.006	16.1360	0.00342	3.2

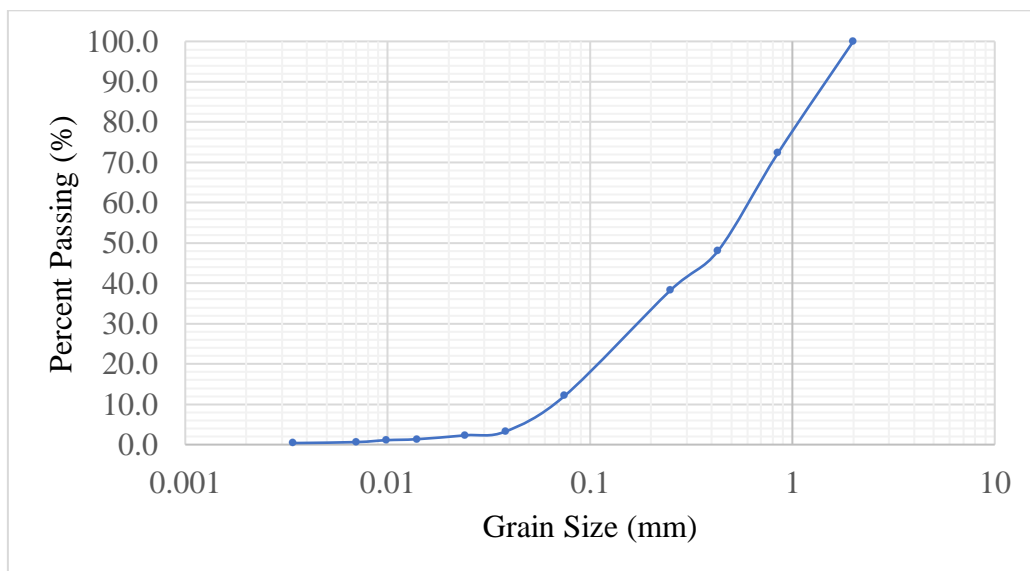


Figure 4.9. Grain size distribution curve according to both sieve and hydrometer analysis.

### 4.3.3. Chemical Composition

#### *X-Ray Diffraction (XRD)*

Clay and lime specimens were tested to find crystalline structures by X-Ray Diffraction (XRD). As can be seen in Figure 4.10, clay specimen contained clay and quartz minerals. Figure 4.11 showed that the lime was hydrated.

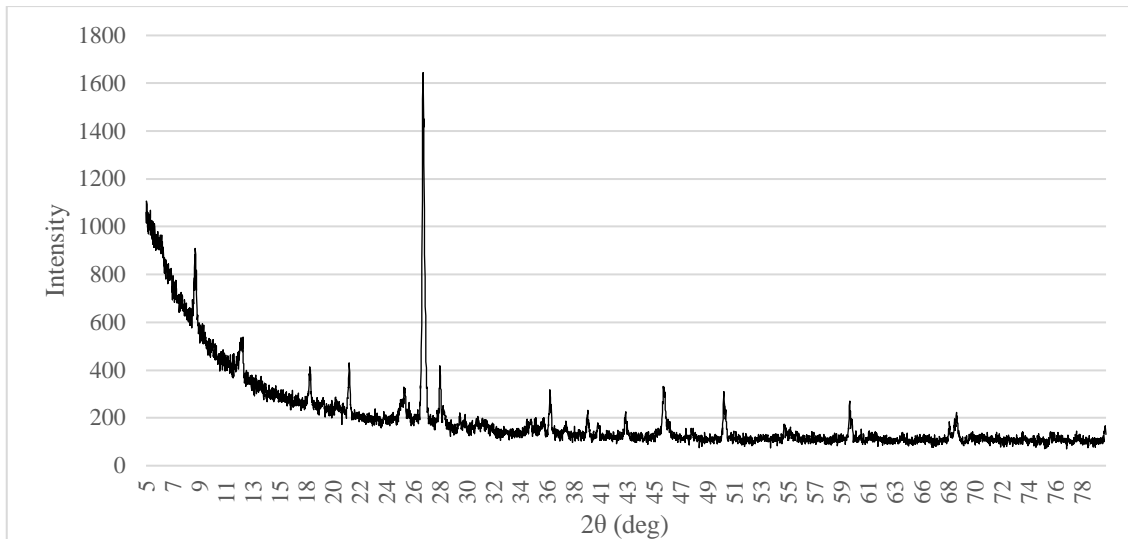


Figure 4.10. XRD pattern of clay specimen.

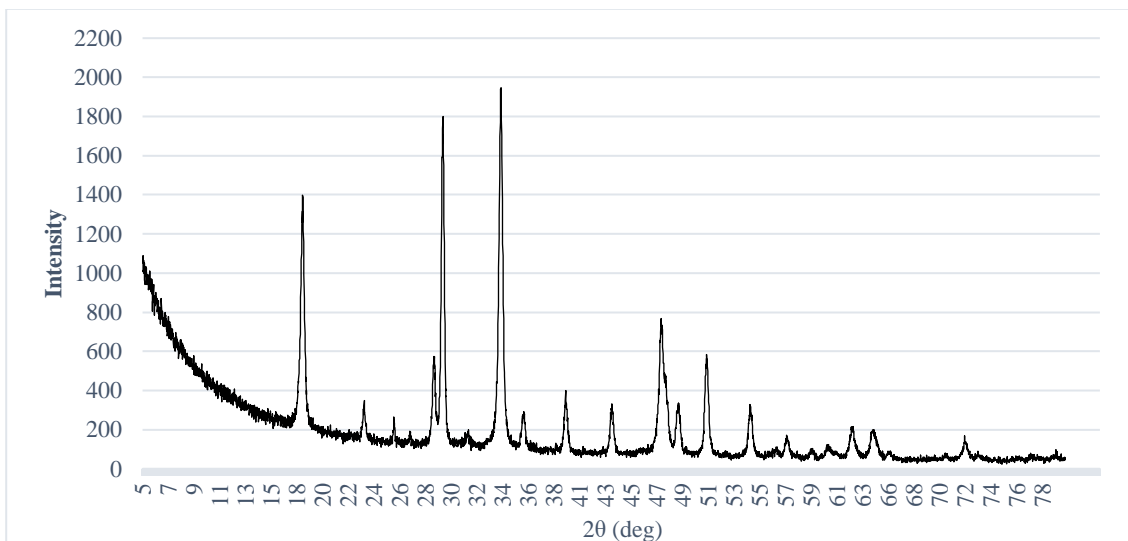


Figure 4.11. XRD pattern of lime specimen

### ***X-Ray Fluorescence (XRF)***

Table 4.6 and 4.7 shows the elemental compositions of clay and lime as the results of XRF tests. According to the XRF results of clay, silicon and aluminum constituted the large part of the material with the share of 55.48 and 27.37 %, respectively. Silicon and aluminum form clay silicates. High amount of SiO<sub>2</sub> and Al<sub>2</sub>O<sub>3</sub> show that the material is

a mix of quartz and clay. In addition, the presence of Al<sub>2</sub>O<sub>3</sub> contributes the strength of material (Müdüroğlu and Atak 1999).

On the other hand, lime specimen comprises high amount of calcium (89.97%) and small amount of sodium (6.69%) as expected.

Table 4.6. XRF results of clay specimen.

Symbol	Element	Percentage (Wt%)
SiO <sub>2</sub>	Silicon	55.48
Al <sub>2</sub> O <sub>3</sub>	Aluminum	27.37
Fe <sub>2</sub> O <sub>3</sub>	Iron	7.81
K <sub>2</sub> O	Potassium	3.18
MgO	Magnesium	2.73
CaO	Calcium	1.96
MnO	Manganese	0.09

Table 4.7. XRF results of lime specimen.

Symbol	Element	Percentage (Wt%)
CaO	Calcium	89.97
Na <sub>2</sub> O	Sodium	6.69
MgO	Magnesium	2.13
AL <sub>2</sub> O <sub>3</sub>	Aluminum	0.69
SO <sub>3</sub>	Sulfur	0.29
Fe <sub>2</sub> O <sub>3</sub>	Iron	0.17
CuO	Copper	0.069

### ***Scanning Electron Microscopy (SEM)***

SEM images of the three materials can be seen in Figure 4.12. It is clearly seen that the hemp has long fibres which are parallel to the surface of the hemp stalk, as the specimen is a chopped stalk. On the other hand, clay and lime specimens were in particle form.

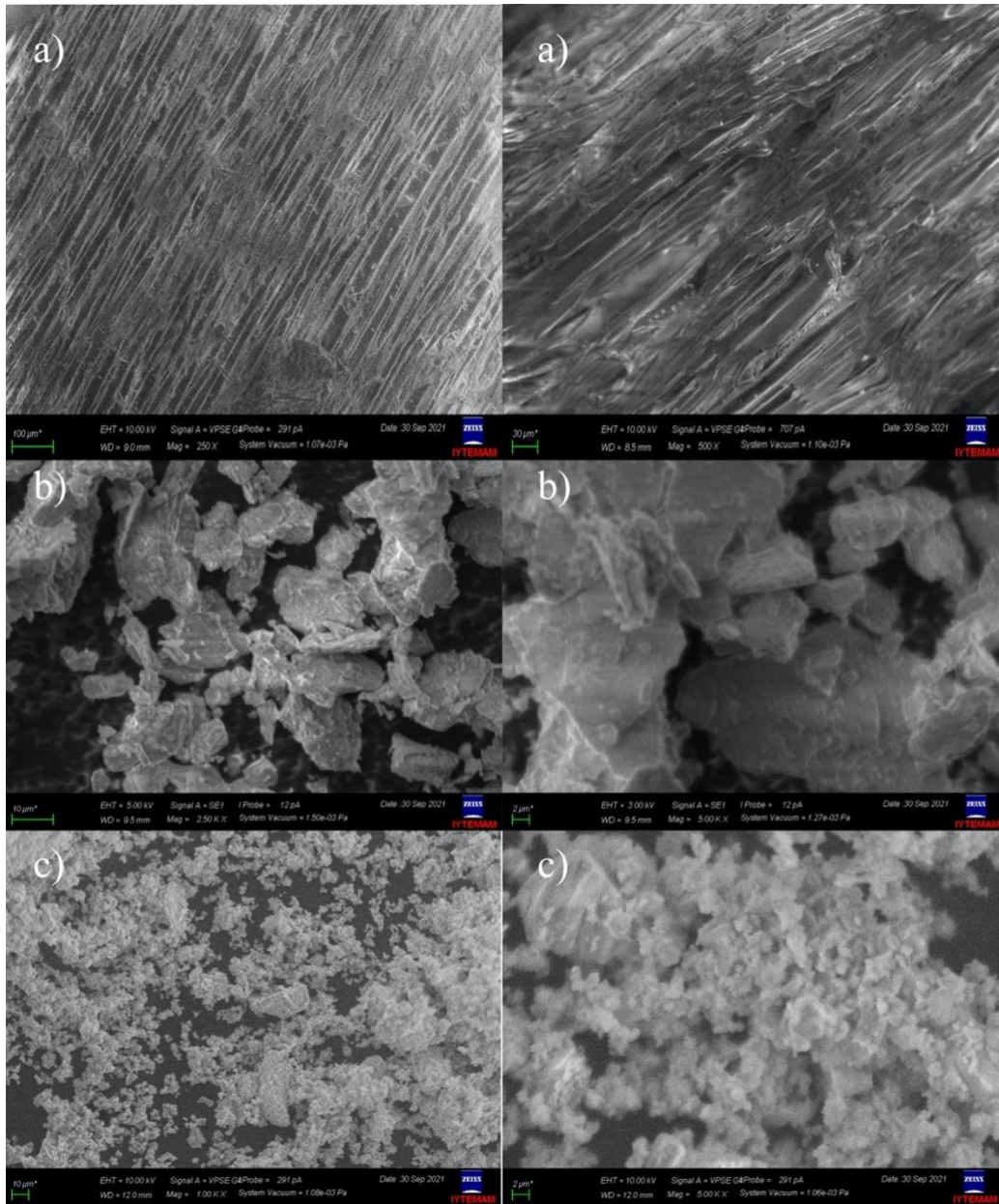


Figure 4.12. SEM images of hemp (a), clay (b) and lime (c).

#### 4.4. Results of Hemp-Clay Block Characterization

In this part of the study, the results which are obtained through material characterization tests on the hemp-clay blocks are presented and explained. Specific density and thermal conductivity values of the material samples with different hemp-clay compositions are evaluated.

#### 4.4.1. Specific Density

Total of 27 hemp-clay blocks were weighted before and after demoulding, and also after 1 month of drying. Densities were measured according to the procedure that is explained in section 3.2.4.1. Densities of each 3 blocks which have the exact mixture composition were averaged to find the ultimate density of samples. In Table 4.8, wet densities stand for the density right after demoulding of hemp-clay blocks while dry densities were measured after 1 month of drying of hemp-clay blocks.

Table 4.8. Density results of hemp-clay samples after demoulding and drying.

Sample Name	H:B	B:W	L	Wet Density (kg/m <sup>3</sup> )	Dry Density (kg/m <sup>3</sup> )	Water Loss (%)
H1B2W2	1:2	1:1	-	721	372	38
H1B2.5W2.5	1:2.5	1:1	-	902	448	42
H1B3W3	1:3	1:1	-	1045	495	43
H1B2W3	1:2	2:3	-	874	367	49
H1BL2W2	1:2	1:1	5	589	352	39
H1BL2.5W2.5	1:2.5	1:1	5	751	427	42
H1BL3W3	1:3	1:1	5	755	467	37
H1BL2W3	1:2	2:3	5	805	394	50
H1BL2W3_L10	1:2	2:3	10	798	400	49

(H:B : Hemp:Binder, B:W : Binder:Water in weight and L: Lime additive ratio in percentage)

According to these findings, wet density of hemp clay blocks varies between 1045 kg/m<sup>3</sup> and 589 kg/m<sup>3</sup> while dry densities change between 495 kg/m<sup>3</sup> and 352 kg/m<sup>3</sup>. For both conditions, densities vary depending on the ratio of clay and water in composition. While the binder ratio increases in the hemp-clay mixture, density of the material rises as expected. Decrease of the density can be explained by the low density of hemp hurds and by the high amount of hemp hurds in composition. This fact also has been mentioned in the previous studies of hempcrete and hemp-clay characterization (Mazhoud 2017).

The amount of water effects the wet density of the hemp-clay while it has not significant influence on dry density. Wet density of sample H1B2W2 was  $721 \text{ kg/m}^3$  while H1B2W3 had a density of  $874 \text{ kg/m}^3$ . On the contrary, these samples had the similar density values when dried. It is due to that hemp-clay blocks lose the water in their composition at a rate changing between 38 and 50% during drying (Table 4.8). More water in the composition resulted in more water loss at the end. Therefore, it can be deduced that hemp-clay blocks hold an amount of its water in equilibrium with the vapor in the air by evaporating the surplus. It may refer to the ability of hemp-clay to balance indoor humidity (Shea, Lawrence, and Walker 2012).

#### **4.4.2. Thermal Conductivity**

Hemp-clay samples produced for this study were tested for thermal properties after 1 month of drying. Total of 27 samples which were composed of 9 different mixture compositions were examined with quick thermal conductivity meter according to the procedure that is explained in Section 3.2.4.

Thermal conductivity values and densities of the samples were presented in Table 4.9. Thermal conductivity values of all hemp-clay blocks produced for this study varies between  $0.108 \text{ W/mK}$  and  $0.1457 \text{ W/mK}$ . The samples with the ratio of 1:2 hemp:binder for both series (H1C2W2 and H1B1W2) have the lowest thermal conductivity values among others while those with the ratio of 1:3 hemp:binder have the highest values of thermal conductivity. It is deduced that the binder amount in the composition has an impact to increase thermal conductivity value of the material. From a similar perspective, it is observed that high density results in high thermal conductivity, which is in strong relation with the clay amount. This result matches up with the previous studies in the literature (Fernea et al. 2019; Busbridge and Rhydwen 2010; Vincelas et al. 2017).

Changes in the thermal conductivity of the second series of hemp-clay blocks which have 5% lime additive in the binder can be seen in Figure 4.13. It is observed that thermal conductivity values of hemp-clay blocks was also influenced by the presence of the lime additive.

Table 4.9. Thermal conductivity results of hemp-clay samples.

Sample Name	H:B	B:W	L	Density (kg/m <sup>3</sup> )	Thermal Conductivity (W/mK)
H1B2W2	0.5	1	-	372	0.1183
H1B2.5W2.5	0.4	1	-	448	0.1355
H1B3W3	0.33	1	-	495	<b>0.1457</b>
H1B2W3	0.5	0.67	-	367	0.1303
H1BL2W2	0.5	1	5	352	<b>0.108</b>
H1BL2.5W2.5	0.4	1	5	427	0.1323
H1BL3W3	0.33	1	5	467	0.1371
H1BL2W3	0.5	0.67	5	394	0.1264
H1BL2W3_10	0.5	0.67	10	400	0.1203

(H:B : Hemp:Binder, B:W : Binder:Water in weight and L: Lime additive ratio in percentage)

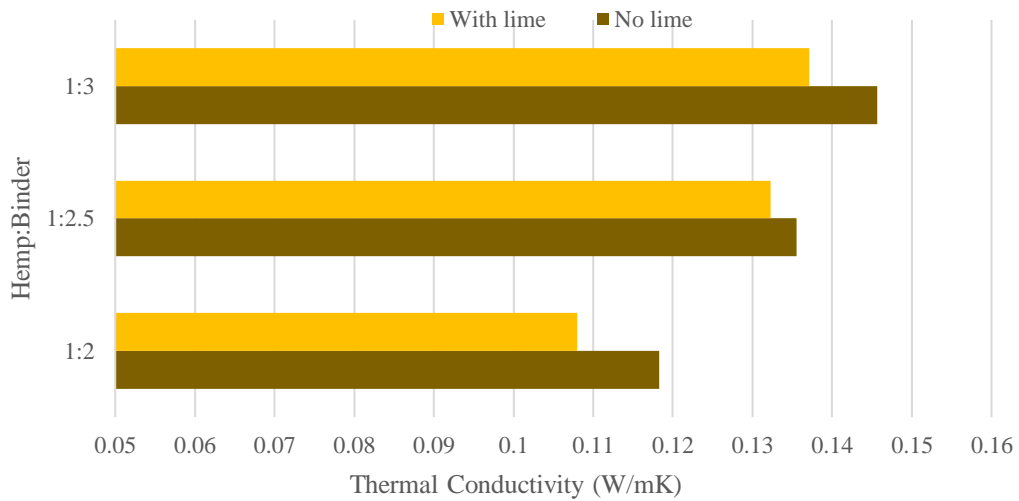


Figure 4.13. Effect of hemp:binder ratio and lime additive on thermal conductivity.

Even if the ratio of hemp:binder in composition was the same, hemp-clay blocks with the lime additive have lower thermal conductivity. 5% of lime addition in the composition of hemp-clay blocks decreases the thermal conductivity values by 5% in average. When the ratio of lime is increased to 10%, the change in thermal conductivity rises up to 7.6%.

## 4.5. Simulation Results

Annual energy consumption results of 24 scenarios are presented in Table 4.10. Simulation scenarios with 8 different wall infills were calculated for annual heating and cooling energy demands. These scenarios were also simulated with the predicted climate data of 2050 and 2080.

In 2020, the building with the hempcrete infill consumes the minimum energy with the value of 8822 kWh and so, reduces the energy consumption by 21.6%. Hempcrete scenario was simulated as being a reference of the targeted material. Besides, hemp-clay which is experimented for this study is seen as the second most energy-efficient material with the annual energy consumption of 9348 kWh. In comparison with the base scenario, hemp-clay wall infill helped to decrease heating, cooling and total energy consumption of the building with the ratio of 21.23%, 14.07% and 16.92%, respectively.

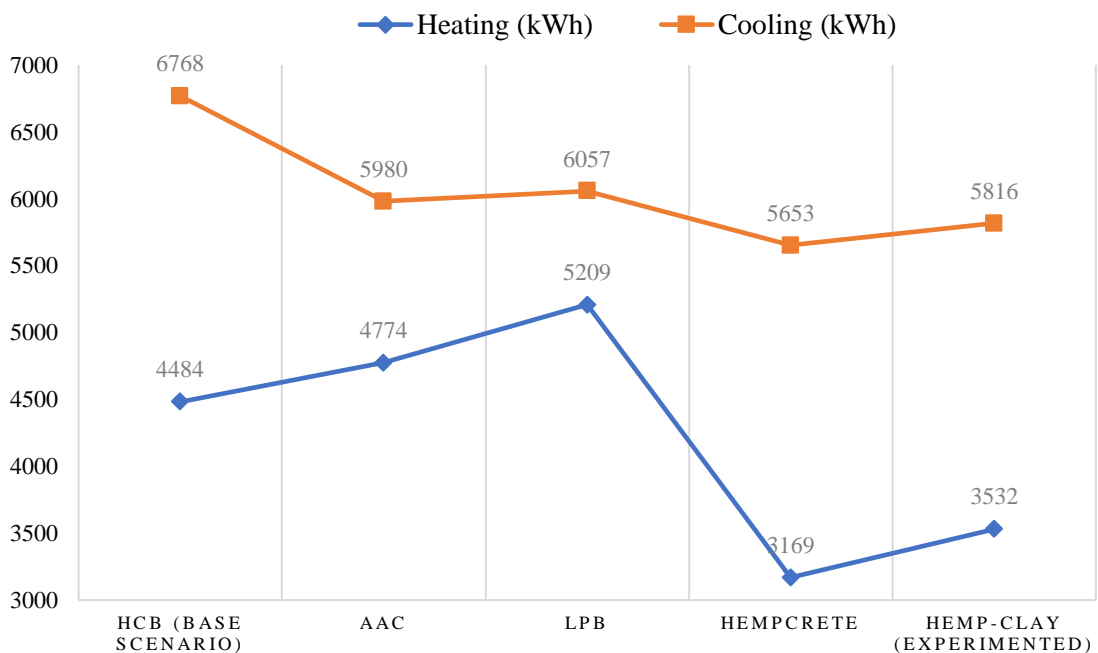


Figure 4.14. Heating and cooling energy consumption of different wall infills within the wall same thickness.

Table 4.10. Annual energy consumption results of all scenarios and change ratio according to the base scenario.

Climate Year	Simulation Scenario	Annual Energy Consumption			Change Ratio		
		Heating (kWh)	Cooling (kWh)	Total (kWh)	Heatin g (%)	Coolin g (%)	Total (%)
2020	HCB (base scenario)	4484	6768	11252	0.00	0.00	0.00
	AAC	4774	5980	10754	6.47	-11.64	-4.43
	LPB	5209	6057	<b>11266</b>	16.17	-10.51	0.12
	Hempcrete	3169	5653	<b>8822</b>	-29.33	-16.47	-21.60
	Hemp-clay (experimented)	3532	5816	9348	-21.23	-14.07	-16.92
	HCB +ins	4171	6442	10613	-6.98	-4.82	-5.68
	AAC +ins	3787	6064	9851	-15.54	-10.40	-12.45
	LPB +ins	3834	6178	10012	-14.50	-8.72	-11.02
2050	HCB (base scenario)	2122	12176	<b>14298</b>	0.00	0.00	0.00
	AAC	2280	11107	13387	7.45	-8.78	-6.37
	LPB	2520	11385	13905	18.76	-6.50	-2.75
	Hempcrete	1460	10104	<b>11564</b>	-31.20	-17.02	-19.12
	Hemp-clay (experimented)	1733	10458	12191	-18.33	-14.11	-14.74
	HCB +ins	1126	12479	13605	-46.94	2.49	-4.85
	AAC +ins	1744	11066	12810	-17.81	-9.12	-10.41
	LPB +ins	1755	11305	13060	-17.30	-7.15	-8.66
2080	HCB (base scenario)	1848	15005	<b>16853</b>	0.00	0.00	0.00
	AAC	1357	14009	15366	-26.57	-6.64	-8.82
	LPB	1497	14402	15899	-18.99	-4.02	-5.66
	Hempcrete	850	12641	<b>13491</b>	-54.00	-15.75	-19.95
	Hemp-clay (experimented)	955	13132	14087	-48.32	-12.48	-16.41
	HCB +ins	1121	14840	15961	-39.34	-1.10	-5.29
	AAC +ins	1011	14004	15015	-45.29	-6.67	-10.91
	LPB +ins	1013	14324	15337	-45.18	-4.54	-9.00

While AAC and LPB increase the heating demand of the building, in total AAC provides a fall by 4.43% and LPB does not make a significant change. The effect of wall options with the same thickness but different wall infill on heating and cooling consumptions can be seen in Figure 4.14. It is deduced that hempcrete targeted and hemp-clay experimented help to reduce heating consumption explicitly beyond AAC and LPB.

As expected, addition of EPS insulation in different thicknesses on HCB, AAC and LPB drops down the annual energy consumption (Table 4.10) In Figure 4.15, annual energy consumptions of different materials with and without the insulation layer were presented. It is considered to have the same U-value while determining the insulation thicknesses for wall options. Therefore, even if the wall options have the same U-value with HCB, AAC, LPB and hempclay infill, the annual energy consumption values range between 10163 kWh and 9348 kWh. In addition, hemp-clay material studied for this thesis gives the lowest value for annual energy consumption in the comparison. It is assumed that the difference in the thermal capacity values of these materials effects their thermal performance.

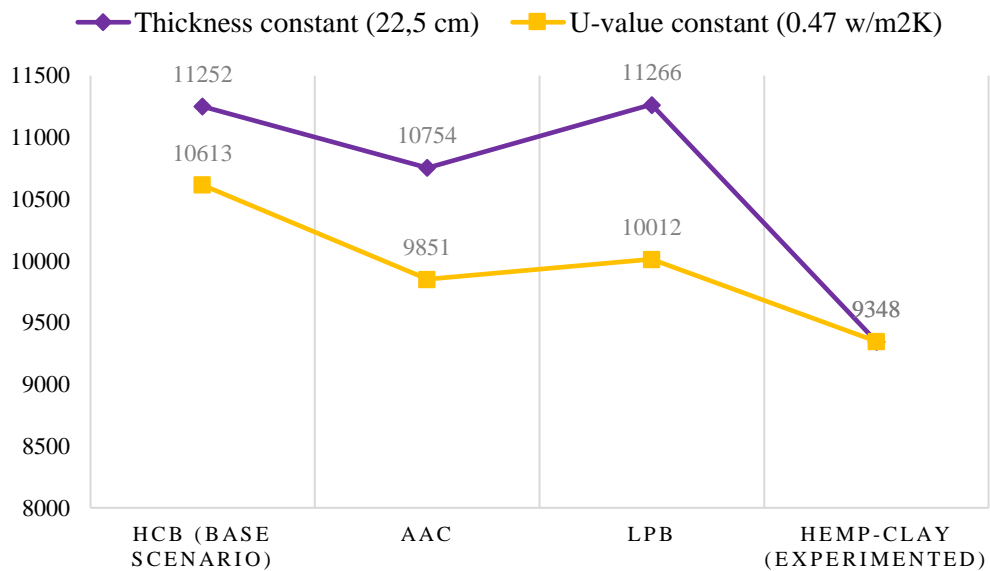


Figure 4.15. Annual energy consumptions of different wall infills with and without insulation layer.

Total of 8 wall options were simulated inserting the predicted climate data of 2050 and 2080 into the simulation model. Annual energy consumption of 5 wall options with the same thickness in 3 different years were imaged in Figure 4.16. According to results of 2050, annual energy consumptions increase in 30 years for all type of walls. It is observed that these rises are at a similar rate. It can be expressed that beyond the other, hemp-clay and hemp-crete show better energy performance in 2050 as well. This deduction is same for the results of year 2080.

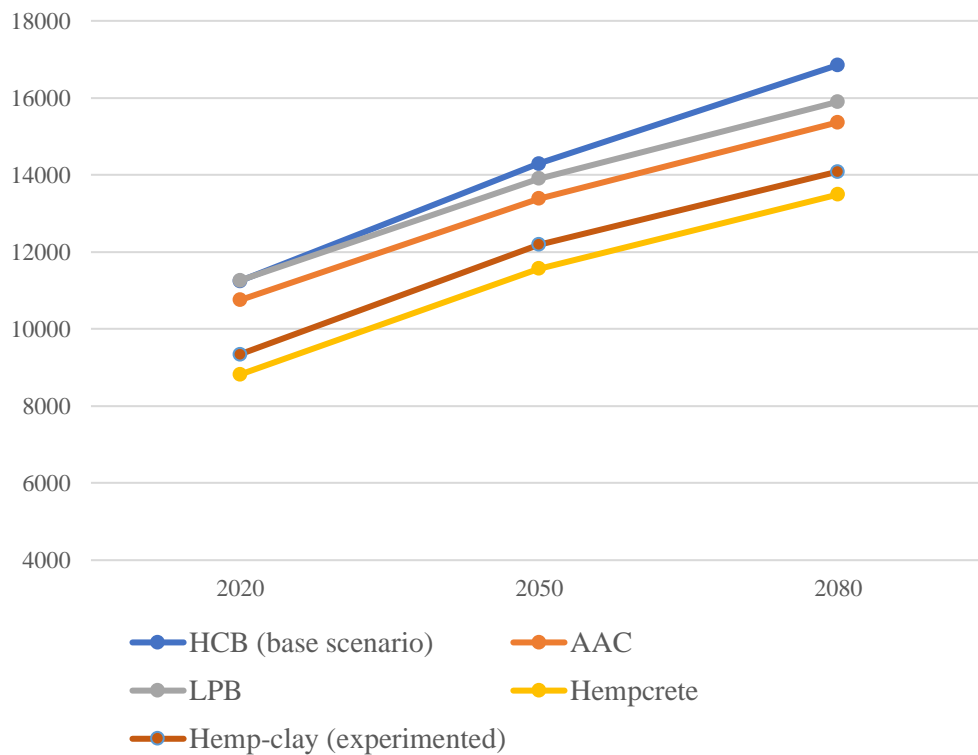


Figure 4.16. Annual energy consumptions of different wall infill materials in 2020, 2050 and 2080.

It is resulted that total energy demand of the case building with HCB will increase by 27.07% in 2050 and by 49.78% in 2080 (Table 4.11). Rates of increase in total annual energy demand for the climate of 2050 range between 23.42% and 31.08% for all wall options. Contary to the ranking on annual energy consumptions, it is observed that hempcrete and hemp-clay are more affected than other materials by the climate change.

Annual total energy consumptions of hempcrete and hemp-clay buildings will rise by 31.08% and 30.41% in 30 years, respectively. However, the values for these parameters still are the lowest among others. It means that hemp-based materials will show better performance in 2050 comparing to others, but they are slightly more vulnerable to be influenced by the climate change. This conclusion can be done for the results of 2080 as well.

Table 4.11. Annual energy consumption of 8 scenarios in 2020, 2050 and 2080 and their change ratios according to present.

	<b>2020</b>	<b>2050</b>		<b>2080</b>	
	<b>Annual Energy Consumption (kWh)</b>	<b>Annual Energy Consumption (kWh)</b>	<b>Change Ratio (%)</b>	<b>Annual Energy Consumption (kWh)</b>	<b>Change Ratio (%)</b>
<b>HCB (base scenario)</b>	11252	14298	27.07	16853	49.78
<b>AAC</b>	10754	13387	24.48	15366	42.89
<b>LPB</b>	11266	13905	23.42	15899	41.12
<b>Hempcrete</b>	8822	11564	31.08	13491	52.92
<b>Hemp-clay (experimented)</b>	9348	12191	30.41	14087	50.70
<b>HCB +ins</b>	10613	13605	28.19	15961	50.39
<b>AAC +ins</b>	9851	12810	30.04	15015	52.42
<b>LPB +ins</b>	10012	13060	30.44	15337	53.19

Besides the rises in total energy consumption, heating energy demands of the scenarios will decrease sharply in years. Heating energy consumption values of scenarios with different wall materials were put in a graph to compare (Figure 4.17). Ranking of wall scenarios will not change in 2050 regarding the heating energy consumptions. Nevertheless, it is observed that LPB shows better performance than HCB to reduce heating energy demand in 2080.

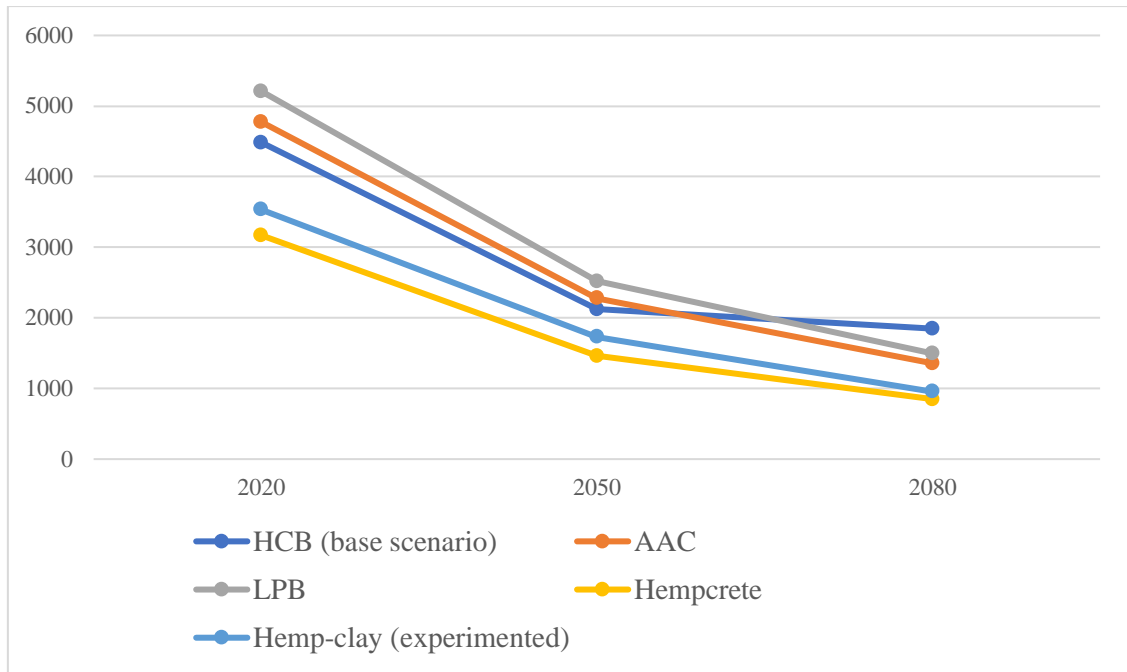


Figure 4.17. Heating energy consumptions of different wall infills in 2020, 2050 and 2080.

# CHAPTER 5

## CONCLUSION

### 5.1. Concluding Regarding the Results

The energy efficiency of building materials is a key concept for the construction sector on the way to achieving sustainability targets. Sustainable materials with high thermal insulation properties, low embodied energy and low-carbon footprint need to be improved urgently to reduce the factors that cause climate change and to build a habitable future. This study questions if hemp-clay building material has the potential to be replaced with existing energy-intensive building materials. The investigation is based on the characterization of hemp-clay building material and comparative energy performance.

In this section, conclusion remarks according to the results that were presented in Chapter 4 were listed based on the research questions in Chapter 1.

- ***What are the physical properties of local hemp and clay?***

According to the results of characterization tests of raw materials, hemp hurds produced from local hemp is lightweight with a density of  $115 \text{ kg/cm}^3$ . Its texture which is similar to wood chips was imaged in scanning electron microscopy. Its long fibrous structure is parallel in the direction that hemp stalks extend and is full of pores shaping like a pipe. It is deduced that the hemp hurds has a high capacity for water absorption according to the results of the density measurement of hemp-clay block samples in Chapter 3.

On the other hand, the clay sample has a density of  $1200 \text{ kg/cm}^3$ . With the method of XRD and XRF, it is observed that the clay sample is a mix of quartz and clay.

- ***In which proportions should hemp and clay combine to be shaped a block?***

For this study, hemp and clay were mixed in ratios of 1:2, 1:2.5 and 1:3. They were defined as workable proportions after several attempts of mixing and molding.

All compositions for this study are suitable to shape a block or any type of wall. In the trial of a ratio of 1:1 hemp:binder, the binder was not in enough amount to connect all hemp hurds together. The ratio of 1:4 hemp:binder was not included in this study.

- ***How does the amount of water or lime affect the drying?***

Observations on drying were made according to the results of water loss after 28 days. It is noticed that the surplus of water in the composition that was absorbed by hemp hurds was evaporated during drying to reach equilibrium with the vapor in the air. Hence, it can be deduced that after 28 days, the densities of the blocks with low and high amounts of water were the same. In addition, when comparing two series with and without lime additive, it is seen that the water loss percentage slightly changed. Therefore, it is confirmed that the water or lime amount does not have a significant effect on drying conditions in this case. Further analysis on hygric properties needs to be done.

- ***How does a small amount of lime change the thermal properties of the material?***

According to the findings of thermal conductivity tests, 5% lime additive in binder reduces the thermal conductivity value by 5%. This alteration can be higher with more addition of lime.

- ***How do the hemp:binder and binder:water ratio affect the density and the thermal conductivity of the novel material?***

As expected, any increase in binder amount results in higher thermal conductivity and density values in hemp-clay materials. While the hemp:binder ratio decreases, the thermal conductivity and density of hemp-clay increase.

On the other hand, it is deduced that the binder:water ratio does not have a significant effect on the density of the dried hemp-clay blocks. However, it is observed that the thermal conductivity value of the blocks that were produced with more water is higher. This could be a result of the different drying requirements of the blocks. The measurements done for this study were not sufficient to make a conclusion on this relationship.

- ***In the end, in which interval do the densities and thermal conductivities of hemp-clay blocks range?***

Densities of the hemp-clay materials which were tested for this study were found between 352 and 495 kg/cm<sup>3</sup> while thermal conductivity values range between 0.108 and 0.1457 W/mK.

- ***Do hemp-clay wall blocks increase the thermal resistance of a wall and decrease the energy consumption of a building?***

Hemp-clay blocks can increase the thermal resistance of a wall with their low thermal conductivity value. Without any insulation layers, a wall that is infilled with hemp-clay blocks has a U-value of 0.47 W/mK. The suggested U-value of an external wall in the Izmir region was defined as 0.7 W/mK in TS-825.

- ***Do hemp-clay building materials show better thermal performance in comparison with hollow clay brick (HCB), aerated autoclaved concrete (AAC), and lightweight pumice blocks (LPB)?***

According to simulation results in section 4.5, the hemp-clay blocks reduced the heating, cooling, and total energy consumption of the case building by 21%, 14% and 16%, respectively when compared with the results of the base scenario. When the wall thicknesses are the same, and any insulation layer was not added to the wall options, the change ratios for the scenarios of AAC and LPB were far lower than hemp-clay's. Therefore, it can be confirmed that hemp-clay building material shows better thermal performance than other conventional materials.

- ***Having the same U-value in the wall, how does the thermal capacity of the materials affect energy consumption?***

According to the data entered in the simulation model, the specific heat capacity of hemp-clay material was higher than others, which is 1550 J/kgK. Even if an insulation layer was added to the external surfaces of other wall options and they have the same U-value, hemp-clay provided better insulation in both cases. It is assumed that the thermal capacity of the hemp-clay wall could affect the energy consumption results.

- *In future climates, 2050's and 2080's, what is the most energy-efficient wall material among them? Could hemp-clay replace the others in the future?*

In 2050 and 2080, due to climate change, heating energy demands drop down and cooling energy demand rises for all cases. The scenario with hemp-clay wall infill material consumes the minimum energy for both heating and cooling in 2050 and 2080, after hempcrete. It can be deduced that hempcrete is the most energy-efficient wall material according to the results of this study. However, hemp-clay show better thermal performance among other conventional materials at present, also in 2050 and 2080. It is suggested that hemp-clay has the potential to be the material of the future and needs to be studied further.

## **5.2. Further Study**

Considering the results of this study, many other studies could be conducted as follows:

- Regarding the material characterization of the hemp-clay building block, 8 different mixture compositions were experienced for this research. For future work, more samples in different compositions could be produced and tested to find a good agreement between the thermal conductivity and mechanical strength or to reach out the suitable material properties for specific uses in the building.
- Density measurements and thermal conductivity tests of the novel material were done in this study. However, the mechanical strength, thermal capacity and moisture buffer values of the novel hemp-clay building block need to be investigated to assess the performance in the strict sense for further studies.
- In specific to the case building of this study, the influence of hemp-clay building block on the energy consumption of the whole building when it is used only in specific façades of the building could also be a topic of another research.
- The benefits of hemp-clay building blocks in reducing energy consumption in buildings were clarified. Indeed, assessing the environmental performance of this material in a broader context could grow up its benefits. In this regard, the life

cycle assessment of the hemp-clay building block could be helpful in future work to improve the hemp-clay.

- As the hemp-clay building block is a natural material produced with raw materials that do not need any heating process, it can be suitable to be reshaped after demolition. Therefore, the recyclability of this building material and its benefits to the circular economy approach could be an interesting topic for future studies.

## REFERENCES

- Ahlberg, Johan, Elza Georges, and Mikael Norlén. 2014. “The Potential of Hemp Buildings in Different Climates : A Comparison between a Common Passive House and the Hempcrete Building System.”
- Ahmed, A T M Faiz, Md Zahidul Islam, Md Sultan Mahmud, Md Emdad Sarker, and Md Reajul Islam. 2022. “Hemp as a Potential Raw Material toward a Sustainable World: A Review.” *Heliyon* 8 (1): e08753.  
<https://doi.org/10.1016/j.heliyon.2022.e08753>.
- Akpınar, Deniz, and Ahmet Nizamoğlu. 2019. “Osmanlı’dan Cumhuriyete Kenevir Üretimi.” *Turkish Studies-Social Sciences* Volume 14 Issue 4 (Volume 14 Issue 4): 1123–1236. <https://doi.org/10.29228/TurkishStudies.23448>.
- Allin, Steve. 2005. *Building With Hemp*. 2nd ed. SEED Press.
- American Lime Technology. n.d. “Hemclad Pre-Cast Wall Systems.” Accessed February 28, 2022. <http://www.americanlimetechnology.com/tradical-hemclad/>.
- Arnaud, L., and V. Cerezo. 2002. “Mechanical, Thermal, and Acoustical Properties of Concrete Containing Vegetable Particles.” In “*SP-209: ACI Fifth Int Conf Innovations in Design with Emphasis on Seismic, Wind and Environmental Loading, Quality Con.*” Vol. 209. American Concrete Institute.  
<https://doi.org/10.14359/12499>.
- Arnaud, Laurent, and Etienne Gourlay. 2012. “Experimental Study of Parameters Influencing Mechanical Properties of Hemp Concretes.” *Construction and Building Materials* 28 (1): 50–56.  
<https://doi.org/10.1016/j.conbuildmat.2011.07.052>.
- ASHRAE14-2002. 2002. *Measurement of energy and demand savings*. ASHRAE Standards Committee.
- Aydoğan, Mehmet, Yunus Emre Terzi, Şahin Gizlenci, Mustafa Acar, Alpay Esen, and Hüseyin Meral. 2020. “Türkiye’de Kenevir Yetiştiriciliğinin Ekonomik Olarak Yapılabilirliği: Samsun İli Vezirköprü İlçesi Örneği.” *ANADOLU JOURNAL OF AGRICULTURAL SCIENCES*, February, 35–50.  
<https://doi.org/10.7161/omuanajas.602585>.

- Aytaç, Selim, Ali Kemal Ayan, and Ş. Funda Arslanoğlu. 2017. “Endüstriyel Tip Kenevir (*Cannabis Sativa* L.) Yetiştiriciliği.” In *KARADENİZ’İN LİF BİTKİLERİ ÇALIŞTAYI Keten – Kenevir – Isırgan*, 27–35. Samsun.  
[https://www.researchgate.net/publication/323541469\\_karadenizin\\_lif\\_bitkileri\\_calistayi\\_Keten-Kenevir-Isirgan/link/5a9b01cd45851586a2ac23bd/download](https://www.researchgate.net/publication/323541469_karadenizin_lif_bitkileri_calistayi_Keten-Kenevir-Isirgan/link/5a9b01cd45851586a2ac23bd/download).
- Balčiūnas, Giedrius, Sigitas Vėjelis, Saulius Vaitkus, and Agnė Kairytė. 2013. “Physical Properties and Structure of Composite Made by Using Hemp Hurds and Different Binding Materials.” *Procedia Engineering* 57: 159–66.  
<https://doi.org/10.1016/j.proeng.2013.04.023>.
- Başer, Uğur, and Mehmet Bozoğlu. 2020. “Türkiye’nin Kenevir Politikası ve Piyasasına Bir Bakış.” *Tarım Ekonomisi Araştırmaları Dergisi*. Tarımsal Ekonomi ve Politika Geliştirme Enstitüsü Müdürlüğü.
- Ben-Alon, Lola. 2020. “Natural Buildings: Integrating Earthen Building Materials and Methods Into Mainstream Construction.” Doctoral Dissertation, Carnegie Mellon University.
- Benfratello, S., C. Capitano, G. Peri, G. Rizzo, G. Scaccianoce, and G. Sorrentino. 2013. “Thermal and Structural Properties of a Hemp–Lime Biocomposite.” *Construction and Building Materials* 48 (November): 745–54.  
<https://doi.org/10.1016/j.conbuildmat.2013.07.096>.
- Bevan, Rachel, and Tom Woolley. 2008. *Hemp Lime Construction: A Guide to Building with Hemp Lime Composites*. 1st ed. London: BRE Press.
- Biokenevir. n.d. “Kenevir Ürünleri.” Accessed April 3, 2022.  
<http://biokenevir.com/kenevir-urunleri.html>.
- Bruijn, Paulien de. 2008. “Hemp Concretes Mechanical Properties Mechanical Properties Using Both Shives and Fibres Using Both Shives and Fi.” Licentiate Thesis, Sweden: Swedish University of Agricultural Sciences.
- Brümmer, Monika, M<sup>a</sup> Paz Sáez-Pérez, and Jorge Durán Suárez. 2018. “Hemp-Clay Concretes for Environmental Building—Features That Attribute to Drying, Stabilization with Lime, Water Uptake and Mechanical Strength.” In *Advances in Natural Fibre Composites*, 249–65. Cham: Springer International Publishing.  
[https://doi.org/10.1007/978-3-319-64641-1\\_21](https://doi.org/10.1007/978-3-319-64641-1_21).
- Busbridge, Ruth, and Ranyl Rhydwen. 2010. “An Investigation of the Thermal Properties of Hemp and Clay Monolithic Walls,” August.

- Busbridge, Ruth. 2009. "Hemp-Clay: An Initial Investigation into the Thermal, Structural and Environmental Credentials of Monolithic Clay and Hemp Walls." MSc Thesis, London: University of East London.
- Cannabric. n.d. "Cannabric : Hempbrick (Bearing +loadbearing." Accessed March 4, 2022.  
[http://www.cannabric.com/catalogo/cannabric\\_bloque\\_de\\_canamo\\_autoportante\\_portante/](http://www.cannabric.com/catalogo/cannabric_bloque_de_canamo_autoportante_portante/).
- Cerezo, Véronique. 2005. "Propriétés Mécaniques, Thermiques et Acoustiques D'un Matériau À Base de Particules Végétales: Approche Expérimentale et Modélisation Théorique."
- Cherney, Jerome, and Ernest Small. 2016. "Industrial Hemp in North America: Production, Politics and Potential." *Agronomy* 6 (4): 58.  
<https://doi.org/10.3390/agronomy6040058>.
- Collet, Florence, and Sylvie Pretot. 2014. "Effect of Temperature on Moisture Buffering of Hemp Concrete." In *10th Nordic Symposium on Building Physics*. Lund, Sweden.
- Collet, Florence, Julien Chamoin, Sylvie Pretot, and Christophe Lanos. 2013. "Comparison of the Hygric Behaviour of Three Hemp Concretes." *Energy and Buildings* 62 (July): 294–303. <https://doi.org/10.1016/j.enbuild.2013.03.010>.
- Cordier, S. 1999. *Caractérisation Thermique et Mécanique Des Bétons de Chanvre*.
- Courgey, S. 1993. *La Construction de Murs À Base de Fibres de Chanvre*.
- Degrave-Lemeurs, Matthias, Philippe Glé, and Arthur Hellouin de Menibus. 2018. "Acoustical Properties of Hemp Concretes for Buildings Thermal Insulation: Application to Clay and Lime Binders." *Construction and Building Materials* 160 (January): 462–74. <https://doi.org/10.1016/j.conbuildmat.2017.11.064>.
- Delannoy, Guillaume, Sandrine Marceau, Philippe Glé, Etienne Gourlay, Marielle Guéguen Minerbe, Dinarzed Diafi, Issam Nour, Sofiane Amziane, and Fabienne Farcas. 2017. "Multi-Scale Analysis of Hemp-Based Insulation Materials."
- ECI. n.d. "Products Details." Accessed April 21, 2022.  
<https://www.eci.com.tr/productdetail/sheep-wool-insulation-batt-blanket>.
- Elfordy, S., F. Lucas, F. Tancret, Y. Scudeller, and L. Goudet. 2008. "Mechanical and Thermal Properties of Lime and Hemp Concrete ('Hempcrete') Manufactured by a Projection Process." *Construction and Building Materials* 22 (10): 2116–23. <https://doi.org/10.1016/j.conbuildmat.2007.07.016>.

- Evrard, Arnaud, and André Herde. 2005. "Bioclimatic Envelopes Made of Lime and Hemp Concrete."
- Evrard, Arnaud. 2003. "Bétons de Chanvre : Synthèse Des Propriétés Physiques, Association Construire En Chanvre."
- Evrard, Arnaud. 2006. "Sorption Behaviour of Lime-Hemp Concrete and Its Relation to Indoor Comfort and Energy Demand." In *The 23rd Conference on Passive and Low Energy Architecture*, Geneva, Switzerland.
- Fawzy, Samer, Ahmed I. Osman, John Doran, and David W. Rooney. 2020. "Strategies for Mitigation of Climate Change: A Review." *Environmental Chemistry Letters* 18 (6): 2069–94. <https://doi.org/10.1007/s10311-020-01059-w>.
- Ferne, Raluca, Daniela Lucia Manea, Daniela Roxana Tămaș-Gavrea, and Ioan Călin Roșca. 2019. "Hemp-Clay Building Materials - An Investigation on Acoustic, Thermal and Mechanical Properties." *Procedia Manufacturing* 32: 216–23. <https://doi.org/10.1016/j.promfg.2019.02.205>.
- Garcia-Jaldon, C. 1992. "Caractérisation Morphologique et Chimique Du Chanvre (Cannabis Sativa) Pré-Traitement À La Vapeur et Valorisation." Doctoral Dissertation, Grenoble: Université de Grenoble.
- Glass, Jacqueline, Andrew R.J. Dainty, and Alistair G.F. Gibb. 2008. "New Build: Materials, Techniques, Skills and Innovation." *Energy Policy* 36 (12): 4534–38. <https://doi.org/10.1016/j.enpol.2008.09.016>.
- Glé, P., E. Gourdon, and L. Arnaud. 2011. "Acoustical Properties of Materials Made of Vegetable Particles with Several Scales of Porosity." *Applied Acoustics* 72 (5): 249–59. <https://doi.org/10.1016/j.apacoust.2010.11.003>.
- Glé, Philippe, Gaudrey Massossa-Telo, Arthur Hellouin de Menibus, Matthias Degrave-Lemeurs, and Emmanuel Gourdon. 2021. "Characterization and Modelling of the Sound Reduction of Hemp-Clay Walls in Buildings." *Journal of Building Engineering* 40 (August): 102315. <https://doi.org/10.1016/j.job.2021.102315>.
- Gołębiewski, Michał. 2018. "Hemp-Lime Bio-Composites – Review and Analysis of World-Wide Architectural Examples." In *Proceedings (International Youth Science Forum "Litteris et Artibus")*. 2018. №1, 51–54. Lviv Polytechnic National University. <https://doi.org/10.23939/lea2018.01.051>.

- Grimes, J, R Walker, S Pavía, and Oliver Kinnane. 2013. “In Situ Measurement of the Sound Absorption Characteristics of Existing Building Fabrics.” In *Proceedings of the Institute of Acoustics*, 35:280–88.
- Haik, R., A. Peled, and I.A. Meir. 2020. “The Thermal Performance of Lime Hemp Concrete (LHC) with Alternative Binders.” *Energy and Buildings* 210 (March): 109740. <https://doi.org/10.1016/j.enbuild.2019.109740>.
- Hamard, Erwan, Bogdan Cazacliu, Andry Razakamanantsoa, and Jean-Claude Morel. 2016. “Cob, a Vernacular Earth Construction Process in the Context of Modern Sustainable Building.” *Building and Environment* 106 (September): 103–19. <https://doi.org/10.1016/j.buildenv.2016.06.009>.
- Hammond, G. P., and C. I. Jones. 2008. “Embodied Energy and Carbon in Construction Materials.” *Proceedings of the Institution of Civil Engineers - Energy* 161 (2): 87–98. <https://doi.org/10.1680/ener.2008.161.2.87>.
- Hemp Block Australia. n.d. “Hemp Block.” Accessed February 28, 2022. <https://hempblockaustralia.com/hemp-block/#data-sheets>.
- Hemp Block USA. n.d. “Hemp Block.” Accessed April 5, 2022. <https://hempblockusa.com/hemp-block/#product-range>.
- Hemp New Zealand. n.d. “The Plant.” <https://hempenz.co.nz/learn/the-plant/>.
- Hempire. n.d. “Hemp Lime Plaster.” Accessed April 21, 2022. <https://hempire.tech/products/hemp-lime-plaster>.
- Hempitecture. n.d. “Hemp Lime Building Systems.” Accessed July 27, 2021. <https://www.hempitecture.com/hempcrete>.
- Hirst, Edward A. J. 2013. “Characterisation of Hemp-Lime as a Composite Building Material.” Doctoral Dissertation, Bath: University of Bath. [https://hempinabox.be/images/pdf/UnivBath\\_PhD\\_2013\\_E\\_Hirst.pdf](https://hempinabox.be/images/pdf/UnivBath_PhD_2013_E_Hirst.pdf).
- Hirst, Edward, Pete Walker, Kevin Paine, and Tim Yates. 2010. “Characterisation of Low Density Hemp-Lime Composite Building Materials under Compression Loading,” August.
- Hu, Ming. 2020. “A Building Life-Cycle Embodied Performance Index—The Relationship between Embodied Energy, Embodied Carbon and Environmental Impact.” *Energies* 13 (8): 1905. <https://doi.org/10.3390/en13081905>.

- International Energy Agency (IEA). 2016. "Evaluation of Embodied Energy and CO<sub>2</sub>eq for Building Construction (Annex 57)." Tokyo. [http://www.iea-ebc.org/Data/publications/EBC\\_Annex\\_57\\_Results\\_Overview.pdf](http://www.iea-ebc.org/Data/publications/EBC_Annex_57_Results_Overview.pdf).
- IPCC. 2014. "Climate Change 2014: Synthesis Report." Geneva, Switzerland. [https://www.ipcc.ch/site/assets/uploads/2018/02/SYR\\_AR5\\_FINAL\\_full.pdf](https://www.ipcc.ch/site/assets/uploads/2018/02/SYR_AR5_FINAL_full.pdf).
- Isohemp. 2022. "Technical Documentation." 2022. <https://www.iso hemp.com/en/technical-documentation>.
- Izoguard. n.d. "Keten Yalıtım." Accessed April 1, 2022. <https://www.izoguard.com.tr/keten-yalitim>.
- Jami, Tarun, S.R. Karade, and L.P. Singh. 2019. "A Review of the Properties of Hemp Concrete for Green Building Applications." *Journal of Cleaner Production* 239 (December): 117852. <https://doi.org/10.1016/j.jclepro.2019.117852>.
- Jiang, Y., M. Lawrence, M. P. Ansell, and A. Hussain. 2018. "Cell Wall Microstructure, Pore Size Distribution and Absolute Density of Hemp Shiv." *Royal Society Open Science* 5 (4): 171945. <https://doi.org/10.1098/rsos.171945>.
- Johnson, Renée. 2014. "Hemp as an Agricultural Commodity." In . Library of Congress Washington DC Congressional Research Service. [https://www.oran.org.tr/images/dosyalar/20190318134910\\_0.pdf](https://www.oran.org.tr/images/dosyalar/20190318134910_0.pdf).
- Jones, Dennis, and Christian Brischke. 2017. *Performance of Bio-Based Building Materials*. 1st ed. Woodhead Publishing.
- JustBioFiber. n.d. "Product Specifications." Accessed February 28, 2022. <http://justbiofiber.ca>.
- Kara, Feride Çiğdem, and Merve Tuna Kayılı. 2021. "Yapı Malzemelerine Sürdürülebilir Mimarlık Bağlamında Bütüncül Bir Bakış: Duvar Malzemelerinin Çevresel Etkilerinin ve Enerji Performansının Belirlenmesi." *European Journal of Science and Technology*, December. <https://doi.org/10.31590/ejosat.1015367>.
- Karche, Tahseen, and Manager Rajdeo Singh. 2019. "The Application of Hemp (Cannabissativa L.) for a Green Economy: A Review." *TURKISH JOURNAL OF BOTANY* 43 (6): 710–23. <https://doi.org/10.3906/bot-1907-15>.
- Kaya, Seher, and Eren Oner. 2020. "Kenevir Liflerinin Eldesi, Karakteristik Özellikleri ve Tekstil Endüstrisindeki Uygulamaları." *Mehmet Akif Ersoy Üniversitesi Fen Bilimleri Enstitüsü Dergisi*. Burdur Mehmet Akif Ersoy Üniversitesi. <https://doi.org/10.29048/makufebed.693406>.

- Kinnane, Oliver, Aidan Reilly, John Grimes, Sara Pavia, and Rosanne Walker. 2016. "Acoustic Absorption of Hemp-Lime Construction." *Construction and Building Materials* 122 (September): 674–82. <https://doi.org/10.1016/j.conbuildmat.2016.06.106>.
- Lane, Thomas. 2022. "Hempcrete: A Natural Solution in the Quest for Better Materials." January 27, 2022. <https://www.building.co.uk/focus/hempcrete-a-natural-solution-in-the-quest-for-better-materials/5115430.article>.
- Li, Hui-Lin. 1974. "An Archaeological and Historical Account of Cannabis in China." *Economic Botany* 28 (4): 437–48.
- Madurwar, Mangesh v., Rahul v. Ralegaonkar, and Sachin A. Mandavgane. 2013. "Application of Agro-Waste for Sustainable Construction Materials: A Review." *Construction and Building Materials* 38 (January): 872–78. <https://doi.org/10.1016/j.conbuildmat.2012.09.011>.
- Magwood, Chris. 2016. *Essential Hempcrete Construction: The Complete Step-by-Step Guide*. New Society Publishers.
- Marsh, Alastair T. M., and Yask Kulshreshtha. 2022. "The State of Earthen Housing Worldwide: How Development Affects Attitudes and Adoption." *Building Research & Information* 50 (5): 485–501. <https://doi.org/10.1080/09613218.2021.1953369>.
- Mazhoud, B, F Collet, S Prétot, and C Lanos. 2017. "Characterization of Mechanical Properties of Hemp-Clay Composite." *Academic Journal of Civil Engineering* 35 (2). <https://doi.org/10.26168/icbbm2017.50>.
- Mazhoud, Brahim, Florence Collet, Sylvie Prétot, and Christophe Lanos. 2021. "Effect of Hemp Content and Clay Stabilization on Hygric and Thermal Properties of Hemp-Clay Composites." *Construction and Building Materials* 300 (September): 123878. <https://doi.org/10.1016/j.conbuildmat.2021.123878>.
- Mazhoud, Brahim, Florence Collet, Sylvie Pretot, and Julien Chamoin. 2016. "Hygric and Thermal Properties of Hemp-Lime Plasters." *Building and Environment* 96 (February): 206–16. <https://doi.org/10.1016/j.buildenv.2015.11.013>.
- Mommertz, E. 2008. *Acoustics and Sound Insulation*. Berlin: Birkhauser.
- Murphy, F., S. Pavia, and R. Walker. 2010. "An Assessment of the Physical Properties of Lime-Hemp Concrete." In *Proceeding of the Bridge and Concrete Research in Ireland*.

- Müdüroğlu, M., and S. Atak. 1999. "Tuğla Kiremit Yapımında Kullanılan Kil Hammaddelerinin Özelliklerinin İncelenmesi." In *3. Endüstriyel Hammaddeler Sempozyumu*. Izmir, Turkey.
- Nguyen, Tai-Thu, Vincent Picandet, Sofiane Amziane, and Christophe Baley. 2009. "Influence of Compactness and Hemp Hurd Characteristics on the Mechanical Properties of Lime and Hemp Concrete." *Revue Européenne de Génie Civil* 13 (9): 1039–50. <https://doi.org/10.3166/regc.13.1039-1050>.
- Onay, Ahmet. 2020. *Kenevir: Cannabis Sativa L.* . 1st ed. Palme Yayıncılık.
- Oran Kalkınma Ajansı. 2019. "Kenevir Yetiştiriciliği."
- Ordu Ticaret Borsası. 2021. "Kenevir (Kendir) Raporu." Ordu. <https://www.ordutb.org.tr/wp-content/uploads/2021/03/Kenevir-Raporu.pdf>.
- Özdamar, Esen Gökçe. 2021. "Hemp as a Potential Material in Architecture: Is It Possible in Turkey." *Iconarp International J. of Architecture and Planning* 9 (1): 131–54. <https://doi.org/10.15320/ICONARP.2021.153>.
- Pacheco-Torgal, F., and Said Jalali. 2012. "Earth Construction: Lessons from the Past for Future Eco-Efficient Construction." *Construction and Building Materials* 29 (April): 512–19. <https://doi.org/10.1016/j.conbuildmat.2011.10.054>.
- Perrot, A., D. Rangeard, and E. Courteille. 2018. "3D Printing of Earth-Based Materials: Processing Aspects." *Construction and Building Materials* 172 (May): 670–76. <https://doi.org/10.1016/j.conbuildmat.2018.04.017>.
- Santillo, David. 2007. "Reclaiming the Definition of Sustainability (7 Pp)." *Environmental Science and Pollution Research - International* 14 (1): 60–66. <https://doi.org/10.1065/espr2007.01.375>.
- Shea, Andy, Mike Lawrence, and Pete Walker. 2012. "Hygrothermal Performance of an Experimental Hemp–Lime Building." *Construction and Building Materials* 36 (November): 270–75. <https://doi.org/10.1016/j.conbuildmat.2012.04.123>
- Singh, M, Divija Mamania, and Vasant Shinde. 2018. "The Scope of Hemp (Cannabis Sativa L.) Use in Historical Conservation in India." *Indian Journal of Traditional Knowledge* 17 (August).
- Stanwix, William, and Alex Sparrow. 2014. *The Hempcrete Book: Designing and Building with Hemp-Lime (Sustainable Building)*. 1st ed. Green Books.

- Sutton, Andy, Daniel Black, and Pete Walker. 2011. *Hemp Lime: An Introduction to Low-Impact Building Materials*. IHS BRE Press.
- Tran Le, A.D., C. Maalouf, T.H. Mai, E. Wurtz, and F. Collet. 2010. “Transient Hygrothermal Behaviour of a Hemp Concrete Building Envelope.” *Energy and Buildings* 42 (10): 1797–1806. <https://doi.org/10.1016/j.enbuild.2010.05.016>.
- Tronet, Pierre, Thibaut Lecompte, Vincent Picandet, and Christophe Baley. 2016. “Study of Lime Hemp Concrete (LHC) – Mix Design, Casting Process and Mechanical Behaviour.” *Cement and Concrete Composites* 67 (March): 60–72. <https://doi.org/10.1016/j.cemconcomp.2015.12.004>.
- Turkish Standards Institution. 2008. TSE-825 Thermal insulation requirements for buildings. TSE-825, issued 2008.
- United Nations Climate Change. 2019. “Climate Action and Support Trends.” Germany. [https://unfccc.int/sites/default/files/resource/Climate\\_Action\\_Support\\_Trends\\_2019.pdf](https://unfccc.int/sites/default/files/resource/Climate_Action_Support_Trends_2019.pdf).
- United Nations Environment Programme. 2021. “2021 Global Status Report for Buildings and Construction: Towards a Zero-Emission, Efficient and Resilient Buildings and Construction Sector.” Nairobi. [https://globalabc.org/sites/default/files/2021-10/GABC\\_Buildings-GSR-2021\\_BOOK.pdf](https://globalabc.org/sites/default/files/2021-10/GABC_Buildings-GSR-2021_BOOK.pdf).
- Vinceslas, Théo, Thibaut Colinard, Erwan Hamard, Arthur Menibus, Thibaut Lecompte, and Hélène Lenormand. 2017. “Light Earth Performances for Thermal Insulation : Application to Earth-Hemp.”
- Werf, H. van der. 1994. “Crop Physiology of Fibre Hemp.” Doctoral Dissertation, Wagenin, Denmark.
- Wilkinson, S. 2009. “A Study of the Moisture Buffering Potential of Hemp in Combination with Lime and Clay-Based Binders.”
- Yates, Tim. 2002. “Final Report on the Construction of the Hemp Houses at Haverhill, Suffolk.” <https://projects.bre.co.uk/hemphomes/HempHousesatHaverhillfinal.pdf>.
- Zuardi, A.W., J.A.S. Crippa, J.E.C. Hallak, F.A. Moreira, and F.S. Guimarães. 2006. “Cannabidiol, a Cannabis Sativa Constituent, as an Antipsychotic Drug.” *Brazilian Journal of Medical and Biological Research* 39 (4): 421–29. <https://doi.org/10.1590/S0100-879X2006000400001>.

## APPENDIX A

### SIMULATION INPUT PARAMETERS IN DESIGN BUILDER

Table A.1. Activity, opening and HVAC input parameters of the study room, bedroom and master bedroom.

		Study Room	Bedroom	M. Bedroom	
<b>A C T I V I T Y</b>	<b>Floor Area (m<sup>2</sup>)</b>	8.1	12.5	15.64	
	<b>Zone Volume (m<sup>3</sup>)</b>	21.23	32.75	40.97	
	<b>Occupancy</b>	Density (people/m <sup>2</sup> )	0.123	0.08	0.133
		Schedule	Through: 31 Dec, Until: 09:00, 0, Until: 19:00, 0.5, Until: 24:00, 1;	Through: 31 Dec, Until: 09:00, 1, Until: 12:00, 0.5, Until: 19:00, 0.25, Until: 24:00, 1;	Through: 31 Dec, Until: 08:00, 1, Until: 09:00, 0.5, Until: 22:00, 0, Until: 24:00, 0.5;
	<b>Metabolic Factor</b>	0.9	0.85	0.9	
	<b>Clothing (clo)</b>	Winter	1	1	1
		Summer	0.5	0.5	0.5
	<b>Heating Setpoint Temperatures</b>	Heating (°C)	23	22	22
		Heating Setback (°C)	19	19	19
	<b>Cooling Setpoint Temperatures</b>	Cooling (°C)	25	25	25
		Cooling Setback (°C)	28	28	28
	<b>Computers</b>	Power Density (W/m <sup>2</sup> )	17	-	-
		Radiant Factor	0.2	-	-
		Operation	Through: 31 Dec, Until: 09:00, 0, Until: 19:00, 0.5, Until: 24:00, 1;	-	-

(con. on next page)

**Table A.1. (Cont.)**

			<b>Study Room</b>	<b>Bedroom</b>	<b>M. Bedroom</b>
	<b>Miscellaneous</b>	Power Density (W/m <sup>2</sup> )	-	-	-
		Radiant Factor	-	-	-
	<b>Model Infiltration</b>	Constant Rate (ac/h)	0.7	0.7	0.7
		Schedule	ON 7/24	ON 7/24	ON 7/24
<b>O P E N I N G</b>	<b>Window Shading</b>	Type	Shade Roll-Medium Opaque	Drapes- Open Weave Medium	Drapes- Open Weave Medium
		Operation	Through: 1 May, Until: 08:00, 1, Until: 12:00, 0.5, Until: 20:00, 0, Until: 24:00, 1, Through: 1 Oct, Until: 12:00, 1, Until: 20:00, 0.5, Until: 24:00, 0.5, Through: 31 Dec, Until: 08:00, 1, Until: 12:00, 0.5, Until: 20:00, 0, Until: 24:00, 1,	Through: 1 May, Until: 08:00, 1, Until: 12:00, 0.5, Until: 20:00, 0, Until: 24:00, 1, Through: 1 Oct, Until: 12:00, 1, Until: 20:00, 0.5, Until: 24:00, 1, Through: 31 Dec, Until: 08:00, 1, Until: 12:00, 0.5, Until: 20:00, 0, Until: 24:00, 1,	Through: 1 May, Until: 08:00, 1, Until: 12:00, 0.5, Until: 20:00, 0, Until: 24:00, 1, Through: 1 Oct, Until: 12:00, 1, Until: 20:00, 0.5, Until: 24:00, 1, Through: 31 Dec, Until: 08:00, 1, Until: 12:00, 0.5, Until: 20:00, 0, Until: 24:00, 1,
	<b>Door</b>	% Area Door Opens	100	80	60
<b>H V A C</b>	<b>Mechanical Ventilation</b>		OFF	OFF	OFF
	<b>Auxiliary Energy</b>		0	0	0
	<b>Heating</b>	Fuel	Natural Gas (COP 0.85)	Natural Gas (COP 0.85)	Natural Gas (COP 0.85)
		Operation	Through: 1 May, Until: 10:00, 1, Until: 20:00, 0.5, Until: 24:00, 1, Through: 15 Oct, Until: 24:00, 0, Through: 31 Dec, Until: 10:00, 1, Until: 20:00, 0.5, Until: 24:00, 1;	Through: 1 May, Until: 10:00, 1, Until: 20:00, 0.5, Until: 24:00, 1, Through: 15 Oct, Until: 24:00, 0, Through: 31 Dec, Until: 10:00, 1, Until: 20:00, 0.5, Until: 24:00, 1;	Through: 1 May, Until: 10:00, 1, Until: 20:00, 0.5, Until: 24:00, 1, Through: 15 Oct, Until: 24:00, 0, Through: 31 Dec, Until: 10:00, 1, Until: 20:00, 0.5, Until: 24:00, 1;

(con. on next page)

**Table A.1. (Cont.)**

			<b>Study Room</b>	<b>Bedroom</b>	<b>M. Bedroom</b>
<b>H V A C</b>	<b>Natural Ventilation</b>	Outside air (ac/h)	20	20	20
		Operation	Through: 1 Jun, Until: 24:00, 0, Through: 1 Oct, Until: 07:00, 1, Until: 19:00, 0, Until: 24:00, 1, Through: 1 Nov, Until: 08:00, 0, Until: 20:00, 1, Until: 24:00, 0.5, Through: 31 Dec, Until: 24:00, 0;	Through: 1 Jun, Until: 24:00, 0, Through: 1 Oct, Until: 07:00, 1, Until: 19:00, 0, Until: 24:00, 1, Through: 1 Nov, Until: 08:00, 0, Until: 20:00, 1, Until: 24:00, 0.5, Through: 31 Dec, Until: 24:00, 0;	Through: 1 Jun, Until: 24:00, 0, Through: 1 Oct, Until: 07:00, 1, Until: 19:00, 0, Until: 24:00, 1, Through: 1 Nov, Until: 08:00, 0, Until: 20:00, 1, Until: 24:00, 0.5, Through: 31 Dec, Until: 24:00, 0;
	<b>Cooling</b>		OFF	OFF	OFF
	<b>Humidification</b>		OFF	OFF	OFF
	<b>DHW</b>		OFF	OFF	OFF

Table A.2. Activity, opening and HVAC input parameters of the kitchen, living room and bathroom.

		<b>Kitchen</b>	<b>Living Room</b>	<b>Bathroom</b>	
<b>A C T I V I T Y</b>	<b>Floor Area (m<sup>2</sup>)</b>		9.05	27.11	8.26
	<b>Zone Volume (m<sup>3</sup>)</b>		23.7	71.03	21.64
	<b>Occupancy</b>	Density (people/m <sup>2</sup> )	0.33	0.0167	0.12
		Schedule	Through: 31 Dec, Until: 07:00, 0, Until: 10:00, 0.3, Until: 13:00, 1, Until: 19:00, 0.3, Until: 20:00, 0.66, Until: 24:00, 0;	Through: 31 Dec, Until: 09:00, 0, Until: 10:00, 0.2, Until: 18:00, 0.7, Until: 21:00, 1, Until: 22:00, 0.7, Until: 24:00, 1;	Through: 31 Dec, Until: 06:00, 0, Until: 07:00, 0.25, Until: 09:00, 1, Until: 10:00, 0.25, Until: 18:00, 0, Until: 19:00, 0.5, Until: 21:00, 1, Until: 22:00, 0.3, Until: 24:00, 0,
	<b>Metabolic Factor</b>		0.9	0.9	0.9
	<b>Clothing (clo)</b>	Winter	1	1	1
		Summer	0.5	0.5	0.5
	<b>Heating Setpoint Temperature</b>	Heating (°C)	23	23	23
		Heating Setback (°C)	19	19	19
	<b>Cooling Setpoint Temperature</b>	Cooling (°C)	25	25	25
		Cooling Setback (°C)	28	28	28
	<b>Computers</b>	Power Density (W/m <sup>2</sup> )	-	-	-
		Radiant Factor	-	-	-
		Operation	-	-	-
<b>Miscellaneous</b>	Power Density (W/m <sup>2</sup> )	26	7.5	-	
	Radiant Factor	0.2	0.2	-	

(con. on next page)

**Table A.2. (Cont.)**

			<b>Kitchen</b>	<b>Living Room</b>	<b>Bathroom</b>
	<b>Model Infiltration</b>	Constant Rate (ac/h)	0.7	0.7	0.7
		Schedule	ON 7/24	ON 7/24	ON 7/24
<b>OPENING</b>	<b>Window Shading</b>	Type	Blind with medium reflectivity slats	-	-
		Operation	Through: 31 Dec, Until: 24:00, 0.5,	-	-
	<b>Door</b>	% Area Door Opens	100	100	5
<b>H V A C</b>	<b>Mechanical Ventilation</b>		OFF	OFF	OFF
	<b>Auxiliary Energy</b>		0	0	0
	<b>Heating</b>	Fuel	Natural Gas (COP 0.85)	Natural Gas (COP 0.85)	Natural Gas (COP 0.85)
		Operation	Through: 1 May, Until: 10:00, 1, Until: 20:00, 0.5, Until: 24:00, 1, Through: 15 Oct, Until: 24:00, 0, Through: 31 Dec, Until: 10:00, 1, Until: 20:00, 0.5, Until: 24:00, 1;	Through: 1 May, Until: 10:00, 1, Until: 20:00, 0.5, Until: 24:00, 1, Through: 15 Oct, Until: 24:00, 0, Through: 31 Dec, Until: 10:00, 1, Until: 20:00, 0.5, Until: 24:00, 1;	Through: 1 May, Until: 10:00, 1, Until: 20:00, 0.5, Until: 24:00, 1, Through: 15 Oct, Until: 24:00, 0, Through: 31 Dec, Until: 10:00, 1, Until: 20:00, 0.5, Until: 24:00, 1;
	<b>Natural Ventilation</b>	Outside air (ac/h)	20	20	0
		Operation	Through: 1 Jun, Until: 24:00, 0, Through: 1 Oct, Until: 07:00, 1, Until: 19:00, 0, Until: 24:00, 1, Through: 1 Nov, Until: 08:00, 0, Until: 20:00, 1, Until: 24:00, 0.5, Through: 31 Dec, Until: 24:00, 0;	Through: 1 Jun, Until: 24:00, 0, Through: 1 Oct, Until: 07:00, 1, Until: 19:00, 0, Until: 24:00, 1, Through: 1 Nov, Until: 08:00, 0, Until: 20:00, 1, Until: 24:00, 0.5, Through: 31 Dec, Until: 24:00, 0;	-
	<b>Cooling</b>		OFF	OFF	OFF
	<b>Humidification</b>		OFF	OFF	OFF
	<b>DHW</b>		OFF	OFF	OFF